UNIVERSIDADE DE BRASÍLIA

FACULDADE DE TECNOLOGIA

DEPARTAMENTO DE ENGENHARIA CIVIL E AMBIENTAL

ANÁLISE HIDROMECÂNICA ACOPLADA CONSIDERANDO COMPRESSIBILIDADE DO FLUIDO E DOS SÓLIDOS

SYLVIA REGINA CORRÊA BRANT PEREIRA DE JESUS

ORIENTADOR: MANOEL PORFÍRIO CORDÃO NETO
COORIENTADOR: IGOR FERNANDES GOMES

DISSERTAÇÃO DE MESTRADO EM GEOTECNIA

PUBLICAÇÃO: G.DM-207/12

BRASÍLIA-DF, ABRIL DE 2012.

UNIVERSIDADE DE BRASÍLIA
FACULDADE DE TECNOLOGIA
DEPARTAMENTO DE ENGENHARIA CIVIL E AMBIENTAL

ANÁLISE HIDROMECÂNICA ACOPLADA CONSIDERANDO COMPRESSIBILIDADE DO FLUIDO E DOS SÓLIDOS

SYLVIA REGINA CORRÊA BRANT PEREIRA DE JESUS

DISSERTAÇÃO DE MESTRADO SUBMETIDA AO DEPARTAMENTO DE ENGENHARIA CIVIL E AMBIENTAL DA UNIVERSIDADE DE BRASÍLIA COMO PARTE DOS REQUISITOS NECESSÁRIOS PARA A OBTENÇÃO DO GRAU DE MESTRE.

APROVADA POR:

_____

Prof. Manoel Porfírio Cordão Neto, DSc (UnB)
(ORIENTADOR)

_____

Prof. Leonardo José do Nascimento Guimarães, PhD (UFPE)
(EXAMINADOR EXTERNO)

_____

Prof. Márcio Muniz de Farias, PhD (UnB)
(EXAMINADOR INTERNO)

BRASÍLIA/DF, 13 de abril de 2012.

FICHA CATALOGRÁFICA

JESUS, SYLVIA REGINA CORRÊA BRANT PEREIRA DE
Análise Hidromecânica Acoplada Considerando Compressibilidade do Fluido e dos Sólidos [Distrito Federal] 2012
xxii, 122 p., 210x297 mm (ENC/FT/UnB, Mestre, Geotecnia, 2012).
Dissertação de Mestrado - Universidade de Brasília. Faculdade de Tecnologia.
Departamento de Engenharia Civil e Ambiental.

1. Numerical modeling
2. Hydro-mechanical coupling
3. Compressible fluid
4. Petroleum reservoirs
I. ENC/FT/UnB
II. Título (série)

REFERÊNCIA BIBLIOGRÁFICA

JESUS, S.R.C.B.P. de (2012). Análise Hidromecânica Acoplada Considerando Compressibilidade do Fluido e dos Sólidos. Dissertação de Mestrado, Publicação G.DM-207/12, Departamento de Engenharia Civil e Ambiental, Universidade de Brasília, Brasília, DF, 122 p.

CESSÃO DE DIREITOS

NOME DO AUTOR: Sylvia Regina Corrêa Brant Pereira de Jesus.
TÍTULO DA DISSERTAÇÃO DE MESTRADO: Análise Hidromecânica Acoplada Considerando Compressibilidade do Fluido e dos Sólidos.
GRAU / ANO: Mestre / 2012.

_____

Sylvia Regina Corrêa Brant Pereira de Jesus
SQS 207 Bl. B Apto. 203
70253-020 - Brasília/DF - Brasil

DEDICATÓRIA

Dedico este trabalho à minha família toda,
pelo amor e apoio incondicionais,
mas especialmente ao meu avô,
Sylvio Pereira de Jesus,
por todo incentivo ao estudo,
pela inspiração e pelo exemplo de vida.

AGRADECIMENTOS

Primeiramente, agradeço a Deus, por todas as oportunidades que me foram dadas.

Agradeço infinitamente à minha mãe, Sandra e meu pai, Sylvio. O carinho, a compreensão, a paciência (e que paciência!), as contribuições e, acima de qualquer coisa, o amor incondicional de vocês me fez chegar até esse momento. Quando achei que não ia conseguir, vocês me ajudaram a levantar e a seguir em frente. Sem vocês, eu não seria nada. Obrigada por tudo, sempre! Eu amo vocês!

Agradeço à minha irmã, Sabrina. Seu jeitinho doce, alegre, feliz, bobo me animam para continuar nos momentos em que acho que não vou conseguir. Suas palavras amigas, suas contribuições importantíssimas sempre foram essenciais e também não estaria aqui hoje se não fosse por você! Obrigada, Bia! Te amo!

Agradeço aos meus avós, por sempre compreenderem e estimularem a minha vontade de estudar e de querer realizar esse trabalho que estou apresentando. Seu carinho e suas palavras de incentivo sempre estão comigo. Amo vocês!

Agradeço às minhas tias Solange e Sônia, primas Camila e Débora e primo Erick, que sempre me animam, me alegram e me inspiram a continuar. Vocês todos são muito importantes para mim! Amo vocês!

Agradeço muito ao meu namorado Gabriel. Sua compreensão, sua contribuição, sua paciência e seu incentivo me ajudaram a continuar e a ter êxito nessa difícil tarefa. Você faz parte desse momento que eu tanto desejava alcançar e eu não poderia estar mais feliz com você ao meu lado, com todo seu carinho, respeito e amor! Sou muito grata a você! Obrigada por ser essa pessoa tão especial! Te amo!

Agradeço imensamente ao meu professor orientador Manoel Porfírio Cordão Neto. Professor, jamais esquecerei a confiança que você depositou em mim, a credibilidade que você teve no meu trabalho e as horas que você investiu para que tudo desse certo. Não há palavras para descrever o quão grata sou a você por isso. Obrigada pela paciência comigo, obrigada por tudo! Tenho um carinho muito grande por você!

Agradeço aos professores Márcio, André Assis, Hernán, Ennio e aos demais professores do Programa de Pós-graduação em Geotecnia da Universidade de Brasília pelo auxílio, pela inspiração e por todo o trabalho ao longo desse percurso.

Agradeço ainda ao auxílio da UFPE para a realização deste trabalho, mais especifcamente ao Professor Igor Gomes pela contribuição, pela disponibilidade, mesmo a distância, e pelo auxílio durante o processo de coorientação da presente pesquisa.

Agradeço também aos funcionários do programa pelo apoio dado durante a realização desta pesquisa e à CAPES pelo apoio financeiro.

Agradeço muito à minha amiga Juliana. Obrigada por me escutar, por me aconselhar, por compartilhar suas experiências com seu próprio trabalho, por ouvir e compreender minhas dificuldades e meus sucessos e, por fim, por me animar para a realização deste trabalho. Suas palavras de incentivo sempre foram importantes e, nesse momento, foram essenciais para eu ter força para continuar! Muito obrigada! Te amo muito! Saudades sempre...

Por fim, mas não por isso menos importantes, agradeço aos amigos e colegas do Programa de Pós-graduação em Geotecnia. Durante o curso e durante a elaboração deste trabalho, suas contribuições foram sempre muito importantes. O carinho e a gentileza de todos vocês auxiliou muito para que eu pudesse cumprir esta jornada. Agradeço em especial aos amigos Caroline, Jaime, Robinson (obrigada pelas figuras!), Leonardo, Camilla e Ígor que, sem dúvida, marcaram muitos momentos divertidos e importantes durante a realização deste trabalho e que sempre me incentivaram para que tudo desse certo.

O resultado final aqui apresentado é muito mais que um trabalho acadêmico para cumprir requisitos necessários para a obtenção de um título. É a realização de um sonho, é uma realização pessoal, é o fim de uma difícil tarefa, é a superação de diversos obstáculos. Representa uma série de aprendizados inesquecíveis, que levarei para sempre comigo. Fico muito feliz e muito honrada com a oportunidade de apresentar este trabalho.

Muito obrigada a todos que de alguma forma contribuíram para que esse trabalho pudesse ser feito e que compreendem a importância disso. Muito obrigada!

RESUMO

A relação entre comportamento mecânico e hidráulico de meios porosos é objeto de estudo da geotecnia. Ferramentas numéricas são amplamente utilizadas para a solução de problemas que envolvem esses fenômenos. Há aplicação desse tipo de estudo na geomecânica de reservatórios de petróleo, que trata especificamente do comportamento hidromecânico das rochas-reservatório e dos fluidos em seu interior. Os modelos numéricos usualmente empregados na simulação de reservatórios adotam hipóteses simplificadoras que, geralmente, não implicam perdas na representatividade do modelo. Há casos, porém, em que as condições do problema exigem o desenvolvimento dessas hipóteses. O objetivo desta pesquisa foi definir uma formulação hidromecânica acoplada para análise do problema de compactação em reservatórios de petróleo considerando compressibilidade do fluido e dos sólidos. Conceitos de engenharia de reservatórios ajudaram a definir tendências de comportamento dos reservatórios. Estratégias de acoplamento e aspectos relacionados a modelos numéricos foram discutidos. Assim, a formulação foi definida, com solução detalhada das equações de equilíbrio e de conservação de massa. Essa formulação foi implementada no programa de elementos finitos ALLFINE e testada para casos de adensamento unidimensional e bidimensional. Foram feitas análises de sensibilidade para parâmetros mecânicos (compressibilidade do fluido e dos sólidos) e hidráulicos (variação da permeabilidade combinada com compressibilidade do fluido). As análises mostraram que para um fluido mais compressível, a poropressão é significativamente afetada, com retardo em sua dissipação durante o adensamento. Além disso, observou-se que tensões elevadas ampliam os efeitos da compressibilidade do fluido. Isso é extremamente relevante na geomecânica de reservatórios, considerando o nível de tensão a que os reservatórios, geralmente, estão submetidos. A compressibilidade dos sólidos também foi avaliada, mostrando-se importante para níveis de tensão elevados, com variação significativa do coeficiente de Biot. As análises para permeabilidade mostraram que sua variação não sofre influência da compressibilidade do fluido. Esses efeitos puderam ser separados, com definição da zona de influência de cada. Observou-se, ainda, a formação de regiões com baixa permeabilidade em camadas que adensaram mais rapidamente, alterando o fluxo. A formulação proposta é adequada para descrever os parâmetros estudados. Os efeitos de compressibilidade do fluido e dos sólidos foram simulados e analisados, oferecendo resultados significativos.

PALAVRAS-CHAVE: geomecânica de reservatórios, reservatórios de petróleo, acoplamento hidromecânico, compressibilidade do fluido, compressibilidade dos sólidos.

ABSTRACT

The mechanical and hydraulic behavior of porous media is studied in geotechnics. The solution of many geotechnical problems is performed using numerical modeling. This type of tool can be applied in reservoir geomechanics simulation, which comprises hydro-mechanical behavior analyses. The numerical model representation of reservoirs is usually simplified and, in certain cases, simplifications do not imply on losses in results and behavior prediction. However, some situations require more comprehensive approaches, with development of previously neglected conditions. The main objective of this research is to define a formulation for fully coupled hydro-mechanical analyses for compaction in petroleum reservoirs considering fluid and solids compressibility valid. This model can also be used for general application in geotechnics. Throughout this research, the concepts of reservoir engineering presented helped defining behavior tendencies of reservoirs. Also, coupling strategies and specific features for the numerical model were discussed. Then, the formulation was defined with a detailed description of equilibrium and mass conservation equations solution. This formulation was implemented in Finite Element program ALLFINE and tested for one and two-dimensional consolidation cases, with sensitivity analyses for mechanical (fluids and solids compressibility) and hydraulic parameters (permeability and its combined effect with fluid compressibility). Fluid compressibility analyses reveal that this consideration affects fluid pressure responses significantly, with a delay in fluid pressure dissipation during consolidation process. Also, high stress levels magnify fluid compressibility effects. This is extremely relevant for reservoir engineering, considering the stress level to which reservoirs are usually subjected. Solids compressibility is also evaluated. Values of Biot's coefficient change significantly when high stress levels are imposed, highlighting the importance of considering solids compressibility in these cases. Permeability analyses showed that permeability variation is not influenced by fluid compressibility. These effects can be separated, being possible to define their influence range. Another effect is the formation of low-permeability zones for layers the consolidation process occurs faster, altering fluid flow. The proposed formulation is adequate to describe the studied parameters. The effects of fluid and solids compressibility could be simulated and thoroughly analyzed in this research, providing remarkable results for reservoir geomechanics simulation.

KEYWORDS: reservoir geomechanics, petroleum reservoirs, hydro-mechanical coupling, fluid compressibility, solids compressibility.

CONTENTS

LIST OF TABLES

LIST OF FIGURES

LIST OF SYMBOLS

p	Fluid pressure
T	Temperature
ρ_s or ρ^s	Solids density
M_s	Mass of solids
V_s	Volume of solids
G_s	Specific gravity
ρ_w	Water density
ρ_f or ρ^f	Fluid density
M_f	Mass of fluid
V_f	Volume of fluid
$d\rho_f$	Differential of the density of the fluid
C_f	Fluid compressibility
dp	Differential of pressure
γ_o	Ratio between oil and water density
ρ_o	Oil density
μ	Dynamic viscosity of the fluid
C_{ef}	Effective compressibility of the rock
ϕ_0	Initial porosity of the rock
$\Delta\phi$	Porosity variation
Δp	Pressure variation
k_{ro}	Relative permeability of the oil
k_{rw}	Relative permeability of the water
k_{rg}	Relative permeability of gases
k_o	Effective permeability of the oil
k_w	Effective permeability of the water
k_g	Effective permeability of the gases
k	Absolute permeability
S_o	Degree of saturation for the oil
S_w	Degree of saturation for the water
S_g	Degree of saturation for the gases

V_o	Oil volume
V_w	Water volume
V_g	Gas volume
V_v	Pore volume of the reservoir
σ_{ij}	Stress tensor
b_i	Body forces vector
x_j	Coordinate system
$\{\delta\varepsilon^*\}$	Virtual strains vector
$\{\delta u^*\}$	Virtual displacements vector
$\{b\}$	Body forces (in the domain)
$\{\tau\}$	Boundary superficial stresses
$\{\dot{x}\}$	Time derivative of variable x
$\{u^*\}$	Virtual displacements vector
$\{\varepsilon^*\}$	Virtual strains vector
$[N]$	Displacements interpolation matrix
$[B]$	Displacement-strain matrix
$\{\bar{u}\}$	Displacement vector in the domain
$\{d\sigma'\}$	Effective stress vector
$[D^{ep}]$	Elastoplastic constitutive matrix
$\{d\varepsilon\}$	Strain vector
α_b	Biot parameter
k_s	Solids bulk modulus
$\{\sigma'\}$	Effective stress vector
$\{\sigma\}$	Total stress vector
$[N^P]$	Pore pressure interpolation matrix
$[K]$	Stiffness matrix
$\{\dot{u}\}$	Nodal displacement rate vector
$[C]$	Solid-fluid coupling matrix

$\{\dot{p}\}$	Nodal pore water pressure rate vector
$\{\dot{F}\}$	External forces rate vector
$\dot{U}_i$	Real fluid velocity vector
$\dot{u}_i$	Velocity of the solids vector
w_i^f	Fluid velocity due to percolation vector
θ	Volumetric fluid content
n or ϕ	Porosity
S_r	Degree of saturation
k_f	Fluid bulk modulus
χ_s	Parameter related to degree of saturation of liquid phase
p^g	Gas pressure
$\{n\}$	Normal vector
Ω	Domain of the problem
Γ	Boundary of the problem
$\bar{q}$	Fluid discharge
$[K]$	Intrinsic permeability tensor
$\{g\}$	Gravity vector
y	Direction coincident with gravity
$[B^P]$	Derivatives of fluid pressure shape function
$[M]$	Mass matrix
$[L]$	Fluid-solids coupling matrix
$[R]$	Flow matrix
$\{p\}$	Nodal fluid pressure vector
$\{Q\}$	External discharges vector
$[W]$	System of equations matrix
$[Y]$	System of equations matrix
$\{x\}$	System of equations vector (vector of unknowns)
$\{\dot{x}\}$	System of equations vector (vector of unknowns)
$\{Z\}$	System of equations vector
α	Controlling parameter for the integration scheme

$\{x\}_t$	Vector of unknowns at initial time stage
$\{x\}_{t+\Delta t}$	Vector of unknowns at calculated time stage
c	Concentration
k	Evaluated space
C	Courant number
F	Yielding function
p'	Effective mean stress
q	Deviator stress
p_0	Preconsolidation stress
M	CSL projection inclination (modified Cam-clay model)
ν	Specific volume (ν = 1 + e)
λ	Inclination of the compression segment
κ	Inclination of the recompression segment
G	Plastic potential function
de	Void ratio increment
dp’	Increment of effective mean stress
de^e	Elastic component of the incremental void ratio
$d\varepsilon_v$	Volumetric strain component
e_0	Initial void ratio
H	Hardening modulus
$d\varepsilon^P$	Plastic strain increment
χ	Plastic multiplier
$\left\{\frac{\partial G}{\partial \sigma}\right\}$	Projection of the vector normal to the potential plastic surface in stress space
$\{d\varepsilon^e\}$	Elastic strain vector increment
$\{d\varepsilon^p\}$	Plastic strain vector increment
$\{d\varepsilon\}$	Strain vector increment
$[D^{ep}]$	Elastoplastic constitutive matrix
T	Time factor
c_v	Coefficient of consolidation
t	Elapsed time

h_d	Drainage height
k	Permeability
γ_f	Fluid unit weight
m_v	Coefficient of volume compressibility
E	Young modulus
ν	Poisson coefficient
$\Delta\sigma$	Load increment
w_{inf}	Initial uniform displacement
l	$l=2b$
b	Extension of application of the load
A	Permeability function parameter (initial permeability value)
B	Permeability function parameter
C	Permeability function parameter (equivalente to reference void ratio value)
e	Void ratio
k_1	Permeability function 1
k_2	Permeability function 2
k_3	Permeability function 3

1 INTRODUCTION

1.1 THEME CONTEXTUALIZATION AND MOTIVATION

Peculiar features characterize a petroleum reservoir. The fluids within this porous medium, oil, water and gases, create behavior conditions quite unique, which stimulate researches related to petroleum reservoirs.

In reservoir geomechanics, there are many study fields in order to better understand physical properties and behavior of a petroleum reservoir. Some of them are (Samier & De Gennaro, 2007; Pereira, 2007):

- Geological storage and petroleum production fluid reinjection;
- Tide effects analysis in mechanical properties of a reservoir;
- Constitutive modeling for reservoir rocks;
- Fault reactivation;
- Compaction and subsidence.

In reservoir geomechanics, compaction is the gradual closing of reservoir rock pores due to an increase in effective stress, consequence of fluid pressure decrease during oil production. Subsidence corresponds to the collapse of superficial zones above the reservoir which has suffered compaction.

When the first oil fields started to being monitored, data of surface displacements have been registered, indicating that during oil production some kind of phenomenon took place and induced surface subsidence. There are registered data of known petroleum fields in which the displacements reached 4,3 m. This magnitude of displacements may damage equipments used during oil production process, altering their performance.

These displacements may also affect oil recovery rates. The pore volume reduction may influence oil recovery in two ways. Depending on how pore closing occurs, oil can be trapped within the voids of the reservoir rock, decreasing recovery rate. Another possibility is that the oil is forced out of the pores, increasing oil production rate.

Considering the presented issues, engineers and technicians have realized the need of modeling and simulation in order to perform prediction analyses for petroleum reservoirs.

However, representing a complex medium such as petroleum reservoirs may be difficult. The stress state of the rock, the fluid pressure, the peculiarities of the fluids within the rock, all this influence the responses obtained with reservoir simulation. Representing all these variables and parameters may be difficult and the evolution of the type of performed

analyses for petroleum reservoirs led researchers to developing more accurate prediction methods.

Numerical modeling may be an important ally in reservoir geomechanics. Studies of behavior prediction may help increase productivity of a reservoir, therefore being of great interest of the petroleum industry.

In many cases, numerical modeling for reservoir geomechanics is restricted. There are many features involved in the studied problems, such as number of phases within the reservoir, pressure and temperature conditions, specific properties of the fluids and the rock (e.g., compressibility). The reproduction of all these variables is difficult and it may limit the possibilities of numerical simulations.

Many simplifying hypotheses are made in typical reservoir geomechanics studies, such as considering the fluids within the reservoir incompressible. There are fluids in a petroleum reservoir which have a considerable level of compressibility, such as oil and gases. Therefore, considering these fluids incompressible may neglect hydro-mechanical effects which influence directly porous medium physical behavior.

1.2 RESEARCH OBJECTIVES

The main objective of this research is to define a fully coupled hydro-mechanical formulation considering fluid and solids compressibility valid. The proposed numerical model can be employed in compaction problems for petroleum reservoirs and it can also be used for general purpose applications in geotechnics, especially consolidation problems.

The intention with this study is to verify the influence of fluid and solids compressibility and gradual void closure with fluid flow on the porous medium physical behavior. Some simplifying hypotheses are made in this research, such as considering the porous medium totally saturated with one type of fluid and in isothermal condition.

The fluid compressibility mentioned as one of the main topics of study in this dissertation refers only to liquid fluids, not being related to gases theory. The focus of this research is to study the effect of liquid fluids compressibility in porous media physical behavior. Therefore, the simulations performed in this study consider only one liquid fluid within the porous medium.

The specific objectives of this research are:

- To implement the proposed mathematical formulation in the finite element program ALLFINE (Farias, 1993; Cordão Neto, 2005);

- To validate and calibrate this formulation through sensitivity analyses for mechanical and hydraulic parameters;
- To verify the fluid compressibility (liquid) influence in physical behavior of porous media;
- To verify the solids compressibility influence in physical behavior of porous media;
- To compare the results of simulations performed with linear elastic model and modified Cam-clay during the sensitivity analyses;

It is also important to highlight that the numerical model proposed and implemented in ALLFINE is the first step for future improvement of the software. In further research, this program will be enabled to simulate behavior of multiphase petroleum reservoirs with geomechanical and hydraulic coupling.

1.3 OUTLINE OF THE DISSERTATION

This dissertation is divided in 7 chapters:

- Chapter 1 – a brief introduction is presented, with the contextualization of the studied problem and the main objectives of this research.

- Chapter 2 – it contains a review of the concepts required for the development of this research, with an overview of researches concerning reservoir geomechanics, description of petroleum and reservoir features and physical properties. Then, the compaction is defined and discussed.

- Chapter 3 – the formulation of the problem is introduced. The detailed deduction of this formulation is presented, with all assumptions and established conditions described. Then, a brief description of the constitutive models employed in the simulations is made.

- Chapter 4 – two specific topics are covered in this chapter, coupling strategies and description of the program used for the implementation of the formulation and simulations.

- Chapter 5 – tests for the mechanical parameters fluid and solids compressibility are performed for the proposed formulation, with simulation of two different cases. A

sensitivity analysis of these parameters is made in order to evaluate the degree of influence of each parameter in the hydro-mechanical behavior of porous media.

- Chapter 6 – tests for a hydraulic parameter, permeability, are performed. A permeability function is established based on void ratio changes of the porous medium and a sensitivity analysis is made for incompressible and compressible fluids with two different constitutive models, linear elastic and modified Cam-clay.

- Chapter 7 – a discussion with the conclusions over the reported topics through this research is presented, including the main results and suggestions for further research.

2 LITERATURE REVIEW

The study of reservoir geomechanics is related to different application fields. In this dissertation, the main goal is the study of compaction problems.

Compaction is defined as the gradual closing or collapse of the pores of the reservoir rock due to fluid pressure decrease and effective stress increase during oil production.

The volume changes of the reservoir with the compaction process can induce displacements of the surface, known as subsidence. These concepts are thoroughly explained in section 2.5.

Being the compaction a major concern in reservoir geomechanics, several studies have been made in order to clarify these problems. Therewith, the understanding of specific features of petroleum and the reservoirs becomes essential.

This chapter contains the main concepts related to reservoir engineering, with a review of studies made in this area. Then, features regarding petroleum generation process, petroleum reservoir and its physical properties are discussed. Finally, compaction and subsidence problems are presented, with their features, their triggering mechanisms and the cases reported in literature.

2.1 RESEARCH AND ADVANCES IN RESERVOIR GEOMECHANICS

The first studies of compaction and subsidence performed in reservoir geomechanics were related to magnitude estimation of surface displacements. According to Geertsma (1973), there have been published some papers with information concerning the causes of surface subsidence. Some researches relating reservoir compaction and surface subsidence were performed, as well as studies to determine mechanical and hydraulic changes which may influence these phenomena.

Settari (2002) defines compaction and the conditions for its occurrence, definitive for evaluating oil field exploitation viability. When these mechanisms are known, it is possible to estimate the oil reserves in a field, optimizing oil production. In this paper, it is also pointed out the importance of studies of coupled hydro-mechanical approaches in compaction analysis, making this type of technology used in large scale.

Representing the rock, the fluids and the surroundings of the reservoir is necessary in order to evaluate reservoir physical behavior and its productivity. However, there are many factors involved in assembling an adequate model.

Specific features of the fluids, such as its compressibility, viscosity, phase changes and gases release with pressure decrease, may be difficult to represent. These difficulties could be

related to computational limitations or even partial understanding of the physics of the problem. Either way, accurate models of petroleum reservoirs are difficult to be made and numerical analysis is not as representative as it should be.

Many authors highlight the importance of focusing on researches which could make possible a more appropriate representation of petroleum reservoirs. This would allow more precise predictions based on numerical modeling, with responses of recovery rate and surface displacements closer to the observed in oil fields.

A proper way of representing mechanical and hydraulic phenomena in porous media is defining a coupled hydro-mechanical formulation. Thus, it is possible to visualize the responses in terms of displacements of the rock matrix and fluid pressure. This allows a better understanding of the problem, being possible to portray the stress-strain state and the fluid flow through and out of the reservoir (Settari & Walters, 2001; Dean et al., 2006; Samier & De Gennaro, 2007).

However, a fully coupled approach may be quite difficult to perform in terms of computational cost required to it. Therefore, other analysis options, such as iterative solving of the equilibrium and the flow equations, can be employed as alternative (Settari & Walters, 2001). The results may not be as accurate as in a fully coupled approach, but are useful as response estimates. More information on coupling strategies is reported in chapter 4.

Another significant aspect in numerical simulation of petroleum reservoirs are the constitutive models. There should be specific and appropriate models for the reservoir rock, in terms of stress-strain responses, for the fluids, in terms of compressibility, and for the fluid-rock interaction, in terms of saturation and permeability. Settari & Walters (2001) highlight the importance of defining the constitutive models adequately, making comparison of the rock behavior with a non-linear elastic model and an elastoplastic model (Drucker-Prager failure criterion).

In parallel, many studies in order to clarify the aspects involved during compaction and subsidence of a petroleum reservoir have been developed (Pastor, 2001; Falcão, 2002; Wan, 2002; Dung, 2007; Pereira, 2007; Gomes, 2009). Authors have identified and studied many variables which may affect the mechanical and the hydraulic behavior of a reservoir during oil production. The mechanisms which could trigger compaction and subsidence have been discussed thoroughly. Many simulations have been performed as an attempt of refining the available numerical models in different softwares. Results from this type of research are still being collected and reported in literature, providing basis for the growth and development of new reservoir geomechanics studies.

Computational difficulties are nowadays the most significant barrier for numerical modeling in reservoir geomechanics, especially in compaction and subsidence simulation. Scientists and engineers study different options to develop accurate numerical simulation of petroleum reservoir for compaction and subsidence problems. The mechanical and the hydraulic aspects of the problem are considered, with its coupling taken into account.

For representing an oil reservoir, the usual approach is based on biphase models. The formulation for this type of problem is complex due to the various factors which interfere in reservoir physical behavior (oil, water and gas flow, interaction among phases, pressure interference in fluid responses).

Considering the difficulties inherent to this type of study, many simplifications are made in the formulations proposed for solution of these problems. The fluids within the porous medium, including oil, are considered incompressible. There are few researches in reservoir geomechanics in which the assumption of a significant compressibility of the fluid is made. Also, the compressibility of the solids is not taken into consideration in most researches.

The study made by Jha (2005) presents some results of oil compressibility consideration in reservoir simulation, comparing model responses for different compressibility values. However, it is not the focus of his work and the consideration is not thoroughly explored.

The study proposed in this research is an attempt of making the compaction problem more generalized, including specific properties of the oil and the porous medium in the coupled hydro-mechanical formulation.

Considering fluid (liquids) and solids compressibility in a coupled hydro-mechanical analysis may alter the predicted oil recovery rate of a reservoir and its estimated displacements. This could contribute to a better understanding of the reservoir physical behavior during oil production, being this the main goal of this study.

Taking into account the research context of reservoir geomechanics studies nowadays, it is important to define some concepts related to this area. Therefore, in the following sections, petroleum generation process, physical properties of reservoirs and specific topics regarding compaction and subsidence problems are presented.

2.2 PETROLEUM GENERATION PROCESS

Petroleum is derived from the sedimentary basins formation, with the settling of layers of organic and inorganic matter in seabed or lakes. Under proper conditions of temperature

and pressure, the organics decompose and form a mixture of hydrocarbons known as petroleum. Due to its sedimentary origin, petroleum is usually found in reservoir rocks such as sandstones, limestones and shales.

Considering its process of generation, one can deduce that petroleum is composed of different organic chemicals, with small and large molecules. It is typical to have hydrocarbon gas (natural gas) or liquid (crude oil) depending on pressure and temperature conditions to which the reservoir is subjected. Larger-chained hydrocarbons form heavier fractions of petroleum and smaller chains, lighter fractions.

A review of the behavior of petroleum organic compounds may be important to characterize this fluid (McCain Jr., 1933), defining properties like compressibility, viscosity and volatility, which influence flow through the reservoir directly.

In a petroleum reservoir, there are pressure and temperature conditions to which the fluids are subjected. During petroleum production, the oil suffers pressure and temperature changes when going from the reservoir to the production well and later to the surface. Therewith, tendencies of behavior of the fluid may be established, as illustrated in Figure 2.1. In Figure 2.1 (a) and (b), the expansion of the liquid may be observed, only by the pressure decrease effect. In Figure 2.1 (b) and (c), there is vaporization of the liquid and in Figure 2.1 (c) and (d), more expansion takes place, in this case, for both fluid phases. Finally, in Figure 2.1 (e), there is temperature decrease, which has effects on fluids volume.

The vaporization observed at a certain pressure level is justified by the bubble-point pressure concept, explained in details in section 2.3.1.

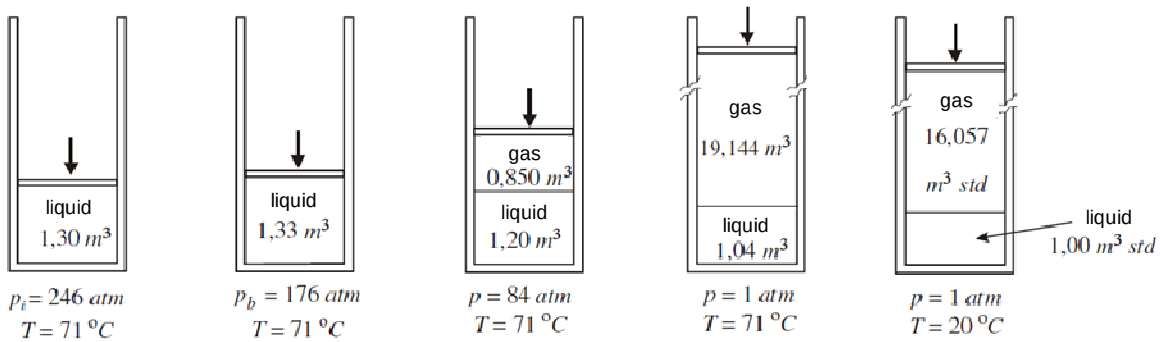

Figure 2.1 – Changes of pressure and temperature during petroleum recovery process (modified Rosa et al., 2006).

The behavior of the fluid in certain pressure conditions highlights the great influence compressibility can have, justifying once more the proposed study. Again, it is important to

highlight that this research comprises only the behavior of compressible liquid fluids, with no mention to gas phase.

2.3 PETROLEUM RESERVOIRS

Petroleum generation process is characterized by the layering of sediments create a geological formation quite porous, with decomposed organic matter (petroleum) intertwined with the rock. This is known as source rock (Dake, 1978).

Specific features of petroleum, such as the density of its compounds, may induce the crude oil and the natural gases to migrate from the profound zones where the source rock is located to much shallower depths. The migration of petroleum is interrupted when a very low permeability zone is reached. Therewith, petroleum is trapped by cap rocks in porous zones of the rock matrix, the reservoir rocks.

It is important to highlight that given the formation process of a reservoir, there are oil, gases and water in it, constituting the three-phased fluid system studied in reservoir geomechanics.

Many aspects influence petroleum generation, inducing a great variability in the process. So reservoir fluid composition may differ, being some only composed by gas, other exclusively by oil. Defining the fluids in a reservoir allows the evaluation of proper numerical modeling to be employed and, at a later stage, the adequate techniques for petroleum exploitation.

For that reason, there is a classification system for petroleum reservoirs, presented in the following section. In sequence, it is made a description of petroleum recovery processes.

2.3.1 CATEGORIES OF PETROLEUM RESERVOIRS

The variability in petroleum reservoir generation processes makes each reservoir unique, with different properties. Thus, it is essential to classify the different types of reservoirs. Categorizing helps on the definition of the requirements for performing numerical analysis. The fluids in the reservoirs, its different phases and coexistence reflect on the modeling and, therefore, this classification is necessary. Thus, each reservoir category may be described with proper physical models.

A petroleum reservoir may be assorted in different ways, depending on many variables, such as (Ahmed, 2001):

- The composition of the hydrocarbon mixture in the reservoir;
- The initial conditions of pressure and temperature;

- Pressure and temperature of the surface production.

Considering the fluids in a reservoir as a multicomponent system and also the pressure and the temperature conditions by which they may be influenced, it is convenient to express this system in a phase diagram, as shown in Figure 2.2. The fluids within a reservoir may be characterized with this pressure-temperature diagram (p-T diagram), which relates pressure and temperature conditions of these fluids. Therewith, the coexistence of phases and particular conditions of the fluids are defined.

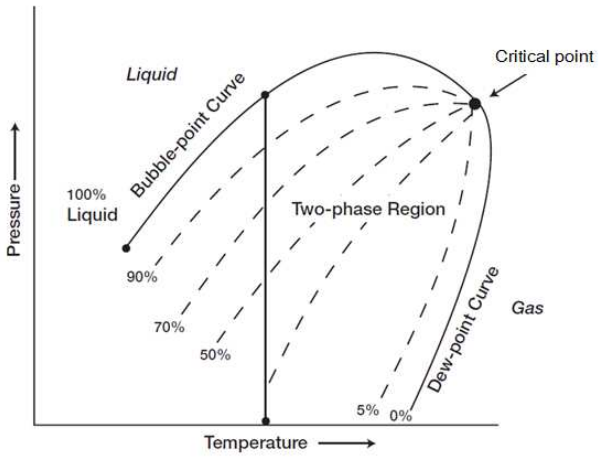

Figure 2.2 - Pressure-temperature diagram for a multicomponent system (modified Ahmed, 2001).

Consequently, petroleum reservoirs may be grouped into categories given their phase composition. The temperature to which the reservoir is subjected reflects on this classification. If such temperature is lower than the critical temperature of the hydrocarbon fluid (Critical point - Figure 2.2), it is an oil reservoir. If such temperature is greater than the critical temperature of the hydrocarbon fluid, it is a gas reservoir (Ahmed, 2001).

Pressure is also used to categorize petroleum reservoir. For such, some importance may be given to the bubble-point curve (Figure 2.2). In certain pressures, the gas which could be within the reservoir is completely dissolved in the crude oil. Therefore, it does not compose a continuous and movable phase. During the process of petroleum exploitation, pressure decreases in the reservoir and bubbles start to arise gradually in the oil. The pressure limit for the appearance of a gas phase (bubbles) in the reservoir is the bubble-point. The bubble-point pressure is a parameter used for classifying reservoirs in three categories:

- Undersaturated reservoir: the initial reservoir pressure is greater than the bubble-point pressure;
- Saturated reservoir: the initial reservoir pressure is equal to the bubble-point pressure;

- Gas-cap reservoir: the initial reservoir pressure is lower than the bubble-point pressure – there are two distinct, continuous and movable phases in the reservoir – gaseous phase and oil phase.

The development of appropriate numerical models for representation of multiphase reservoirs is possible with the understanding of the conditions of pressure and temperature of a reservoir.

Even though not very common in practice, the formulation developed and tested in this research is specific for a monophase reservoir (oil saturated reservoir, e.g.) in isothermal conditions.

2.4 PHYSICAL PROPERTIES OF A PETROLEUM RESERVOIR

In reservoir geomechanics, researches related to oil and natural gas production are developed. Maximizing the recovery rate is the main goal: greater production means quicker financial response. Therefore, studies regarding physical aspects of phenomena in oil and gas reservoirs are important. It is necessary to improve numerical modeling of reservoirs in order to predict reservoir behavior due to changes in stress-strain state.

Foremost, characteristics of the reservoir must be established, not only for the reservoir rock itself, but also for the fluid and the fluid-rock interaction.

There are some characteristics of fluid-rock interaction which must be considered in cases of a multiphase flow. For that reason, there are some specific features regarding multiphase reservoirs which will not be described in this review, taking into account this research focus, a monophase, oil-saturated reservoir. In the following section, the main aspects regarding reservoir features are presented.

2.4.1 DENSITY AND VISCOSITY

The fluids within the rock and the reservoir itself must be characterized to their behavior be properly represented in numerical models. The density is a basic feature commonly described for fluid and rock matrix.

The density is defined as the ratio of mass to volume. Specifically for the solid particles, for the rock matrix, this ratio is:

$$\rho_s = \frac{M_s}{V_s} \tag{2.1}$$

where: ρ_s is the density of the solid particles, M_s is the mass of solids and V_s is the volume of solids.

The specific gravity G_s is a dimensionless variable also used to express the density of solid particles. It is a normalized value of solids density relative to water density.

$$G_s = \frac{\rho_s}{\rho_w} \tag{2.2}$$

where: G_s is the specific gravity, ρ_s is the density of the solid particles and ρ_w is the density of the water.

For a fluid within the rock, the density is defined as:

$$\rho_f = \frac{M_f}{V_f} \tag{2.3}$$

where: ρ_f is the density of the fluid, M_f is the mass of fluid and V_f is the volume of fluid.

There are cases in which the rock is saturated with only one fluid. When this happens, the volume of fluid corresponds to the pore volume of the reservoir.

It is important to highlight that the density of the fluid varies progressively with changes of pressure, determining the compressibility of the fluid. In general, the pressure variation rate is not significant and the density changes might be neglected in modeling. However, in some particular cases, like in petroleum reservoirs, the effects of pressure changes are greatly noticed and must be taken into account. The density of liquid fluids varies with pressure like expressed in Eq. (2.4) (Peaceman, 1977; Rosa et al, 2006):

$$d\rho_f = C_f \rho_f dp \tag{2.4}$$

where: $d\rho_f$ is the differential of the density of the fluid, C_f is the fluid compressibility and dp is the differential of pressure.

Another feature quite important in cases of oil reservoir analysis is the viscosity of the fluid. This property represents the resistance of the fluid to a shearing force. As well as the density, the viscosity of a fluid also depends on the pressure to which it is subjected. The temperature of the fluids influences its viscosity as well, decreasing as temperature increases (Fredlund & Radharjo, 1993).

In reservoir engineering, there are several empirical methods proposed for oil viscosity estimative. Usually, these methods determine a correlation between the oil viscosity and the API gravity of the crude oil. The API gravity is a parameter to compare the oil density to water density, given by the following expression:

$$^{\circ}API = \frac{141,5}{\gamma_o} - 131,5 \tag{2.5}$$

where: $\gamma_o = \rho_o / \rho_w$, ρ_o is the oil density at 60 ºF (15,6 ºC) and ρ_w is the water density at 60 ºF.

One empirical method for estimating oil viscosity is Beal's correlation, function of the temperature and the API gravity. It is known as:

$$\mu = \left(0,32 + \frac{1,8.10^7}{^{\circ}API^{4,53}}\right)\left(\frac{360}{T-200}\right)^a \tag{2.6}$$

$$a = 10^{\left(0,43+8,33/^{\circ}API\right)} \tag{2.7}$$

where: $\mu$is the dynamic viscosity of the fluid and *T* is the reservoir temperature, in ºF.

2.4.2 POROSITY

In order to understand the behavior of the reservoir rock, porosity is one of the first features which should be defined. It refers to the reservoir volume that is empty or filled by fluids, particularly the pores of the solid matrix. There are two distinct types of porosity – the absolute and the effective porosity (Ahmed, 2001).

The absolute porosity is attributed to all voids of the rock, presented in Figure 2.3. The effective porosity, however, it is related to the interconnected pores, as shown in Figure 2.4 (b). This represents the preferential paths through which fluids can run.

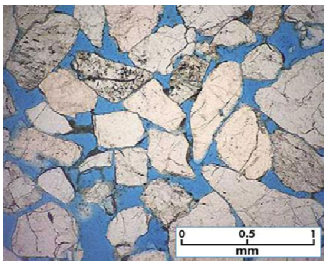

Figure 2.3 - Absolute porosity of a rock (Iglesias, 2009).

(a) (b)

Figure 2.4 – (a) Non-interconnected pores of a rock; (b) Interconnected pores of a rock (Iglesias, 2009).

2.4.3 ROCK COMPRESSIBILITY

A quite relevant property is the compressibility of the rock. The reservoir rock is subjected to a stress state and fluid pressure, which adjust throughout petroleum recovery process. These variations may induce volume changes in the grains (solids), in the pores or even in the whole reservoir rock. The ratio between volume variation and stress/pressure changes defines rock compressibility.

There are three categories of compressibility which can be distinguished in rocks (Rosa et al, 2006):

- Compressibility of the rock matrix: it takes into account the fractional variation of the volume of solids of the rock with pressure changes;
- Pore compressibility: it takes into account the fractional variation of the volume of the pores (voids) of the rock with pressure changes;
- Total compressibility of the rock: it takes into account the fractional variation of the total volume of the rock (solids and voids) with pressure changes.

In reservoir geomechanics, the most significant volume changes are those observed in the pores of the rock. This phenomenon characterizes the effective compressibility of the reservoir, described in Eq. (2.8).

$$C_{ef} = \frac{1}{\phi_0}\frac{\Delta\phi}{\Delta p} \tag{2.8}$$

where: C_{ef} is the effective compressibility of the rock, ϕ_0 is the initial porosity of the rock, $\Delta\phi$ is the porosity variation and Δp is the pressure variation.

For reservoir geomechanics, this definition (Eq. (2.8)) is particularly important. Most of commercial softwares for reservoir geomechanics simulation use this equation to describe the porosity changes in terms of compressibility.

Pore compressibility may be quite significant in shallow unconsolidated reservoirs, with values of 6,89 x 10^{-4}/kPa being measured, for instance, in the Bolivar Coast fields in Venezuela. It is essential to consider the effects of pore compressibility in cases like this (Dake, 1978).

2.4.4 WETTABILITY

As already mentioned, petroleum is stored in highly porous layers, the reservoir rocks. The main features of the rock and the fluid-rock interaction must be specified in order to have the information required for reservoir modeling.

An important characteristic is wettability. This property concerns the contact angle between the solid matrix (surface) and the fluid. Intermolecular forces which connect the compounds of each petroleum liquid phase – crude oil and water – influence the fluid-rock interaction. In crude oil, fairly small intermolecular forces between hydrocarbon molecules make the oil-rock adherence minimum. Therewith, the contact angle of oil with the reservoir rock is null, distinguishing it as the non-wetting phase. The water phase found in the reservoir, on the other hand, adheres completely to the solid matrix, characterizing the wetting phase (Ahmed, 2001), as shown in Figure 2.5.

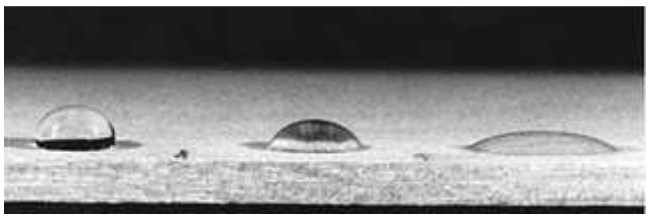

Figure 2.5 – Water wettability (from internet).

2.4.5 PERMEABILITY AND SATURATION

Given the distinct fluids that may be within the pores of a petroleum reservoir, it is important to establish some aspects regarding permeability.

Permeability is defined as the measure of transmissibility of a fluid in a porous medium. This measure may vary depending on the type of fluid, its viscosity and density. Therefore, in the same medium, the flow of different fluids occurs in different rates. This is particularly important for petroleum reservoirs in which, in general, there is more than one phase of fluid.

There are three categories of permeability which can be determined in a given medium: absolute permeability, effective permeability and relative permeability.

The absolute permeability of the reservoir rock is determined with an inert fluid, usually nitrogen or hydrogen gases, which saturates completely the intertwined pores.

The effective permeability is a specific measure for the petroleum composing fluids. Therefore, the effective permeability of the oil, water and gas are determined for the reservoir rock. Finally, the relative permeability is a normalized ratio between the effective permeability for each fluid and the absolute permeability (Eqs. (2.9), (2.10) and (2.11)).

$$k_{ro} = \frac{k_o}{k} \tag{2.9}$$

$$k_{rw} = \frac{k_w}{k} \tag{2.10}$$

$$k_{rg} = \frac{k_g}{k} \tag{2.11}$$

where: k_{ro}, k_{rw}, k_{rg} are the relative permeabilities of the oil, water and gases, respectively, k_o, k_w *e* k_g are the effective permeabilities of the oil, water and gases and k is the absolute permeability.

The distribution of the different fluids in the pores of the rock is important to define flow occurrence in a reservoir. Therefore, concepts regarding saturation are important and should be stated.

The degree of saturation of a sample is related to the volume of fluid within the rock. The saturation may be established for the different fluids which compose petroleum – oil, gas and water – and this reflects directly on reservoir behavior.

$$S_o = \frac{V_o}{V_v} \tag{2.12}$$

$$S_w = \frac{V_w}{V_v} \tag{2.13}$$

$$S_g = \frac{V_g}{V_v} \tag{2.14}$$

where: S_o, S_w and S_g are the degrees of saturation for the oil, the water and the gases in the reservoir, respectively; V_o, V_w, V_g and V_v are the oil volume, the water volume, the gas volume and the pore volume of the reservoir, respectively.

In order to flow being established through the reservoir, there is a minimum volume of fluid necessary. For this reason, defining the degree of saturation of each fluid within the rock is essential to understand how fluid flow occurs in the reservoir. There are three limit values which delineate what happens to each fluid, depending on its degree of saturation in a petroleum reservoir. For the oil phase, the following limits should be taken into account (Ahmed, 2001):

- Residual oil saturation: it is related to a volume of oil impossible to be removed from the pores of the reservoir rock;
- Critical oil saturation: it is the minimum degree of saturation required to the occurrence of oil flow;
- Movable oil saturation: it refers to any value of degree of saturation greater than the critical saturation. Therefore, in this case, the volume of oil in the reservoir is always more than the necessary to establish flow through the rock.

There are some important phenomena dependent on the degree of saturation of the water and gases in the reservoir. It is necessary to define for those phases these two concepts (Ahmed, 2001):

- Critical water saturation: this refers to the minimum water saturation at which the water phase remains immobile. This remaining water in the reservoir is also known as connate water, as shown in Figure 2.6;

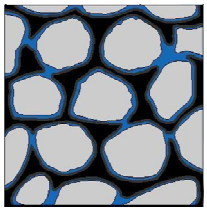

Figure 2.6 - Connate water in an oil reservoir (Iglesias, 2009).

- Critical gas saturation: when a multiphase reservoir is subjected to high pressure (greater than the bubble-point pressure), the gases remain dissolved in the oil. Therefore, the gas does not form visible bubbles. When reservoir pressure declines above the bubble-point pressure, bubbles start to appear, but still do not form a movable phase. The critical gas saturation limit is reached when above it, gas begins to move, as illustrated in Figure 2.7.

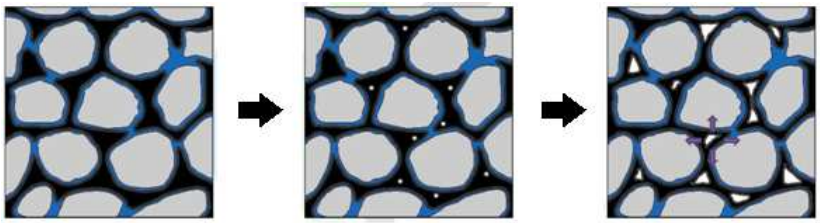

Figure 2.7 – Petroleum despressurization – movable gaseous phase formation (Iglesias, 2009).

The definition of the degree of saturation of the fluids in a reservoir is more significant for multiphase reservoir analysis. However, the critical gas saturation definition may be useful in order to visualize the compressibility of petroleum composing fluids.

The basic concepts presented in this section are necessary to understand the behavior of a petroleum reservoir, making possible a more adequate numerical representation of this type of medium.

2.5 GEOMECHANICAL IN RESERVOIRS: COMPACTION AND SUBSIDENCE

The maximum productivity of a petroleum reservoir is the main goal in reservoir geomechanics. The process of oil recovery from a petroleum reservoir implies in fluid withdrawal from the rock, which causes fluid pressure decrease. This alters the stress-strain state of the rock and fluids within and these variations guide the production process.

In reservoir geomechanics, many studies can be made in order to comprehend the physical behavior of the reservoir rock and the fluids within (Samier & De Gennaro, 2007; Pereira, 2007). The proper understanding of the reservoir behavior may help in future performance prediction. Therefore, the study of phenomena which may influence petroleum recovery rate is of great importance.

In this section, some aspects regarding petroleum driving mechanisms and production processes are discussed, followed by a specific analysis of influence of the compaction and subsidence in petroleum recovery.

2.5.1 PETROLEUM DRIVING MECHANISMS

The process of petroleum recovery is greatly influenced by driving mechanisms of the fluids within the petroleum reservoir. These driving mechanisms are established due to energy provided to the reservoir, which controls flow mechanisms that ensure oil recovery.

For a multiphase reservoir, there are basically six driving mechanisms necessary for oil recovery (Ahmed & McKinney, 2005):

- Rock and liquid expansion drive;
- Depletion drive;
- Gas cap drive;
- Water drive;
- Gravity drainage drive;
- Combination drive.

In the rock and liquid expansion drive mechanism, when oil recovery is initiated, with fluid pressure decrease, the fluids within the reservoir and the reservoir rock itself tend to expand due to their individual compressibility (sections 2.4.1 and 2.4.3). This causes reduction in pore volume, forcing the fluids out of the reservoir to the wellbore.

The depletion drive mechanism is significant for undersaturated reservoirs. During the production process, pressure declines in the reservoir. When the bubble-point pressure is reached (section 2.3.1), gas bubbles are liberated within pore spaces of the rock. The bubbles gradually expand and force oil out of the pores. This mechanism takes place until critical gas saturation is reached. When this happens, free gas begins to flow toward the wellbore and vertically, forming a secondary gas cap.

In a multiphase reservoir with a gas cap, the existent gases within the reservoir expand with pressure decrease and this also forces fluids out of the pores rocks, characterizing gas cap drive mechanism (Figure 2.8). This mechanism may be associated to dissolved gas liberation, like mentioned in depletion drive mechanism (Ahmed & McKinney, 2005).

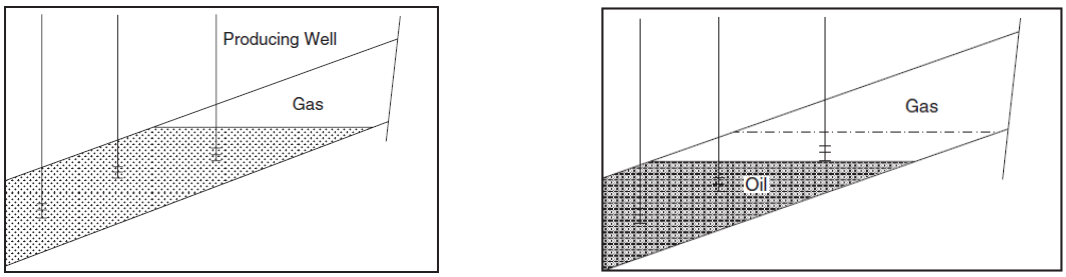

Figure 2.8 – Gas cap drive mechanism – (a) initial condition of the reservoir; (b) gas cap expansion and oil production (Ahmed & McKinney, 2005).

In some cases, there is an aquifer underneath the reservoir. When fluids are extracted, water from the aquifer fills in the pores of the reservoir (Figure 2.9). Thus, during production process, it is not established a significant pressure decrease within the reservoir and oil withdrawal is much less productive. In some situations, it is also initiated water production, a non-profitable situation. The ideal is to minimize water and gas production, so oil recovery is maximized.

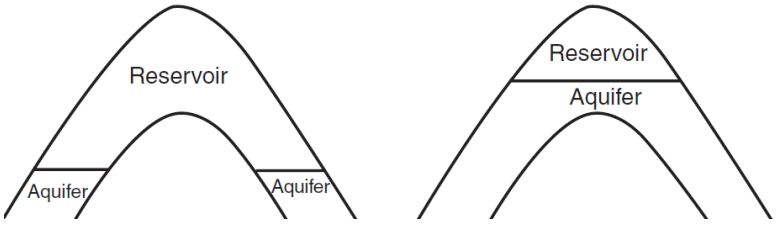

Figure 2.9 – Water from aquifer filling oil reservoir (Ahmed & McKinney, 2005).

The gravity drainage drive mechanism is a result of the difference in densities of the fluids in a reservoir. With petroleum formation process and natural migration within the reservoir, the fluids are mixed. After a period of time, the fluids tend to separate, the more dense fluid settling to the bottom of the reservoir, the water. In this way, the fluids have been separated as a result of gravitational forces action. Considering the period involved in petroleum formation and migration processes, followed by the large time with no flow processes within the reservoir, i.e. before production, this system of fluids is assumed to be in equilibrium. It may be established then that the contacts between fluids are horizontal, as illustrated in Figure 2.10.

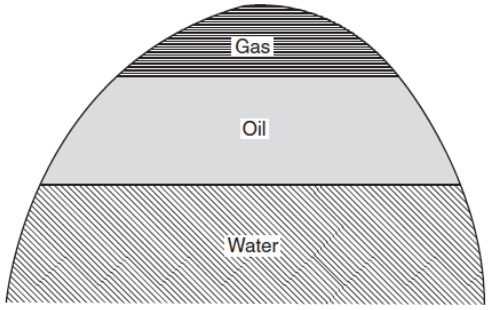

Figure 2.10 – Initial fluids distribution in an oil reservoir (Ahmed & McKinney, 2005).

The fluid segregation observed in this type of reservoir may contribute substantially to oil production. The fluids are separated in zones and this facilitates their recovery.

Finally, the combined drive mechanisms are the most commonly observed during oil production. The combinations of different drive mechanisms usually present are:

- Depletion drive and water drive;
- Depletion drive with gas cap drive and water drive.

It is important to highlight the special role of gravity drainage drive mechanism, which enhances oil recovery in most cases.

The understanding of the physical behavior of the reservoir and the drive mechanisms of the fluids within is essential in order to predict reservoir behavior and production performance.

2.5.2 PETROLEUM PRODUCTION PROCESSES

Once a zone with petroleum is located, it is fundamental to study the initial conditions of pressure and temperature of the reservoir. Thus, it can be possible to define the appropriate method of petroleum recovery. It is necessary to study the aspects which may influence petroleum production in order to evaluate the profitability of the project. Different techniques

may be applied and, consequently, the appropriate one is chosen not only by physical aspects, but so by financial aspects (Chen *et al*, 2006).

Petroleum recovery is made by drilling a well in the surface (land, seabed or bottom of lakes) to the reservoir. After this, there are three types of recovery processes which can be applied (Dake, 1978).

The primary recovery takes place due to a pressure gradient between the reservoir and the well. Considering that the reservoir is under greater pressure than the well, the difference of pressure between them makes the fluids flow from the reservoir to the well, characterizing primary recovery. During this process, the internal pressure of the reservoir decreases and, consequently, the effective stress on the reservoir increases. This makes pore volume decrease, inducing the oil flow out of the reservoir. Another important aspect to consider is the fluid expansion given the decrease of pressure inside the reservoir. This also helps the extraction of crude oil and water from the reservoir (Rosa et al., 2006).

During the continuous process of petroleum production, a stage of balance between the pressure in the well and in the reservoir is reached. When this is observed, it is required the development of a different method of petroleum recovery. Auxiliary methods might be needed to increase recovery rates if petroleum production becomes not sufficient in terms of financial response.

The secondary and the tertiary petroleum recovery processes are based on the idea of increasing natural energy of the reservoir with fluid injection (Dake, 1978). This procedure forces petroleum to flow out of the reservoir, continuing its production and increasing recovery rate. The secondary and tertiary recovery procedures are methods which follow primary recovery.

Secondary recovery refers to procedures of water flooding and water steam injection in the reservoir. This makes the gradient of pressure sufficient to induce oil flow out of the reservoir, increasing its recovery rate.

Tertiary recovery process corresponds to procedures to recover residual oil within the reservoir, therefore being the last method employed to recover fluids from the reservoir. The type of injected fluids in this recovery process, carbonic gas, polymers or surfactants, is reactive to the water or the oil in the reservoir, triggering chemical and thermal effects. Changes in water viscosity or in oil miscibility can take place, affecting positively petroleum recovery rate. This type of recovery is used only when the secondary recovery is not possible (Dake, 1978).

The injection of other fluids could influence the simulation results for fluid pressure estimative. Therefore, in order to isolate the effects of fluid and solids compressibility, only primary recovery is considered in this research. Thus, the evaluation of compressibility effects on model responses is more accurately registered.

2.5.3 COMPACTION AND SUBSIDENCE

During the oil production, fluid pressure declines, inducing effective stress increase in the reservoir. With the load of overburdens, sideburdens and underburdens layers and pressure changes, processes of strain and rock matrix properties changing are observed. A gradual closing or collapse of the pores of the reservoir rock is established, characterizing the phenomenon known as compaction (Lewis et al, 2003; Pereira, 2007; Gomes, 2009).

Volume reduction caused in compaction may induce surface displacements above the reservoir rock. This particular phenomenon is known as subsidence. Both compaction and subsidence are illustrated in Figure 2.11.

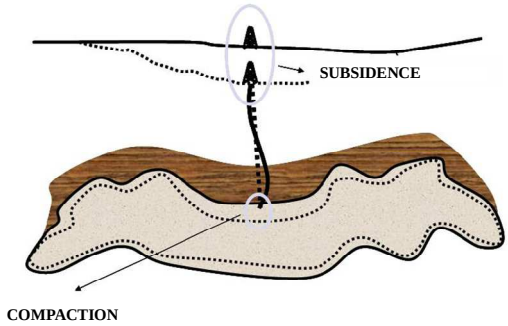

Figure 2.11 - Compaction and subsidence in a petroleum reservoir (Pereira, 2007).

The fluid pressure decrease during oil recovery is the cause of compaction and subsidence mechanisms. Depending on how pore closing takes place, oil might be trapped in the voids of the rock, making oil recovery rate decline.

On the other hand, these phenomena may also enhance oil recovery through a process named compaction drive. During oil production, the stress-strain state changes induce collapse of the pores of the reservoir rock. This pore volume reduction forces fluids out of the voids of the rock. This process of pore closing increases the oil production rate, characterizing the compaction drive mechanism (Gomes, 2009).

Compaction and subsidence occurrence is determined by the depth and the mechanical properties of the reservoir rock, the geometry of its burdens and the contrast between mechanical properties of the reservoir rock and its surroundings.

In some cases, there are no significant losses in oil recovery specifically due to compaction and subsidence. Then subsidence may be admissible if it does not imply on great damage to the surface. However, other cases can induce different phenomena in the reservoir, such as fault reactivation, fracture propagation and damage to the production well (Gomes, 2009).

Some cases of compaction and subsidence are reported in literature and are briefly described in this section.

2.5.3.1 BOLIVAR COAST (VENEZUELA)

In this region, three oil fields have been affected by subsidence after three years production has started. Landmarks were installed in 1939 and periodic measures have been made in order to check subsidence evolution in the area.

With a maximum displacement of the surface of 4,3 m in 1978, there was need of construction of dikes to prevent flooding of some areas. However, there were still some regions with inundation and the vegetation became submersed in all field extension. There have been reported damages in tubes and wells of the oil production area.

Even though many losses have been reported in Bolivar coast, oil production has been enhanced due to reservoir compaction. Primary recovery was the main production technique employed in this region and a compaction drive mechanism has been established, contributing to a greater oil production rate.

To avoid more structural damage in the platforms, water injection has been implemented, maintaining fluid pressure within the reservoirs and preventing from more subsidence.

2.5.3.2 EKOFISK FIELD (NORWAY - NORTH SEA)

This reservoir, located in the Norwegian sector of the North Sea, started to have subsidence registries in 1984. The measure displacement in 1989 was approximately 4,3 m, with predictions of 6,1 m for 2011. Studies in the area have proved that compaction mechanism was responsible for the surface displacements, as a result of fluid pressure decline during oil production (Lewis et al, 2003). The subsidence may be easily seen in Figure 2.12.

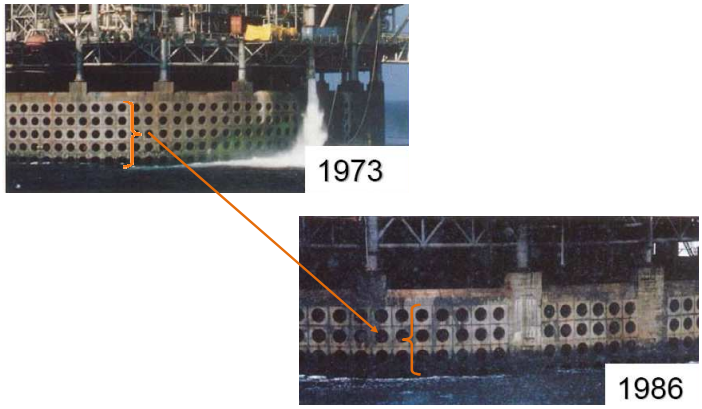

Figure 2.12 - Subsidence in Ekofisk field (Pereira, 2007).

Due to the compaction and subsidence problem in this reservoir, oil production has reduced significantly and water injection procedures have been started in the area. This has induced a great increase in oil production rate.

This procedure has controlled quite well the depletion mechanism in the reservoir. However, compaction has still taken place in the region at constant rates. It has been stated that the injected water reacted to the rock, causing its weakening and consequent compaction (Pereira, 2007).

2.5.3.3 VALHALL FIELD (NORWAY - NORTH SEA)

This is an offshore petroleum field with highly porous reservoir rocks, located in the norwegian sector of the North Sea, 190 km far from the coast. This field was discovered in 1975 and its exploitation began in 1981 (Pereira, 2007).

After three years of oil production, the measured values of pressure within the reservoir were lower than the expected given numerical predictions, suggesting that a specific phenomenon should be taking place in this field. In fact, in 1986, satellites images registered subsidence in this region, attesting the occurrence of the compaction mechanism.

Numerical modeling studies and computational analysis based on data field revealed that 70% of the petroleum production in this area was due to compaction drive mechanism.

2.5.3.4 WILMINGTON FIELD (UNITED STATES)

In this field, located in California, United States, subsidence has been documented four years after the start of the oil production process. Large horizontal displacements have taken place in the region (approximately 3,7 m), causing damages to an industrial area in the Long Beach port (Lewis et al, 2003). The subsidence control has been achieved with water injection technique (Pastor, 2001).

2.5.3.5 SOUTH BELRIDGE FIELD (UNITED STATES)

This petroleum field is a composition of an unconsolidated sandstone reservoir (122 to 183 m thick) and highly compressible adjacent formations (305 m thick), located in California, United States.

Compaction and subsidence phenomena started to be taken into account when field operators realized that some wells had their casing damaged. Besides that, horizontal fissures in the surface over the reservoir were registered, parallel to maximum horizontal stresses direction, attesting that compaction and subsidence mechanisms have taken place (Pereira, 2007).

Observing the registered cases of compaction and subsidence and given the properties of the reservoir rock and the fluids related to compaction and subsidence mechanisms, it may be inferred that stress-strain changes and fluid flow are greatly relevant for reservoir analyses.

Therefore, it is important to state that performing analyses with both hydraulic and mechanical approaches is the most adequate. Thus, physical phenomena involved in the recovery process are appropriately represented.

Coupling strategies for these phenomena should be taken into account, in order to properly represent the reservoir in numerical modeling.

2.6 SUMMARY

In this chapter, basic concepts of reservoir engineering have been presented. Firstly, aspects regarding specific research of reservoir engineering are discussed, highlighting the importance of studying compaction and subsidence mechanisms.

Later, the understanding of petroleum formation process helps in determining some properties which delineate reservoir behavior. Therewith, it is possible to classify petroleum reservoir, defining the type of formation by verifying the conditions of the fluids within.

Then, some aspects of reservoir rock and petroleum properties are established. This is of paramount importance, given the necessity of defining properties and parameters for posterior numerical modeling.

Finally, petroleum reservoir phenomena are discussed, with the definition of petroleum driving mechanisms, petroleum production processes and specific features of compaction and subsidence.

All concepts discussed in this chapter were important in the definition of the numerical modeling procedures performed in this research.

3 FORMULATION

The solution of many engineering problems is only possible when representative models are established and their numerical modeling is performed. Different approaches are required in order to represent physical phenomena. Specifically for geotechnics, the mechanical and the hydraulic behavior of a porous media are completely interrelated.

In this chapter, some aspects regarding possible coupling strategies for the solution of hydro-mechanical problems are presented. Then the studied phenomena are outlined, with definition of the mechanical and the hydraulic approaches assumed in this research.

3.1 DESCRIPTION OF THE MECHANICAL AND THE HYDRAULIC BEHAVIOR EQUATIONS

Models which represent physical processes in porous media more commonly take into account the mechanical behavior and the hydraulic behavior, delineated by equilibrium and fluid mass conservation equations. Therewith, the coupled hydro-mechanical approach is important, being adequate to describe the physical phenomena studied in reservoir geomechanics (Samier et al, 2003).

However, in some cases, there is also some influence of specific characteristics of the porous media. Porosity variation of the solid matrix may be observed given the changes in stress-strain state. Coupled analysis then may be enhanced by taking into account the effects of porosity variation. This can be done by considering the solids mass conservation.

Considering these equations, the compaction and the subsidence phenomena can have their solutions determined by numerical modeling. It allows prediction of changes in stress-strain state, representing more appropriately what occurs in a petroleum reservoir. Therefore, it is possible to evaluate petroleum production rates with higher precision.

The representative mathematical formulation for these problems is solved with a spatial discretization with the finite element method (FEM) and a time discretization with the finite difference method (FDM). The proposed formulation has been specially developed for studies of monophase reservoirs (only for liquid fluids), even though it can be applied in cases with similar features.

The solution of the problem is divided into four parts for better understanding of the reader. Firstly, it is presented the spatial solution of the equilibrium equation. Then, the mass conservation equation is solved in space as well. These solutions are gathered as a system of equations. Finally, the solution in time is performed for this system of equations.

3.2 SPATIAL SOLUTION OF THE EQUILIBRIUM EQUATION

The equilibrium equation for a petroleum reservoir in the established conditions can be described using indicial notation as:

$$\frac{\partial \sigma_{ij}}{\partial x_j} + b_i = 0 \tag{3.1}$$

where: σ_{ij} is the stress tensor, b_i are the body forces vector and x_j is correspondent to the coordinate system.

Eq. (3.1) can also be written as:

$$\frac{\partial \sigma_x}{\partial x} + \frac{\partial \tau_{yx}}{\partial y} + \frac{\partial \tau_{zx}}{\partial z} + b_x = 0 \tag{3.2}$$

$$\frac{\partial \sigma_y}{\partial y} + \frac{\partial \tau_{xy}}{\partial x} + \frac{\partial \tau_{zy}}{\partial z} + b_y = 0 \tag{3.3}$$

$$\frac{\partial \sigma_z}{\partial z} + \frac{\partial \tau_{xz}}{\partial x} + \frac{\partial \tau_{yz}}{\partial y} + b_z = 0 \tag{3.4}$$

The subsequent description of deduction of the spatial solution of the equilibrium equation is made in matrix notation. Also, the stress and the strain tensors are treated as vectors, following the law of conservation of linear momentum.

The Principle of Virtual Work is employed to solve the equilibrium equation in space. The work due to stress corresponds to the internal work and the work due to body forces and boundary superficial stresses corresponds to the external work. Considering Ω as domain and Γ as boundary of the analyzed problem, we have:

$$\int_{\Omega} \left\{\delta\varepsilon^*\right\}^T \{\dot{\sigma}\} d\Omega - \int_{\Omega} \left\{\delta u^*\right\}^T \{\dot{b}\} d\Omega - \int_{\Gamma} \left\{\delta u^*\right\}^T \{\dot{\tau}\} d\Gamma = 0 \tag{3.5}$$

where: $\left\{\delta\varepsilon^*\right\}$ are virtual strains compatible to displacements $\left\{\delta u^*\right\}$, $\{b\}$ are the body forces (in the domain), $\{\tau\}$ are the boundary superficial stresses and $\{\dot{x}\}$ is the time derivative of the variable *x*.

By definition:

$$\left\{u^*\right\} = [N]\left\{\bar{u}^*\right\} \tag{3.6}$$

$$\left\{\varepsilon^*\right\} = [B]\left\{\bar{u}^*\right\} \tag{3.7}$$

where: $\left\{u^*\right\}$ and $\left\{\varepsilon^*\right\}$ are virtual displacements and strains, respectively, [*N*] is the displacements interpolation matrix, [*B*] is the displacement-strain matrix and $\{\bar{u}\}$ is the displacement vector in the domain.

The stress-strain relation for this problem is based on the definition of the generalized effective stress, given as:

$$\left\{d\sigma'\right\} = \left[D^{ep}\right]\left\{d\varepsilon\right\} \tag{3.8}$$

where: $\left[D^{ep}\right]$ is the elastoplastic constitutive matrix and $\left\{d\varepsilon\right\}$ is the strain vector.

The constitutive matrix depends on which model is going to be applied for the proposed study. Different models can be chosen and in section 3.7 aspects regarding constitutive modeling are described.

There are circumstances in which the stress state of the porous medium may be affected by rock crystals or solids compressibility (Li et al, 1999). This compressibility can be considered in the formulation with the Biot parameter (α_b), defined by the following expression:

$$\alpha_b = 1 - \frac{\left\{m\right\}^T \left[D^{ep}\right] \left\{m\right\}}{9k_s} \tag{3.9}$$

where: k_s is the bulk modulus of solids or rock crystals.

For isotropic, homogeneous and linear elastic media, the Biot parameter is defined as $\alpha_b = 1$. This suggests that the compressibility of the solid matrix does not interfere in the porous medium behavior in these conditions. However, this parameter value may vary for other constitutive models, such as elastoplastic. Thus, the consideration of solids compressibility is important to accurately reproduce solid matrix phenomenon.

With the solids compressibility consideration, the general expression for the effective stress principle is defined, as Eq. (3.10):

$$\left\{\sigma'\right\} = \left\{\sigma\right\} - \alpha_b \left\{m\right\} p \tag{3.10}$$

where: $\left\{\sigma'\right\}$ is the effective stress vector, $\left\{\sigma\right\}$ is the total stress vector, α_b is the Biot parameter, $\left\{m\right\}^T = \left\{1 \quad 1 \quad 1 \quad 0 \quad 0 \quad 0\right\}$ for a 3D analysis and p is the fluid pressure (for a saturated analysis).

With the substitution of Eqs. (3.6), (3.7) and (3.10) into Eq. (3.5), the spatially-solved equilibrium equation may be written as:

$$\left[\int_{\Omega}[B]^T[D][B]d\Omega\right]\{\dot{u}\}+\left[\int_{\Omega}[B]^T\alpha_b\{m\}\left[N^P\right]d\Omega\right]\{\dot{p}\}=\int_{\Omega}[N]^T\{\dot{b}\}d\Omega+\int_{\Gamma}[N]^T\{\dot{\tau}\}d\Gamma \quad (3.11)$$

where: $\left[N^P\right]$ is the fluid pressure interpolation matrix.

The matrixes that represent the solved equilibrium equation are assembled and may be written as:

$$[K]\{\dot{u}\}+[C]\{\dot{p}\}=\{\dot{F}\} \quad (3.12)$$

where:

$[K]=\int_{\Omega}[B]^T[D][B]d\Omega$, stiffness matrix, (3n x 3n), $[F][L]^{-1}$;

$\{\dot{u}\}$, nodal displacement rate vector, (3n x 1), $[L][T]^{-1}$;

$[C]=\int_{\Omega}[B]^T\alpha_b\{m\}\left[N^P\right]d\Omega$, solids-fluid coupling matrix, (3n x m), $[L]^{-2}$;

$\{\dot{p}\}$, nodal fluid water pressure rate vector, (m x 1), $[F][L]^{-2}[T]^{-1}$;

$\{\dot{F}\}=\int_{\Omega}[N]^T\{\dot{b}\}d\Omega+\int_{\Gamma}[N]^T\{\dot{\tau}\}d\Gamma$, external forces rate vector, (3n x 1), $[F][T]^{-1}$.

The dimension of the matrixes and vectors corresponds to three-dimensional element analyses, with *n* nodes in which the displacements are calculated (*3n* degrees of freedom for displacements) and *m* nodes in which the fluid pressure is calculated (*m* degrees of freedom for fluid pressure).

3.3 SPATIAL SOLUTION OF THE MASS CONSERVATION EQUATION

The mass conservation law description involves both liquid and solid phases. Compaction and subsidence problems, by its physics, are hydro-mechanical and, therefore, changes in the solid matrix of the reservoir reflect directly in storage and flow of fluids. Besides, solids mass variation should also be considered, given its effect in reservoir displacements.

Regarding this consideration, in a given control volume, the real velocity to which the fluid is subjected depends on fluid velocity due to percolation (Darcy's law) and also depends

on the velocity of the solids (Li et al, 1999, Schrefler & Scotta, 2001). The real velocity can be expressed in indicial notation as:

$$\dot{U}_i = \dot{u}_i + \frac{w_i^f}{\theta} \tag{3.13}$$

where: $\dot{U}_i$ is the real fluid velocity vector, $\dot{u}_i$ is the velocity of the solids vector and w_i^f is the fluid velocity due to percolation vector.

The real fluid velocity assumption implies on taking into account the effects of porosity changes in the porous medium. The velocity of the solids $\dot{u}_i$ is related to the displacements in the reservoir. Thus, it may be inferred that there is no need of expanding the porosity term in the proposed formulation. This is the same approach used by Cordão Neto (2005).

It is important to define the expression for the volumetric fluid content, which is associated with porosity as shown in Eq. (3.14):

$$\theta = nS^f \tag{3.14}$$

where: θ is the volumetric fluid content of the medium, *n* is the porosity of the medium and S^f is the degree of saturation of the medium.

In reservoir engineering, it is common to use the symbol ϕ to make reference to medium porosity. So, in this formulation, the porosity is represented as ϕ.

The fluid mass conservation equation is presented in Eq. (3.15). The density changes due to fluid compressibility during the flow and the real fluid velocity are considered in this formulation. Once more, it is emphasized that only liquids fluid are taken into account in the formulation.

$$\frac{\partial}{\partial t}\left(\theta\rho^f\right) + \frac{\partial}{\partial x_i}\left(\theta\rho^f\dot{U}_i\right) = 0 \tag{3.15}$$

where: θ is the volumetric water content, ρ^f is the fluid density and $\dot{U}_i$ is the real fluid velocity.

When expanding the terms of the fluid mass conservation equation, it should be taken into account that the porosity must not be derivate. With this, only the changes in the degree of saturation are considered. The formulation for fluid mass conservation is finally shown in Eq. (3.16):

$$\phi S^f \frac{\partial \rho^f}{\partial t} + \rho^f \phi \frac{\partial S^f}{\partial t} + \phi S^f \rho^f \frac{\partial}{\partial x_i}\left(\dot{u}_i + \frac{w_i^f}{\theta}\right) + \phi S^f \dot{U}_i \frac{\partial \rho^f}{\partial x_i} + \rho^f \dot{U}_i \phi \frac{\partial S^f}{\partial x_i} = 0 \qquad (3.16)$$

where: θ is the volumetric fluid content, ρ^f is the fluid density, ϕ is the porosity of the medium, S^f is the degree of saturation, $\dot{u}_i$ is the solids velocity, w_i^f is the fluid velocity due to percolation (Darcy's law) and $\dot{U}_i$ is the real fluid velocity.

The solids mass conservation equation may be presented as (Li et al, 1999, Schrefler & Scotta, 2001):

$$\frac{\partial}{\partial t}\left[(1-\phi)\rho^s\right] + \frac{\partial}{\partial x_i}\left[(1-\phi)\rho^s \dot{u}_i\right] = 0 \qquad (3.17)$$

where: ϕ is the material porosity, ρ^s is the solids density and $\dot{u}_i$ is the solids velocity vector.

Considering the complete mass conservation requires both fluid and solids mass balance (Li et al, 1999, Schrefler & Scotta, 2001). In order to set this, it is necessary to establish a way of analyzing fluids and solids mass conservation together.

It is possible to balance the volume of solids and the volume of fluid within a finite element, in a total element volume approach. For that reason, in order to assemble a single mass conservation equation, fluid and solids mass conservation equations are converted into volume (Li et al, 1999).

Analyzing the fluids mass conservation equation with a volume approach is possible when dividing it by $\rho^f S^f$, as shown:

$$\frac{(\phi S_r)}{\rho^f S^f}\frac{\partial \rho^f}{\partial t} + \frac{\rho^f \phi}{\rho^f S^f}\frac{\partial S^f}{\partial t} + \frac{(\phi S_r)\rho^f}{\rho^f S^f}\frac{\partial \dot{u}_i}{\partial x_i} + \frac{\left(\phi S^f\right)\rho^f}{\rho^f S^f \left(\phi S^f\right)}\frac{\partial \dot{w}_i^f}{\partial x_i} + \frac{\left(\phi S^f\right)\dot{U}_i}{\rho^f S^f}\frac{\partial \rho^f}{\partial x_i} + \frac{\rho^f \dot{U}_i \phi}{\rho^f S^f}\frac{\partial S^f}{\partial x_i} = 0 \qquad (3.18)$$

where: θ is the volumetric fluid content, ρ^f is the fluid density, S^f is the degree of saturation, ϕ is the porosity of the medium, $\dot{u}_i$ is the solids velocity, w_i^f is the fluid velocity due to percolation (Darcy's law) and $\dot{U}_i$ is the real fluid velocity.

The solids mass conservation equation is converted to a volume approach when divided by ρ^s. Assuming this and expanding this equation, we have:

$$\frac{(1-\phi)}{\rho^s}\frac{\partial \rho^s}{\partial t}+(1-\phi)\frac{\partial \dot{u}_i}{\partial x_i}+\frac{(1-\phi)}{\rho^s}\dot{u}_i\frac{\partial \rho^s}{\partial x_i}=0 \tag{3.19}$$

where: ϕ is the porosity of the rock, ρ^s is the solids density and $\dot{u}_i$ is the solids velocity.

Assembling both fluid and solids mass conservation equations (Eqs. (3.18) and (3.19)) and substituting Eq. (3.14), we have:

$$\begin{aligned}&\frac{(1-\phi)}{\rho^s}\frac{\partial \rho^s}{\partial t}+(1-\phi)\frac{\partial \dot{u}_i}{\partial x_i}+\frac{(1-\phi)}{\rho^s}\dot{u}_i\frac{\partial \rho^s}{\partial x_i}+\\&\frac{\theta}{\rho^f S^f}\frac{\partial \rho^f}{\partial t}+\frac{\rho^f\phi}{\rho^f S^f}\frac{\partial S^f}{\partial t}+\frac{\theta\rho^f}{\rho^f S^f}\frac{\partial \dot{u}_i}{\partial x_i}+\frac{\theta\rho^f}{\rho^f S^f\theta}\frac{\partial \dot{w}_i^f}{\partial x_i}+\frac{\theta\dot{U}_i}{\rho^f S^f}\frac{\partial \rho^f}{\partial x_i}+\frac{\rho^f\dot{U}_i\phi}{\rho^f S^f}\frac{\partial S^f}{\partial x_i}=0\end{aligned} \tag{3.20}$$

There are laws which define the variation of the density of liquid fluids (Peaceman, 1977; Rosa et al., 2006) and the density of solids (Li et al., 1999). They are expressed in Eqs. (3.21) and (3.22), respectively.

$$\frac{d\rho^f}{\rho^f}=\frac{1}{k_f}dp \tag{3.21}$$

where: ρ^f is the fluid density, k_f is the bulk modulus of the fluid and p is the fluid pressure.

$$\frac{(1-\phi)}{\rho^s}\frac{D\rho^s}{Dt}=\left[\frac{(\alpha_b-\phi)}{k_s}\frac{Dp^R}{Dt}-(1-\alpha_b)\dot{u}_{i,i}\right] \tag{3.22}$$

where: ρ^s is the solids density, k_s is the bulk modulus of rock crystals, α_b is the Biot parameter, ϕ is the porosity of the rock and p^R is the pressure of the fluids.

This pressure of the fluids p^R is used in cases in which there are two fluid phases within the porous medium, gas and liquid. In these situations, the pressure of the fluids may be defined by the following expression.

$$p^R = \chi_s p + (1-\chi_s)\, p^g \tag{3.23}$$

where: p^R is the pressure of the fluids, χ_s is a parameter related to the degree of saturation of the liquid phase (for a porous medium fully saturated with liquid, $\chi_s = 1$) and p^g is the gas pressure.

For this particular study, the medium is assumed to be fully saturated with liquid. Therefore, $\chi_s = 1$ and, with this, $p^R = p$.

The degree of saturation is:

$$dS^f = \frac{\partial S^f}{\partial p} dp \tag{3.24}$$

where: S^f is the degree of saturation and p is the fluid pressure.

As defined previously, it is made the assumption of a fully liquid saturated medium. Therefore, there is no variation of the degree of saturation and it may be established that $S_r = 1$ and $dS_r / dp = 0$.

Substituting the Eqs. (3.21), (3.22) and (3.23) and knowing that $S^f = 1$ and, therefore, $p^R = p$ and $dS^f / dp = 0$, in Eq. (3.20), we have:

$$\begin{aligned} &\frac{(\alpha_b - \phi)}{k_s}\frac{\partial p}{\partial t} + \frac{(\alpha_b - \phi)}{k_s}\dot{u}_i \frac{\partial p}{\partial x_i} - (1-\alpha_b)\frac{\partial \dot{u}_i}{\partial x_i} + (1-\phi)\frac{\partial \dot{u}_i}{\partial x_i} + \frac{\phi}{k_f}\frac{\partial p}{\partial t} + \phi \frac{\partial \dot{u}_i}{\partial x_i} + \frac{\partial w_i^f}{\partial x_i} \\ &+ \frac{\phi \dot{U}_i}{k_f}\frac{\partial p}{\partial x_i} = 0 \end{aligned} \tag{3.25}$$

Putting the similar terms together, we have:

$$\left[\frac{(\alpha_b - \phi)}{k_s} + \frac{\phi}{k_f}\right]\frac{\partial p}{\partial t} + \left[\frac{(\alpha_b - \phi)}{k_s}\dot{u}_i + \frac{\phi \dot{U}_i}{k_f}\right]\frac{\partial p}{\partial x_i} + \alpha_b \frac{\partial \dot{u}_i}{\partial x_i} + \frac{\partial w_i^f}{\partial x_i} = 0 \tag{3.26}$$

The spatial solution for the mass conservation equation via FEM can be made with the weighted residual method. More specifically, Galerkin method is employed in this particular situation (Zienkiewicz, 1977). Using this method, one can proceed with the solution of Eq. (3.26):

$$\int_{\Omega}\left(N^{P}\right)_{j}^{T}\left\{\left[\frac{(\alpha_b-\phi)}{k_s}+\frac{\phi}{k_f}\right]\frac{\partial p}{\partial t}+\left[\frac{(\alpha_b-\phi)}{k_s}\dot{u}_i+\frac{\phi\dot{U}_i}{k_f}\right]\frac{\partial p}{\partial x_i}+\alpha_b\frac{\partial \dot{u}_i}{\partial x_i}+\frac{\partial w_i^f}{\partial x_i}\right\}d\Omega=0 \tag{3.27}$$

Eq. (3.27) may be represented in matrix notation as:

$$\int_{\Omega}\left[N^{P}\right]^{T}\left(\left[\frac{(\alpha_b-\phi)}{k_s}+\frac{\phi}{k_f}\right]\frac{\partial p}{\partial t}+\left[\frac{(\alpha_b-\phi)}{k_s}\{\dot{u}\}+\frac{\phi\{\dot{U}\}}{k_f}\right]\nabla.p+\alpha_b\nabla.\{\dot{u}\}+\nabla.\{w^f\}\right)d\Omega=0 \tag{3.28}$$

Considering the following mathematical identity:

$$f\nabla\cdot g=\nabla\cdot(fg)-\nabla\cdot(f)g \tag{3.29}$$

For the highlighted term of Eq. (3.28), we have:

$$\int_{\Omega}\left[N^{P}\right]^{T}\nabla\cdot\{w^f\}d\Omega=\int_{\Omega}\nabla\cdot\left(\left[N^{P}\right]^{T}\{w^f\}\right)d\Omega-\int_{\Omega}\left(\nabla\cdot\left[N^{P}\right]^{T}\right)\{w^f\}d\Omega \tag{3.30}$$

The highlighted term of Eq. (3.30) should be treated with the divergence theorem. Therefore, we have:

$$\int_{\Omega}\nabla\cdot\left[\left[N^{P}\right]^{T}\{w^f\}\right]d\Omega=\int_{\Gamma}\left[N^{P}\right]^{T}\{w^f\}\cdot\{n\}d\Gamma \tag{3.31}$$

where: $\{n\}$ is normal vector, Ω is the domain and Γ is the boundary of the studied problem.

The boundary of the problem can be divided into two parts. In the first one (Γ_1), essential boundary conditions are prescribed. In the second one (Γ_2), natural boundary conditions are prescribed.

$$\int_{\Gamma}\left[N^{P}\right]^{T}\{w^f\}\cdot\{n\}d\Gamma=\int_{\Gamma_1}\left[N^{P}\right]^{T}\{w^f\}\cdot\{n\}d\Gamma+\int_{\Gamma_2}\left[N^{P}\right]^{T}\{w^f\}\cdot\{n\}d\Gamma \tag{3.32}$$

For this mass conservation equation term, the boundary conditions are:

- Γ_1 : prescribed values of pore pressure

$$p = \bar{p} \tag{3.33}$$

- Γ_2 : prescribed values of fluid discharge

$$\left\{\dot{w}^f\right\}\{n\}^T = \bar{q} \tag{3.34}$$

In Γ_1, pore pressures are considered null and, therefore, so is velocity. In Γ_2, there is a prescribed value for fluid discharge ($\bar{q}$). Thus for this term (Eq. (3.31)):

$$\int_{\Gamma}\left[N^P\right]^T\left\{\dot{w}^f\right\}\{n\}^T d\Gamma = \int_{\Gamma_2}\left[N^P\right]^T \bar{q} d\Gamma \tag{3.35}$$

For the fluid mass conservation equation solution, some relations must be taken into account (Peaceman, 1977). The fluid velocity due to percolation (Darcy's law) (Eq. (3.36)) is given as:

$$\left\{\dot{w}^f\right\} = -\frac{[K]}{\mu}\left(\nabla p - \rho^f \{g\}\nabla y\right) \tag{3.36}$$

where: [*K*] is the intrinsic permeability tensor, μ is the dynamic viscosity of the fluid, {*g*} is the gravity vector and *y* is the direction coincident with gravity direction in the coordinate system used.

There are some expressions which define some variables of the mass conservation equation. Those are:

$$p = \left[N^P\right]\bar{p} \tag{3.37}$$

$$u = \left[N^P\right]\bar{u} \tag{3.38}$$

$$\left(\nabla.\left[N^P\right]\right)\{p\} = \left[B^P\right]\{p\} \tag{3.39}$$

where: $\left[N^P\right]$ is the fluid pressure interpolation matrix and $\left[B^P\right]$ is equivalent to the derivatives of fluid pressure shape function.

Taking into account all the considerations already mentioned, the spatial solution for the mass conservation equation via FEM (using Galerkin method) is:

$$\left[\int_{\Omega}\left[N^{P}\right]^{T}\left[\frac{(\alpha_b-\phi)}{k_s}+\frac{\phi}{k_f}\right]\left[N^{P}\right]d\Omega\right]\{\dot{p}\}+\left[\int_{\Omega}\left[N^{P}\right]^{T}\alpha_b\{m\}^{T}[B]d\Omega\right]\{\dot{u}\}+$$
$$\left[\int_{\Omega}\left[N^{P}\right]^{T}\left[\frac{(\alpha_b-\phi)}{k_s}\{\dot{u}\}+\frac{\phi}{k_f}\left(\{\dot{u}\}+\frac{\{w^{f}\}}{\phi}\right)\right]\left[B^{P}\right]d\Omega+\int_{\Omega}\left[B^{P}\right]^{T}\frac{[K]}{\mu}\left[B^{P}\right]d\Omega\right]\{p\}= \quad (3.40)$$
$$\left[\int_{\Omega}\left[B^{P}\right]^{T}\frac{[K]}{\mu}\rho^{f}\{g\}(\nabla.y)d\Omega\right]-\int_{\Gamma_2}\left[N^{P}\right]^{T}\bar{q}d\Gamma$$

The matrixes that represent the solved mass conservation equation are assembled and may be written as:

$$[M]\{\dot{p}\}+[L]\{\dot{u}\}+[R]\{p\}=\{Q\} \quad (3.41)$$

where:

$[M]=\int_{\Omega}\left[N^{P}\right]^{T}\left[\frac{(\alpha_b-\phi)}{k_s}+\frac{\phi}{k_f}\right]\left[N^{P}\right]d\Omega$, mass matrix, (m x m), $[M]^{-1}[L]^{4}[T]^{2}$;

$\{\dot{p}\}$, nodal fluid pressure rate vector, (m x 1), $[M][L]^{-1}[T]^{-3}$;

$[L]=\int_{\Omega}\left[N^{P}\right]^{T}\alpha_b\{m\}^{T}[B]d\Omega$, fluid-solids coupling matrix, (m x 3n), $[L]^{2}$;

$\{\dot{u}\}$, nodal displacements rate vector, (3n x 1), $[L][T]^{-1}$;

$[R]=\int_{\Omega}\left[N^{P}\right]^{T}\left[\frac{(\alpha_b-\phi)}{k_s}\{\dot{u}\}+\frac{\phi}{k_f}\left(\{\dot{u}\}+\frac{\{w^{f}\}}{\phi}\right)\right]\left[B^{P}\right]d\Omega+\int_{\Omega}\left[B^{P}\right]^{T}\frac{[K]}{\mu}\left[B^{P}\right]d\Omega$, flow matrix, (m x m), $[M]^{-1}[L]^{4}[T]$;

$\{p\}$, nodal fluid pressure vector, (m x 1), $[M][L]^{-1}[T]^{-2}$;

$\{Q\}=\left[\int_{\Omega}\left[B^{P}\right]^{T}\frac{[K]}{\mu}\rho_f\{g\}(\nabla.y)d\Omega\right]-\int_{\Gamma_2}\left[N^{P}\right]^{T}\bar{q}d\Gamma$, external discharges vector, (m x 1), $[L]^{3}[T]^{-1}$.

The term with fluid bulk modulus (k_f), correspondent to fluid compressibility, represents pore compressibility in this case, considering the medium is fully saturated. Analogously, the term with solids bulk modulus (k_s) also appears in the formulation, being representative of the solid matrix compressibility. Together, these two terms express the total

compressibility of the medium. It is interesting to highlight that in the deduction of this formulation, these terms have naturally been gathered, as seen in mass and flow matrixes.

3.4 EQUATION SYSTEM

The spatial solution of equilibrium and mass conservation equations may be put together in order to assemble a system of equations. This system permits the time solution of the problem at a later stage. Considering both Eqs. (3.12) and (3.41), we have:

$$\begin{bmatrix} 0 & 0 \\ 0 & [R] \end{bmatrix} \begin{Bmatrix} \{u\} \\ \{p\} \end{Bmatrix} + \begin{bmatrix} [K] & [C] \\ [L] & [M] \end{bmatrix} \begin{Bmatrix} \{\dot{u}\} \\ \{\dot{p}\} \end{Bmatrix} = \begin{Bmatrix} \{\dot{F}\} \\ \{Q\} \end{Bmatrix} \tag{3.42}$$

Then, with this, the system of equations may be expressed by:

$$[W]\{x\} + [Y]\{\dot{x}\} = \{Z\} \tag{3.43}$$

where:

$$\{x\} = \begin{Bmatrix} \{u\} \\ \{p\} \end{Bmatrix} \tag{3.44}$$

$$\{\dot{x}\} = \begin{Bmatrix} \{\dot{u}\} \\ \{\dot{p}\} \end{Bmatrix} \tag{3.45}$$

$$\{Z\} = \begin{Bmatrix} \{\dot{F}\} \\ \{Q\} \end{Bmatrix} \tag{3.46}$$

3.5 TIME SOLUTION FOR THE EQUATION SYSTEM

The proposed formulation has its solution established not only spatially, but also in time. For this, the equation system correspondent to the spatial solution of the problem is solved in time. With this methodology, even though the solution is stationary, it is equivalent to the transient problem.

Firstly, a vector of unknowns $\{x\}$ is evaluated in time for a Δt time interval. This vector is considered to have linear variation, as shown in Eq. (3.47):

$$\{x\}_{t+\alpha\Delta t} = (1-\alpha)\{x\}_t + \alpha\{x\}_{t+\Delta t} \tag{3.47}$$

where: α is the controlling parameter for the integration scheme and $\{x\}_t$ and $\{x\}_{t+\Delta t}$ are the vector of unknowns at the initial time stage and the calculated time stage, respectively.

The time derivative for the vector of unknowns can be defined as:

$$\{\dot{x}\}_{t+\Delta t} = \frac{\{x\}_{t+\Delta t} - \{x\}_t}{\Delta t} \tag{3.48}$$

Thus, Eq. (3.43) is evaluated at $t + \alpha\Delta t$ time stage (Eq. (3.49)):

$$[W]_{t+\alpha\Delta t}\{x\}_{t+\alpha\Delta t} + [Y]_{t+\alpha\Delta t}\{\dot{x}\}_{t+\alpha\Delta t} = \{Z\}_{t+\alpha\Delta t} \tag{3.49}$$

So, substituting Eqs. (3.47) and (3.48) in Eq. (3.49), the solution of the problem is obtained in terms of the increment of the vector of unknowns, $\{\Delta x\}$:

$$\left[\Delta t\alpha[W]_{t+\alpha\Delta t} + [Y]_{t+\alpha\Delta t}\right]\{\Delta x\} = \Delta t\{Z\}_{t+\alpha\Delta t} - \Delta t[W]_{t+\alpha\Delta t}\{x\}_t \tag{3.50}$$

where:

$$[W]_{t+\alpha\Delta t} = \left[W\left(\{x\}_{t+\alpha\Delta t}\right)\right] = \left[W\left((1-\alpha)\{x\}_t + \alpha\{x\}_{t+\Delta t}\right)\right] \tag{3.51}$$

$$[Y]_{t+\alpha\Delta t} = \left[Y\left(\{x\}_{t+\alpha\Delta t}\right)\right] = \left[Y\left((1-\alpha)\{x\}_t + \alpha\{x\}_{t+\Delta t}\right)\right] \tag{3.52}$$

$$\{Z\}_{t+\alpha\Delta t} = \left\{Z\left(\{x\}_{t+\alpha\Delta t}\right)\right\} = \left\{Z\left((1-\alpha)\{x\}_t + \alpha\{x\}_{t+\Delta t}\right)\right\} \tag{3.53}$$

In equations (3.51), (3.52) and (3.53), matrixes [W] and [Y] and vector {Z} have their average evaluated between t and $t + \Delta t$. Vector $\{x\}_{t+\alpha\Delta t}$ is unknown at $t + \Delta t$, being necessary appropriate techniques for the problem solution.

3.6 ASPECTS REGARDING ADVECTIVE FLUX

Observing the proposed formulation, it can be noticed that certain terms in the flow matrix [*R*] (Eq. (3.41)) use solids and fluid velocity. These terms characterize advective flux, the macroscopic movement of fluid or particles through a porous medium in time.

The solution of problems with advective flux can be made with the Finite Differences Method (FDM). Different solution approaches can be performed, using the derivative form of the equation terms.

The equation solution is made in a specific domain, which is discretized in time in this particular studied case. The time derivatives are based on this, with the reference value being calculated with advanced, delayed or centered derivatives.

Different methods of problem solution with FDM can be performed. The main concern in these is numerical instability. Thus, different approaches have been developed in order to

solve this issue, such as differences in advance for time and delay for space method (Eq. (3.54)), Euler method (Eq. (3.55)), Lax method (Eq. (3.56)) and Lax-Wendroff method (Eq. (3.57)).

$$c_k^{n+1} = c_k^n - C\left(c_k^n - c_{k-1}^n\right) \tag{3.54}$$

$$c_k^n = \frac{1}{2}\left(c_{k+1}^n + c_{k-1}^n\right) \tag{3.55}$$

$$c_k^{n+1} = \frac{1}{2}\left(c_{k+1}^n + c_{k-1}^n\right) - \frac{\mathrm{C}}{2}\left(c_{k+1}^n - c_{k-1}^n\right) \tag{3.56}$$

$$c_k^{n+1} = c_k^n - \frac{C}{2}\left(c_{k+1}^n - c_{k-1}^n\right) + \frac{\mathrm{C}^2}{2}\left(c_{k+1}^n - 2c_k^n + c_{k-1}^n\right) \tag{3.57}$$

where: c is the concentration (for contaminant transportation evaluation), n is the evaluated time stage, k is the evaluated space and C is the Courant number, defined as $\mathrm{C} = \mathrm{v}\Delta\mathrm{t}/\Delta\mathrm{x}$.

The presented equations refer to contaminant transportation problems, being calculated in terms of concentration. However, these expressions can be used for other advective flux problems, such as the studied in this research.

The differences in advance for time and delay for space method has an associated error of the order of *dx*. All other mentioned methods have their solutions completely stable when the ratio between physical and numerical distances of transportation is equal 1. This ratio is known as Courant number (*C*). This number is in all expressions which define these methods solutions and it is exclusively used for guaranteeing numerical stability of each method (Jesus & Cavalcante, 2011).

Another important information is related to the Lax and Lax-Wendroff methods. These methods have in their formulation a second-order term. This kind of term represents diffusive behavior during transportation. Therefore, these methods do not solve only advective flux problems. This could influence responses, causing a diffusion phenomenon non-correspondent to advective flux. In Lax-Wendroff, oscillations can be also observed. In general, this oscillation occurs in a certain way that the effect of diffusion is compensated.

Jesus & Cavalcante (2011) show differences in advance and Lax-Wendroff methods as approaches for the solution of advective flux problems. In Figure 3.1 and Figure 3.2, their

results are presented, where the numerical instability is clearly registered, with dissipation of contaminant concentration in a simulation which should represent only the advective phenomenon. Also, the diffusion and oscillations characteristics for Lax-Wendroff can be noticed.

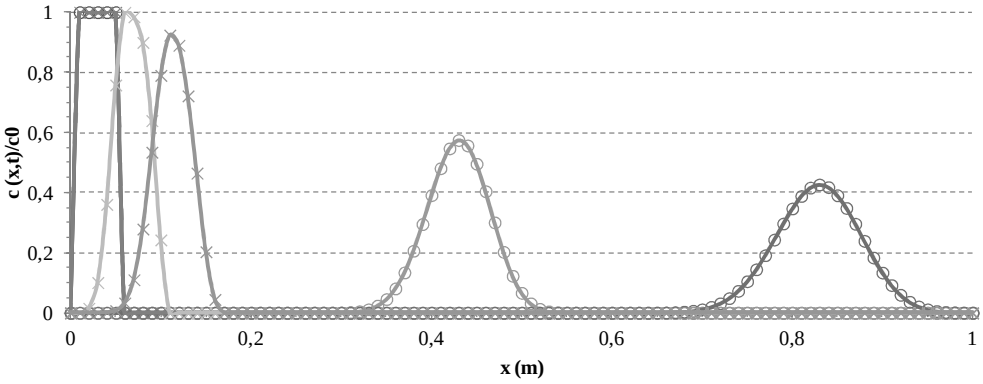

Figure 3.1 - Results of advective flux simulation in two different soils – Differences in advance method (Jesus & Cavalcante, 2011).

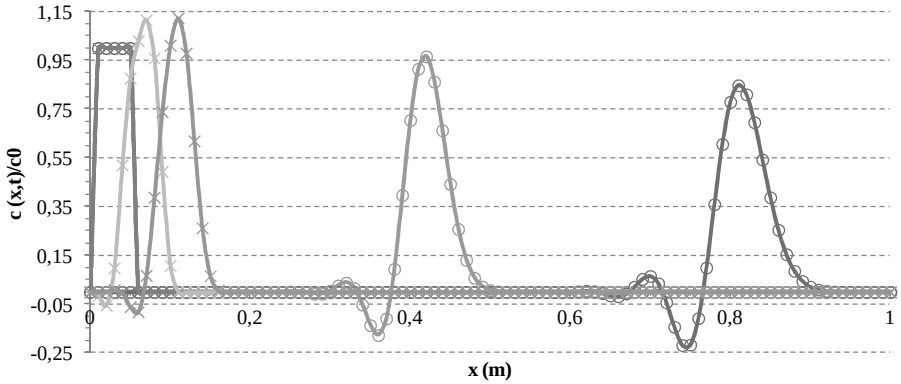

Figure 3.2 - Results of advective flux simulation in two different soils – Lax-Wendroff method (Jesus & Cavalcante, 2011).

Another possible approach for the solution of advective flux equations is using finite element method (FEM). Some solutions are discussed in Dhawan et al. (2011) and Nonaka & Nakayama (1998), both suggesting the use of interpolating functions to perform the solutions. However, their computational cost may difficult their application.

Considering these aspects, the method of discretization in time presented for the formulation complies with the expected results. The small effects of instability observed do not interfere in the problem solution.

3.7 CONSTITUTIVE MODELS

Performing any stress-strain analyses requires the understanding of the material performance. In order to represent the behavior of the material, it is necessary to use models which can reproduce the specific characteristics of the material. These are known as constitutive models.

Constitutive models are employed in mechanical behavior analyses of geologic materials. There are different models used to reproduce the stress-strain relations of a material. In this research, two different models are applied, linear elastic and modified Cam-clay. The modified Cam-clay is described in this section.

These models were chosen to represent the studied porous media, the reservoir rocks. The phenomena reproduced in this study via numerical analysis are compaction and subsidence.

In these processes, the rock is subjected to compression stress paths. Therefore, there is need of constitutive models which can be adequate to capture the specificities of this kind of stress. The modified Cam-clay model is believed to be appropriated for the referred circumstance.

3.7.1 MODIFIED CAM-CLAY

Constitutive modeling was enhanced in the 1960s by Roscoe and collaborators in Cambridge University. The critical state models were the suggested approach to complement the theory of plasticity for soils. With this, many concepts were put together in the same theory:

- Relationship between void ratio and effective stress;
- Plastic strain occurrence on different stress paths, shear and compression included;
- Soil critical state;
- Failure criterion and
- Softening and hardening.

These concepts are united in the Cam-clay model, an elastoplastic model of soil behavior, developed to describe the mechanical responses of a saturated, normally consolidated clay, Cambridge clay, during triaxial tests (undrained and drained).

The physical basis of this model is well-founded and, nowadays, with the appropriate parameters, Cam-clay model is generalized for different types of soils and rocks.

Any material which Cam-clay model represents only reaches critical state after passing through successive states of yielding, during which the material hardens. The continuous

yielding eventually leads the material to the critical state, in which there is no occurrence of volumetric strains, as previously stated (Britto & Gunn, 1987).

The shape of the yield surface depends on the material. Different shapes could be assumed, but specifically for the modified Cam-clay, it is established an elliptical surface. This shape of surface is deducted by hypotheses regarding the plastic work dissipation.

The expression which describes the yielding locus for the modified Cam-clay model is:

$$F\left(p', q, p'_0\right) = M^2 p'^2 - M^2 p'_0\, p' + q^2 \tag{3.58}$$

where: F is the yielding function, p' is the effective mean stress, q is the deviator stress, p'_0 is the preconsolidation stress and M is the inclination of the projection of the CSL.

The yielding surface is represented in Figure 3.3 with all three axes (p', q and v). The projections of the yielding surface and the critical state line are represented in Figure 3.4 and Figure 3.5, respectively.

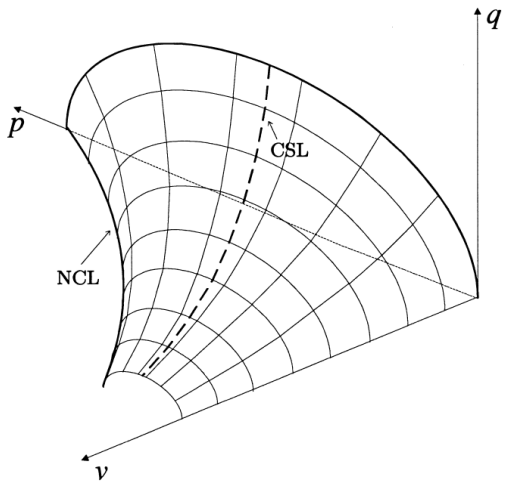

Figure 3.3 - Yielding surface for modified Cam-clay model (Callari et al., 1998).

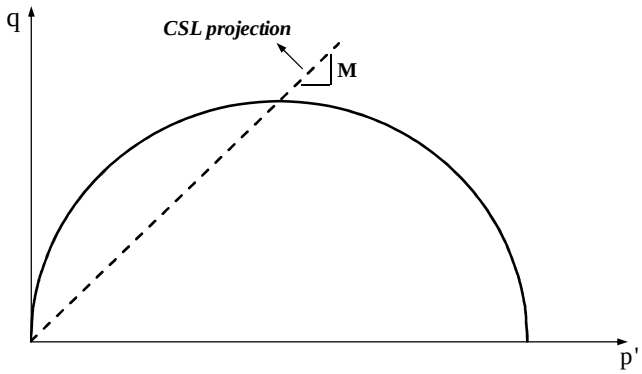

Figure 3.4 - Yielding locus for modified Cam-clay model: projection of the yielding surface (plane *p' versus q*).

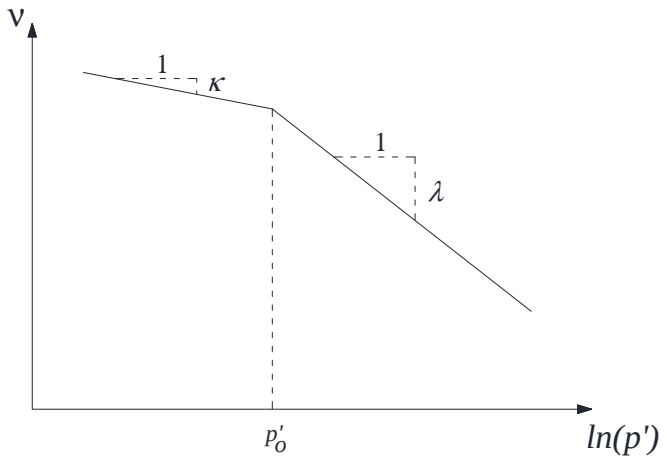

Figure 3.5 - Yielding locus for modified Cam-clay model: projection of the yielding surface (plane ν *versus* ln *p'*).

The modified Cam-clay model is said to have an associated flow. In practical terms, this means the plastic potential surface and the yielding surface have the same shape and they are coincident. Therefore, the plastic flow vector, which is normal to the plastic potential surface, follows the derivate of the plastic potential function (same direction of the yielding function derivate).

The plastic potential function is described by Eq. (3.59):

$$G = F\left(p', q, p'_0\right) = M^2 p'^2 - M^2 p'_0\, p' + q^2 \tag{3.59}$$

where: G is the plastic potential function, F is the yielding function, p' is the effective mean stress, q is the deviator stress, p'_0 is the preconsolidation stress and M is the inclination of the projection line of the CSL.

Defining a constitutive model requires an appropriate hardening law. The hardening effect makes the yielding surface expand, making it adequate to the imposed new stress state. With the internal variables of stress and strain, it is possible to define the stress-strain state conditions to which the material is subjected in present time and how they should evolve. This permits the maintenance of the yielding surface format adequately, with changes only in these internal variables.

When considering a case of volumetric compression, followed by decompression in an isotropic loading, it is fair to say that the expected behavior of the soil sample is portrayed by the represented in Figure 3.6.

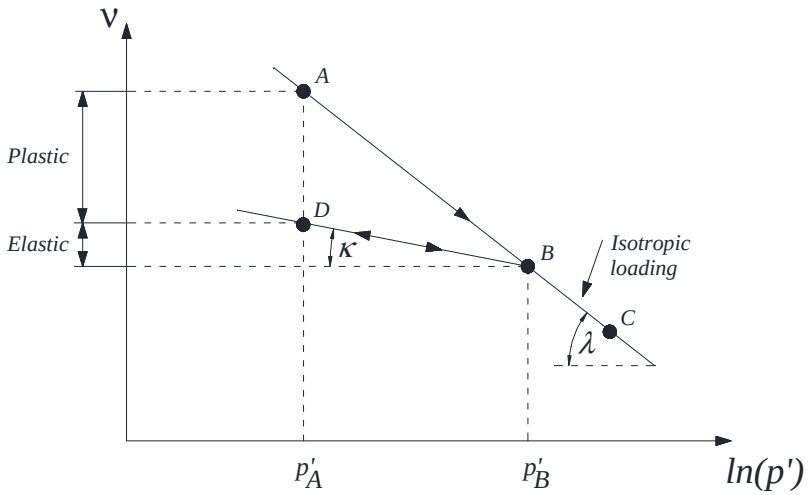

Figure 3.6 - Consolidation behavior in ν - *ln p*' space (modified Desai & Siriwardane, 1984).

During decompression (from B to D), the stress-strain relation is elastic and during compression (from A to B), there are elastic and plastic strains. The strains, represented by void ratio variation, and the stress may have its relation expressed by Eqs. (3.60) and (3.61).

$$de = -\lambda \frac{dp'}{p'_0} \tag{3.60}$$

where: *de* is the void ratio increment, λ is the inclination of the compression segment, *dp*' is the increment of effective mean stress and p'_0 is the preconsolidation stress.

$$de^e = -\kappa \frac{dp'}{p'_0} \tag{3.61}$$

where: de^e is the elastic component of the incremental void ratio and κ is the inclination of the decompression segment.

Defining the volumetric strain of a soil sample, we have:

$$d\varepsilon_v = -\frac{de}{1+e_0} \tag{3.62}$$

where: $d\varepsilon_v$ is the volumetric strain component, *de* is the void ratio increment and e_0 is the initial void ratio.

Substituting Eqs. (3.60) and (3.61) on Eq. (3.62), the volumetric plastic strain may be defined as:

$$d\varepsilon_v^p = -\frac{de^p}{1+e_o} = -\frac{de - de^e}{1+e_o} = \frac{(\lambda-\kappa)}{1+e_o}\frac{dp'_0}{p'_0} \tag{3.63}$$

where: $d\varepsilon_v^p$ is the volumetric strain component in plastic strains and de^p is the plastic component of the incremental void ratio.

Defining the hardening law in this case may be simple when considering the internal variables of stress and strain as p_0 and ε_v^p, respectively. Therefore, the hardening modulus may be defined, as shown in Eq. (3.64).

$$\mathrm{H} = \frac{1+e_0}{(\lambda-\kappa)}\, p'_0 \tag{3.64}$$

where: H is the hardening modulus, e_0 is the initial void ratio, λ is the inclination of the compression segment, κ is the inclination of the decompression segment and p'_0 is the preconsolidation stress.

Finally, the plastic strain potential of the studied porous medium soil may be defined. Eq. (3.65) represents the flow rule:

$$\left\{d\varepsilon^P\right\} = \chi\left\{\frac{\partial G}{\partial \sigma}\right\} \tag{3.65}$$

where: $d\varepsilon^P$ is the plastic strain increment, χ is the plastic multiplier and $\left\{\frac{\partial G}{\partial \sigma}\right\}$ is the projection of the vector normal to the potential plastic surface in stress space.

A basic hypothesis in Plasticity Theory is strain additive decomposition, defined as:

$$\left\{d\varepsilon\right\} = \left\{d\varepsilon^e\right\} + \left\{d\varepsilon^p\right\} \tag{3.66}$$

where: $\left\{d\varepsilon^e\right\}$ is the elastic strain vector increment and $\left\{d\varepsilon^p\right\}$ is the plastic strain vector increment.

Thus, the total strain can be written as:

$$\left\{d\varepsilon\right\} = \left[C^e\right]\left\{d\sigma\right\} + \chi\left\{\frac{\partial G}{\partial \sigma}\right\} \tag{3.67}$$

where: $\{d\varepsilon\}$ is the strain vector increment.

Rearranging this expression, isolating the stress increment term, we have:

$$\{d\sigma\} = \left[D^e\right]\left(\{d\varepsilon\} - \chi\left\{\frac{\partial G}{\partial \sigma}\right\}\right) \tag{3.68}$$

where: $\left[D^e\right]$ is the elastic stress-strain constitutive matrix, with $\left[D^e\right] = \left[C^e\right]^{-1}$.

The stress increment expression, Eq. (3.68), has two unknowns, $\{d\sigma\}$ and χ. The solution of this problem is only possible with another equation. Defining the consistency condition for the yielding locus is essential in this case. According to plasticity theory, the yielding surface is the physical limit for any stress state, which means no conditions allow the porous medium to reach a stress state beyond this limit. This can be expressed as:

$$F\left(p', q, p'_0\right) \leq 0 \tag{3.69}$$

where: F is the yielding function.

Finally, the constitutive matrix for the modified Cam-clay model can be expressed as:

$$\left[D^{ep}\right] = \left[\frac{\kappa}{(1+e)p'}\begin{bmatrix}1 & 0\\ 0 & 2(1+\nu)/9(1-2\nu)\end{bmatrix} + \frac{-1}{\dfrac{\partial f}{\partial p'_o}\left(\dfrac{\partial p'_o}{\partial \varepsilon_v^p}\dfrac{\partial g}{\partial p'} + \dfrac{\partial p'_o}{\partial \varepsilon_d^p}\dfrac{\partial g}{\partial q}\right)}\begin{bmatrix}\dfrac{\partial f}{\partial p'}\dfrac{\partial g}{\partial p'} & \dfrac{\partial f}{\partial q}\dfrac{\partial g}{\partial p'}\\ \dfrac{\partial f}{\partial p'}\dfrac{\partial g}{\partial q} & \dfrac{\partial f}{\partial q}\dfrac{\partial g}{\partial q}\end{bmatrix}\right] \tag{3.70}$$

3.8 SUMMARY

In this chapter, there is a detailed description of the equations proposed in this study. Assuming that the compressibility of the fluid influences the phenomena which take place in porous media requires a formulation considering changes in fluid density. This makes the model much more comprehensive and it may help solving cases in which the fluid compressibility is significant.

The spatial solution of both equilibrium and mass conservation equations are presented, followed by the assembling of the equation system, characterizing the coupled approach. Then, a time solution is made for the system of equations.

Some considerations regarding non linearity in the equilibrium and the flux analyses are discussed. The advective flux term determined in the formulation is also debated, in order to evaluate possible numerical instabilities which may take place when proceeding with the equation solution.

Finally, the mechanical constitutive models utilized in the simulations of this dissertation are presented, including a justification of their usage.

4 COUPLING STRATEGIES AND DESCRIPTION OF ALLFINE

The proposal of this dissertation is the solution of a coupled hydro-mechanical formulation with the consideration of fluid compressibility. This problem is solved via Finite Element Method (FEM), with the implementation of the equations on the FE software ALLFINE (Farias, 1993; Cordão Neto, 2005).

In this chapter, a brief discussion over coupling strategies is presented, followed by some aspects concerning ALLFINE (Farias, 1993; Cordão Neto, 2005).

4.1 COUPLING STRATEGIES

The solution of many engineering problems is only possible when representative models are established and their numerical modeling is performed. Different approaches are required in order to represent physical phenomena. In geotechnics and geomechanics, the mechanical and the hydraulic behavior of a porous media are completely interrelated.

Considering the need of representing simultaneously the observed phenomena, it is appropriate to define an adequate manner to physically describe this kind of problem. This may be established with coupled or mixed formulations.

A coupled formulation can be valid in cases in which there are multiple domains with no possible solution separated from the other. In this type of formulation, it is also observed that the set of dependent variables cannot be explicitly eliminated from the partial differential equations.

On the other hand, a mixed formulation is applicable to a single domain in which equations and boundary conditions describing the physical phenomenon contain a number of dependent variables which could be reduced by elimination, still maintaining a soluble problem (Jha, 2005).

Therefore, a more accurate way of achieving appropriate results in geotechnics and in reservoir geomechanics is possible with coupled analyses. Considering the mechanical and the hydraulic behavior of a reservoir, it can be observed that stress-strain state is affected by fluid pressures and vice-versa. Thus, it is intuitive the understanding of the importance of a coupled analysis, which is a more precise manner of describing how mechanical and hydraulic behavior are connected (Samier et al, 2003).

In this section, some aspects regarding possible coupling strategies for the solution of hydro-mechanical problems are presented.

Coupled analysis may be performed in different ways, depending on each particular case. There are scenarios which require a refined degree of coupling, more appropriate for that specific phenomena representation (Jha, 2005). There are four levels of coupling methods which lead to different strategies of problem solutions, going from a completely separated solution of the equations to a fully coupled approach (Settari & Walters, 2001):

- Decoupled;
- Partially coupled approach – explicit coupling;
- Partially coupled approach – iterative coupling;
- Fully coupled.

In order to describe these different coupling strategies, the formulation proposed in this research, already discretized in space and in time and written in matrix form is used as basis, as shown:

$$\begin{bmatrix} 0 & 0 \\ 0 & [R] \end{bmatrix} \begin{Bmatrix} \{u\} \\ \{p\} \end{Bmatrix} + \begin{bmatrix} [K] & [C] \\ [L] & [M] \end{bmatrix} \begin{Bmatrix} \{\dot{u}\} \\ \{\dot{p}\} \end{Bmatrix} = \begin{Bmatrix} \{\dot{F}\} \\ \{Q\} \end{Bmatrix} \tag{4.1}$$

where: $[R]$ is the flow matrix, $[K]$ is the stiffness matrix, $[C]$ is the solids-fluid coupling matrix, $[L]$ is the fluid-solids coupling matrix, $[M]$ is the mass matrix, $\{u\}$ is the nodal displacements vector, $\{p\}$ is the nodal fluid pressure vector, $\{\dot{u}\}$ is the nodal displacements rate vector, $\{\dot{p}\}$ is the nodal fluid pressure rate vector, $\{\dot{F}\}$ is the external forces rate vector and $\{Q\}$ is the external discharges vector (chapter 3).

A different approach for this equation is required for each of coupling level. It is necessary to identify the impact the type of coupling may have on the simulation. This definition is essential, considering that the main challenges related to coupling strategies are computational efficiency, numerical solution convergence and code combination for the solution of equilibrium and flow equations (Jha, 2005; Gomes, 2009). A more sophisticated coupled analysis should only be made when its advantages are greater than its difficulties.

The different levels of coupling strategies are presented in sections 4.1.1, 4.1.2, 4.1.3 and 4.1.4, following the classification proposed by Settari & Walters (2001).

4.1.1 DECOUPLED APPROACH

The main characteristic observed in this type of approach is that the equilibrium equation is solved separated from the flow equation. Considering the solution like this, the stress changes have no effect in flow and vice-versa, characterizing the type of coupling known as one-way. Firstly, the flow equation is solved and then, its solution is applied in the equilibrium equation, providing geomechanical responses of the analyzed medium. A scheme representing this is portrayed in Figure 4.1.

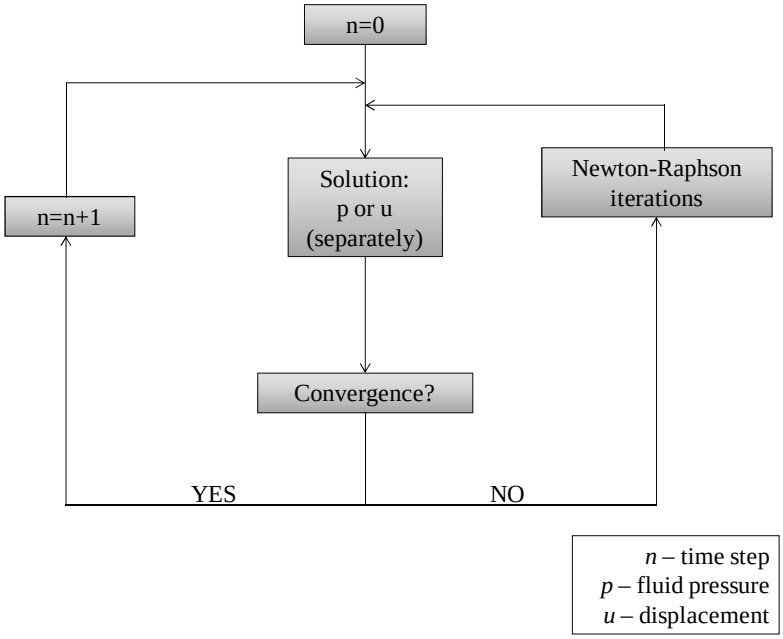

Figure 4.1 - Solution algorithm for a decoupled approach of hydro-mechanical problems.

In some cases, the flow part is aware of the mechanical part of the problem if new or updated permeability and porosity data is incorporated into the flow equation. On the other hand, the mechanical part may be aware of the flow part if pressure loads are applied on the nodes of the mechanical grid as boundary terms (Jha, 2005).

In mathematical terms, the decoupled approach may be represented by considering only flow and then only stress equations (Settari & Walters, 2001). The first is represented by assuming that $\{u\}=0$ and $\{p\}$ is known (imposed as external load), meaning no stress changes during reservoir simulation. Thus, Eq. (4.1) may be rewritten as:

$$[M]\{\dot{p}\}^{n+1} = \{Q\} - [R]\{p\}^{n} \tag{4.2}$$

where: *n* corresponds to each time step.

In Eq. (4.2), the value of $\{\dot{p}\}^{n+1}$ is achieved. So, in order to define $\{\dot{u}\}^{n+1}$, the top half of Eq. (4.1) may be decoupled and rewritten as:

$$[K]\{\dot{u}\}^{n+1} = \{\dot{F}\} - [C]\{\dot{p}\}^{n+1} \tag{4.3}$$

This type of approach represents great simplification of the studied physical phenomena and may not be the most appropriate to reservoir modeling. Decoupled models are usually employed only on predictions of reservoir geomechanical responses (Pereira, 2007).

4.1.2 PARTIALLY COUPLED APPROACH – EXPLICIT COUPLING

The partially coupled approach takes into account the importance of the coupled hydro-mechanical analysis of a porous media, considering that both flow and equilibrium equations should be solved with some connection between them. This is a method in which flow and equilibrium equations are solved separately, but with updates of the results (displacements and fluid pressures) in each mathematical statement. This type of coupling is known as two-way coupling, with the variable update working in both equations. There are two categories of partial coupling, explicit, described in this section and iterative, described in section 4.1.3.

The explicit coupling approach is a special case of the iteratively coupling. The main difference between them is that, in this particular case, flow responses are not affected by the geomechanical responses at a same time step. The flow analysis is performed firstly. The results of this analysis are input for the stress analysis. The stress analysis results are used to compute porosity and permeability explicitly and also in the solution of the flow equation for the following time step. It is important to highlight that the coupling terms are lagged one time step behind and there is no specific coupling variable (Jha, 2005), characterizing the partial coupling of this kind of approach. A scheme representing this type of coupling is shown in Figure 4.2.

In mathematical terms, this approach consists of lagging the coupling terms one time step behind (Settari & Walters, 2001). Firstly, the flow equation is solved:

$$[M]\{\dot{p}\}^{n+1} = \{Q\} - [R]\{p\}^{n} - [L]\{\dot{u}\}^{n} \tag{4.4}$$

When the flow solution $\{\dot{p}\}^{n+1}$ is applied in the stress equation, it can be expressed by:

$$[K]\{\dot{u}\}^{n+1} = \{\dot{F}\} - [C]\{\dot{p}\}^{n+1} \tag{4.5}$$

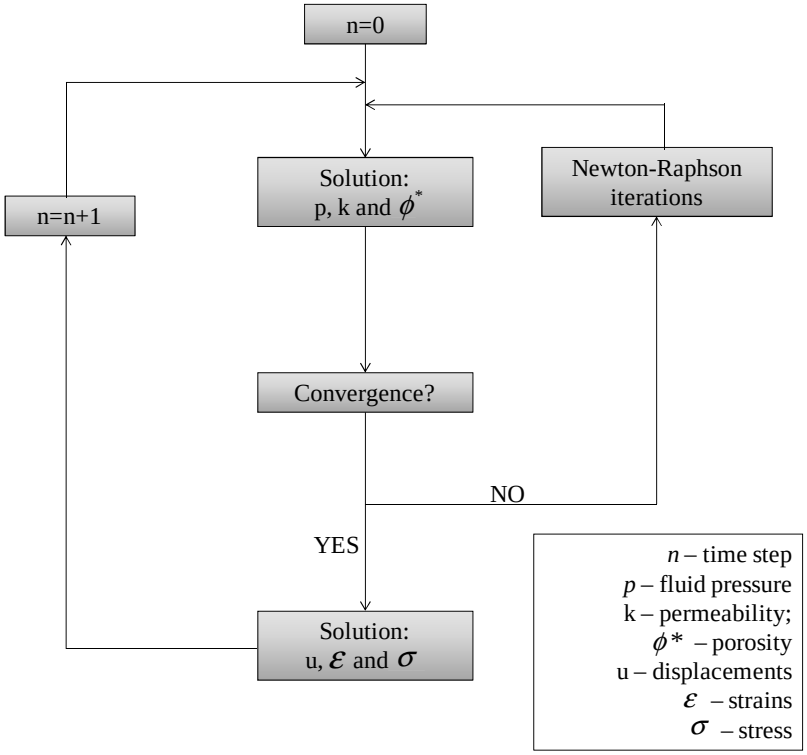

Figure 4.2 - Solution algorithm for an explicit coupling approach of hydro-mechanical problems.

4.1.3 PARTIALLY COUPLED APPROACH – ITERATIVE COUPLING

In iterative coupling, flow and geomechanical variables are computed separately and sequentially. During the solution procedure, many iterations are performed at each time step until the desired degree of convergence is achieved (Jha, 2005).

Firstly, the flow equation solution is executed and its results (fluid pressure) are applied in the mechanical part of the problem. Once this is solved, the displacements are used in the update of values of porosity and permeability. When this iteration is finished, the next one begins with the new values of porosity and permeability, allowing a new solution for the flow equation and for the equilibrium equation at that time step, likewise. This process continues until the solution of the equations converges. Then, the procedure is repeated to the next time step (Pereira, 2007). This approach differs from explicit coupling in the number of iterations in a same time step. A scheme representing this type of coupling is portrayed in Figure 4.3.

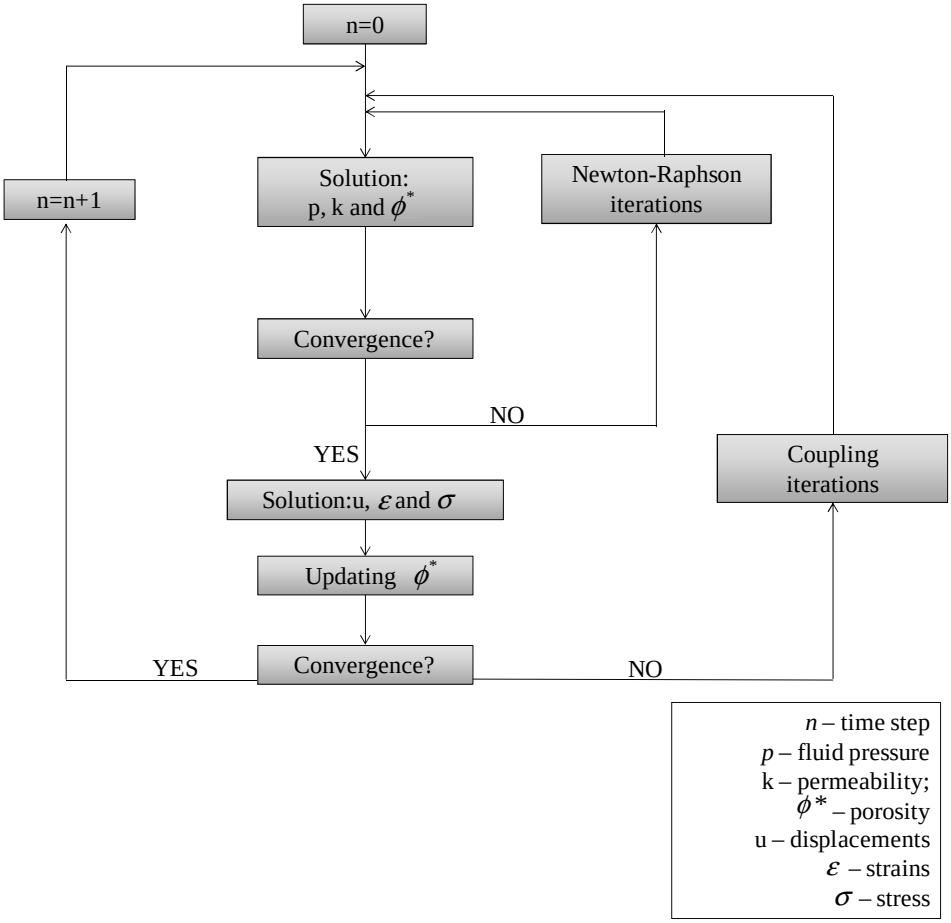

Figure 4.3 - Solution algorithm for an iterative coupling approach of hydro-mechanical problems.

Mathematically, this approach consists of the repeated solution of the flow and the stress equations (ν iterations) in a time step *n* according to these expressions:

$$[M]\{\dot{p}\}^{\nu+1} = \{Q\} - [R]\{p\}^{n} - [L]\{\dot{u}\}^{\nu} \tag{4.6}$$

$$[K]\{\dot{u}\}^{\nu+1} = \{\dot{F}\} - [C]\{\dot{p}\}^{\nu+1} \tag{4.7}$$

It is fair to say that when the iteration converges, $\{p\}^{\nu} = \{p\}^{n+1}$ and $\{\dot{u}\}^{\nu} = \{\dot{u}\}^{n+1}$, the solution is identical to the fully coupled system. Another great advantage of this method is that convergence criteria are easily controlled due to the separated solution of equations. Also, there is the possibility of applying different numerical methods for flow and equilibrium equations solution (Pereira, 2007).

The iterative coupling approach is adequate for representing physical phenomena in primary recovery simulation in an oil reservoir. In this type of problem, the stress state of the

media is influenced only by dissipation of fluid pressure. No external loading is applied during the process. Therewith, the model accuracy is not decreased by using the iterative coupling approach.

However, for traditional geotechnics application, the level of coupling may influence more the results of the simulation. In cases where load is applied, as in consolidation problems, solving the equations separately does not represent adequately the physics of the phenomenon. The undrained condition of the problem at early stages is not well represented with an iterative coupling approach. A fully coupled model is the most appropriate for this type of modeling in terms of portraying the problem, providing greater accuracy to the simulations.

This discussion of coupling approaches takes into consideration media subjected to isothermal conditions. When considering the influence of temperature in the analyses, it is required further explanation regarding the coupling level of the problem.

4.1.4 FULLY COUPLED APPROACH

From all types of coupling approaches, this is the most refined in terms of general representation of the physical phenomena occurring in porous media.

The solution of the flow and the equilibrium equations are performed simultaneously. With this, the flow is affected by the stress and the strain by porosity, and, consequently, permeability, proving this kind of solution to being internally consistent (Tran et al, 2005). Other advantages are the possibility of taking into account the effects of anisotropy and non-linearity of materials (Samier et al, 2003) and the unconditional convergence property for implicit time integration (Jha, 2005).

The disadvantages of this coupling approach are computational cost and consumption of time and the specific application of the same numerical solution method (e.g., Finite Element Method) for both equations (Settari & Walters, 2001; Pereira, 2007). A scheme representing this type of coupling is shown in Figure 4.4.

The fully coupled approach is used in the formulation proposed in this research, as shown in chapter 3. This type of coupling allows the performance of more accurate simulations for traditional geotechnics and it may also improve reservoir geomechanical analyses.

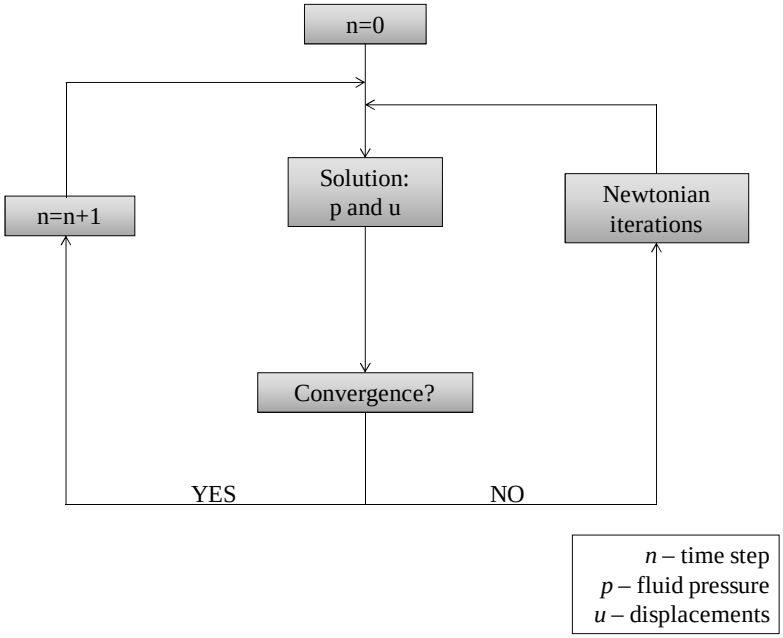

Figure 4.4 - Solution algorithm for a fully coupled approach of hydro-mechanical problems.

4.2 DESCRIPTION OF ALLFINE

ALLFINE (Farias, 1993) was a Finite Element program for geotechnical analyses, originally developed for three-dimensional equilibrium problems and plane-strain consolidation problems in saturated conditions. The solution of the hydro-mechanical behavior of porous media is made with a fully coupled approach. Computational cost and consumption of time are managed with some features incorporated in the program. The simulation options of this program included:

- Drained and undrained analyses;
- Embankment construction simulations;
- Excavation simulations;
- Choice of different constitutive relations, including several elastoplastic models, such as:
    - Linear elastic;
    - Non-linear elastic;
    - Critical State – continuously plastic;
    - Critical State – elastoplastic;
    - Non-linear elastic for resilient sand;
    - Non-linear elastic for resilient clay;
    - Elastic-perfectly plastic (Drucker-Prager failure criterion);
    - Modified Cam-clay;

    - Tij-clay;
    - Tij-sand.
- Collapse settlement analysis;
- Different integration algorithms for stress-strain relation;
- Different solution schemes for non-linear equation systems.

Cordão Neto (2005) added new features to the program, making it suitable for unsaturated conditions. The following options were added to ALLFINE:

- Three-dimensional analysis of unconfined flow in unsaturated media;
- Three-dimensional analysis of consolidation problems in unsaturated condition;
- Choice of an elastoplastic model used for unsaturated soils, the Barcelona Basic Model (Alonso et al., 1990);
- Hydraulic behavior constitutive models.

It is important to highlight that ALLFINE is essentially a processing software. There is need of complementary softwares for pre-processing data and for post-processing the results.

Considering the intention of studying compaction and subsidence problems in petroleum reservoirs, which are essentially consolidation analysis, there is need of ensuring the suitability of ALLFINE for performing these simulations. The consolidation analyses for saturated and unsaturated conditions were thoroughly discussed and tested by Cordão Neto (2005). The possible analysis conditions for both versions of the program were validated by Farias (1993) and Cordão Neto (2005).

The latest version of ALLFINE was used as basis for implementation of the proposed formulation (chapter 3). The constitutive models used in this research were already in the program (linear elastic and modified Cam-clay).

4.3 SUMMARY

In this chapter, coupling strategies were described, with the definition of their main features, the differences among them and the advantages and disadvantages of each.

Then, the FE program ALLFINE (Farias, 1993; Cordão Neto, 2005) was presented. The main analyses this software performs are listed, followed by the program functioning. The need of pre and post-processing complementary is highlighted, with description of the necessary procedures to adequately perform the simulations.

This program is used as basis for the implementation of the coupled hydro-mechanical formulation proposed in chapter 3, with fluid and solids compressibility consideration.

5 SENSITIVITY ANALYSIS FOR MECHANICAL PARAMETERS

The Finite Element program ALLFINE was improved with the implementation of the formulation proposed in this research (chapter 3). Being this formulation new to the software, tests had to be performed in order to verify the validity and to calibrate the proposed numerical model.

Therefore, this formulation was tried with the simulation of two different cases in order to evaluate the influence of mechanical and hydraulic parameters of porous media. In this chapter, only the analyses performed for the mechanical parameters are presented. In the following chapter, the formulation tests for hydraulic parameters are presented and analyzed.

Firstly, there have been performed one-dimensional consolidation simulations in a laterally confined column of soil, based on the simulations made by Farias (1993) and Cordão Neto (2005). The results are compared with the analytical solution of the conventional Terzaghi's problem.

The second case is a two-dimensional consolidation problem, with the behavior analysis of a porous medium subjected to an uniform load, infinite in one direction and with delimited extension on the other, again based on simulations performed by Farias (1993) and Cordão Neto (2005). The results are compared with the analytical solution of the conventional Biot problem (Biot, 1940).

For the first case, the compressibility of the fluid and the soil were varied to control their influence in porous medium responses. For the second case, only the compressibility of the fluid was changed, making possible the evaluation of its influence in the physical behavior of the porous medium.

The results here presented are sensitivity analyses of these parameters, contributing to a better understand of their significance on hydro-mechanical behavior of the porous medium in each simulated situation.

The simulations are performed for two different constitutive models for the solid matrix, linear elastic and modified Cam-clay. Each one of these models requires specific mechanical parameters, which are adequately described on its corresponding sections throughout this chapter.

5.1 ONE-DIMENSIONAL CONSOLIDATION PROBLEM

This first case consists of a laterally confined column of soil, 1 meter high and supporting an uniform load, as illustrated in Figure 5.1.

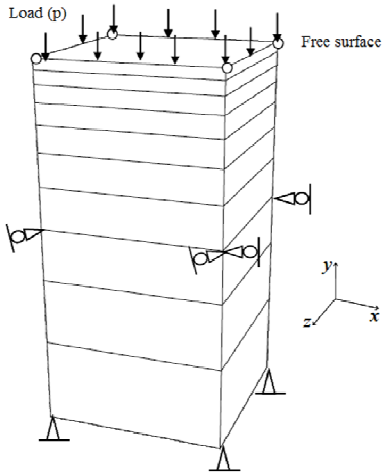

Figure 5.1 - One-dimensional consolidation problem (modified Cordão Neto, 2005).

The soil column is discretized in 10 three-dimensional 8-noded elements (Figure 5.2), making up a mesh with a total of 44 nodes. The division of the soil column is not uniform, each element with a different height, as shown in Figure 5.1.

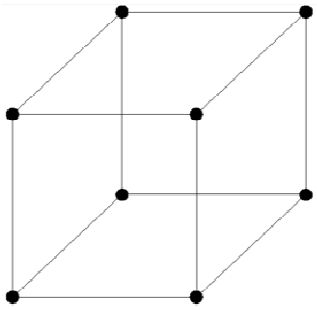

Figure 5.2 - 8-noded 3D element.

The soil sample is assumed to be totally saturated and the fluid flow is restricted in the laterals of the column, but it can occur at the top surface.

The studied problem is a consolidation analysis. The applied load is transferred to the fluid within the sample, configuring an instantaneous increase in fluid pressure. Gradually, over time, the fluid pressure dissipates, as it may be observed in the results.

The performed analyses are compared to the solution as preview by Terzaghi. Simplifying assumptions were made by Terzaghi in his proposal of analysis for the one-dimensional consolidation problem, some of which were:

- Linear elastic model;
- Incompressible fluid.

In the first analysis, using the linear elastic model, the results may be thoroughly compared. On the other hand, when the other models are used, the results are not equivalent to Tergazhi's proposal. Even though it is not appropriate to make a comparison based on the analytical solution, these are the reference values for the proposed problem, so they are used to evaluate the results.

The sensitivity analyses here presented reveal how the hydro-mechanical behavior of porous media is influenced by the compressibility of the fluid and the solids for different mechanical constitutive models.

5.1.1 SENSITIVITY ANALYSIS FOR THE FLUID COMPRESSIBILITY

The simulations performed to evaluate the influence of the fluid compressibility in the hydro-mechanical behavior of porous media were divided in two parts:

- Verification of the influence of fluid compressibility in fluid pressure results;
- Verification of the influence of stress state in fluid pressure results for the same fluid compressibility value.

Firstly, for a 100 kPa load, the values of compressibility of the fluid were varied, as presented in Table 5.1. In these analyses, the compressibility of the solids was kept constant and its value is also shown in Table 5.1. The results of these analyses are presented for time factors T=0; 0,2; 0,5; 0,8.

It is important to highlight that in the formulation (chapter 3), the influence of the fluid pressure in the fluid and solids density is measured with the bulk modulus. This modulus corresponds to the inverse of the compressibility.

Table 5.1 - Parameters for simulation of fluid compressibility influence.

Fluid bulk modulus (k_f)	$1{,}0\text{x}10^{12}$ kPa
	$3{,}7\text{x}10^{6}$ kPa
	$1{,}0\text{x}10^{4}$ kPa
	$1{,}0\text{x}10^{3}$ kPa
	$5{,}0\text{x}10^{2}$ kPa
Solids bulk modulus (k_s)	$1{,}0\text{x}10^{15}$ kPa

Then, in order to verify the influence of the stress state in fluid pressure results for the same fluid compressibility value, the simulations were performed for two different loads, 100

kPa and 10000 kPa. The compressibility of the fluid was kept constant through the tests (k_f = 1,0x10^5 kPa) and the results were evaluated to time factors T=0,05; 0,5; 0,8.

It is important to state the time factors presented in these results correspond to those calculated with the premises of classic consolidation theory - Terzaghi's approach. The time factor is calculated with the following expression:

$$T = \frac{c_v t}{h_d^{\,2}} \tag{5.1}$$

where: T is the time factor, c_v is the coefficient of consolidation [L^2T^{-1}], t is elapsed time [T] and h_d is the largest measured height to a draining surface [L].

$$c_v = \frac{k}{\gamma_f m_v} \tag{5.2}$$

where: c_v is the coefficient of consolidation [L^2T^{-1}], k is the permeability [LT^{-1}], γ_f is the fluid unit weight [$ML^{-2}T^{-2}$] and m_v is the coefficient of volume compressibility [$L^2T^2M^{-1}$].

$$m_v = \frac{(1+\nu)(1-2\nu)}{E(1-\nu)} \tag{5.3}$$

where: m_v is the coefficient of volume compressibility [$L^2T^2M^{-1}$], E is the Young modulus [$ML^{-2}T^{-2}$] and ν is the Poisson coefficient.

The values for time factor are kept constant for each set of simulations, allowing the comparison of results at the same stage of analysis.

5.1.1.1 LINEAR ELASTIC MODEL RESPONSES

The analyses performed with this model use the parameters shown in Table 5.2, besides others previously defined in Table 5.1. The value of Young modulus of the soil for the stress level influence analysis was established 100 times greater for the 10000 kPa load. This was made in order to prevent the soil sample from suffering large straining rates during the simulations, considering the objective of evaluating only the fluid compressibility effect.

Table 5.2 - Parameters for one-dimensional consolidation problem (linear elastic model).

Young modulus (*E*)	For $\Delta\sigma = 100$ kPa	25000 kPa
	For $\Delta\sigma = 10000$ kPa	2500000 kPa
Poisson coefficient (ν)		0,31

Initial void ratio (e_0)	0,90
Density of the solids (ρ_s)	2,65 kg/m³
Permeability (k)	$1{,}0\text{x}10^{-6}$ m/s
Density of the fluid (ρ_f)	1,00 kg/m³

Firstly, a comparison between the analytical solution and the simulation results is made, as shown in Figure 5.3. This comparison is made only for the linear elastic model and incompressible fluid ($k_f = 1{,}0\text{x}10^{12}$ kPa) in order to reproduce the same conditions to which the conventional Terzaghi problem is solved.

The results achieved with the simulation for incompressible fluid are very similar to the analytical solution. This shows the adequacy of the formulation for the proposed simulations. Some difference can be noticed only for the first time factor, T=0. This is expected, since this result represents full load transference for the fluid at the initial time stage of the consolidation analysis. The numerical model responses are not adequate to the analytical solution due to its boundary conditions, which force the porous medium results to go softly from 0 to 100 kPa, while the analytical solution shows an abrupt change on fluid pressure values.

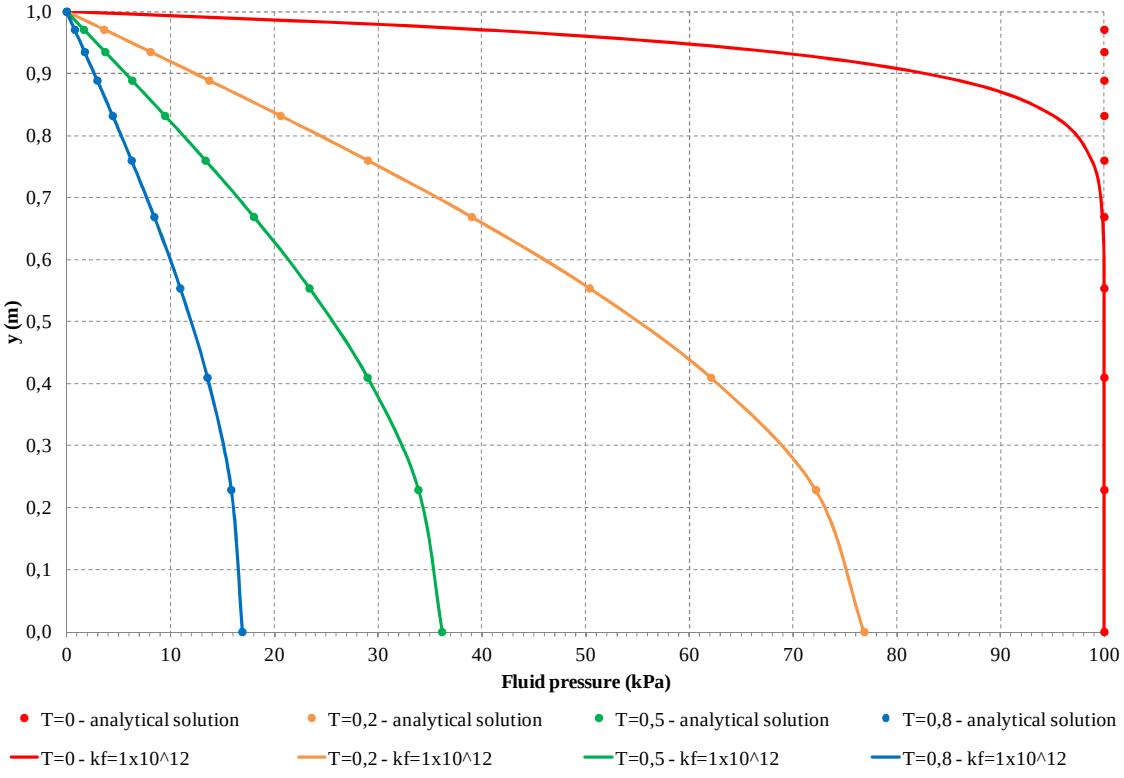

Figure 5.3 - Comparison between simulation results and analytical solution for an incompressible fluid case.

It is important to highlight that the results for lower layers of the porous medium (y=0m) should become constant, being perpendicular to the x-axis. This is not noted in the presented results due to little discretization of the domain to these lower layers. With more analysis points, this tendency would certainly be observed.

Then, the influence of fluid compressibility in the hydro-mechanical behavior of the porous medium is evaluated with the results of fluid pressure. The evolution of the fluid pressure during the simulation of the consolidation process is monitored for specific time factors (T=0; 0,2; 0,5 e 0,8). They are presented in Figure 5.4.

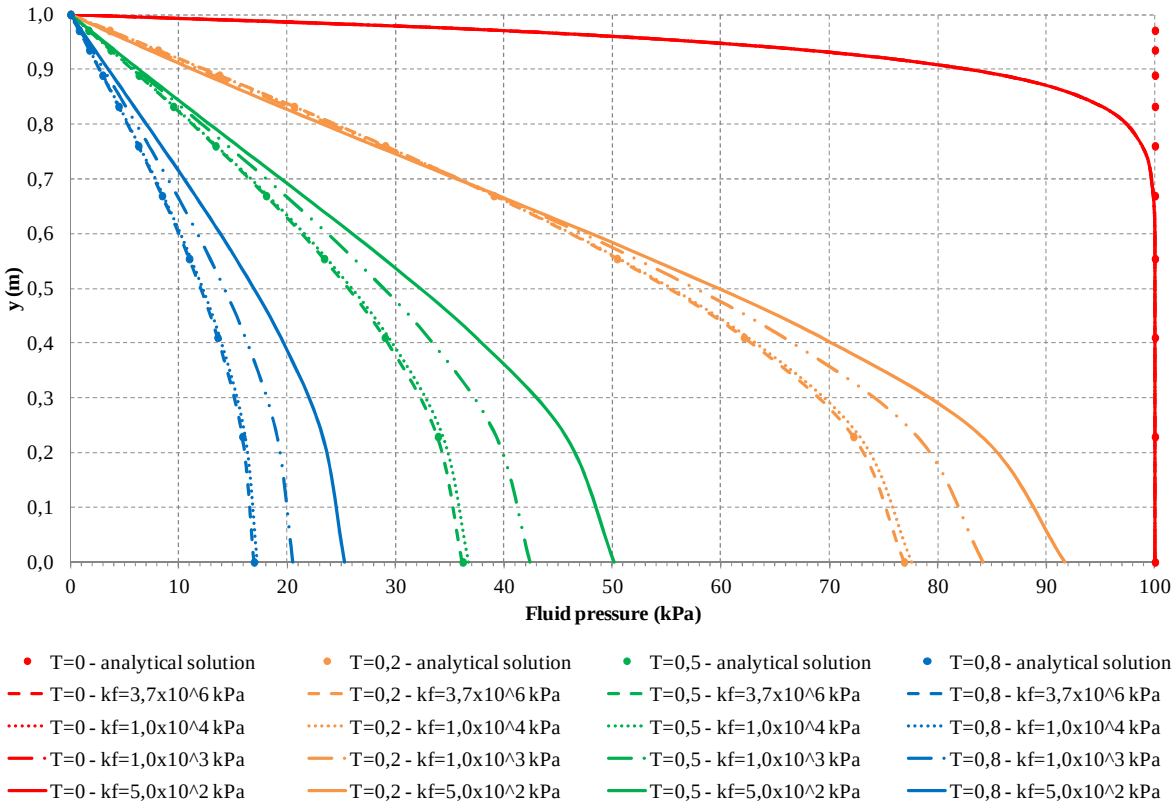

Figure 5.4 - Results of fluid pressure for 100 kPa load in soil column
(fluid compressibility analysis – linear elastic model).

For time factor T=0, the first analyzed stage of the simulations, the curves of fluid pressure are overlap, regardless the fluid compressibility. This occurs due to the short elapsed time of the phenomenon. In an initial moment, the imposed load goes directly to the fluid, making the values of fluid pressure equal.

In the following stages, the responses start to change. For greater values of k_f (lower compressibility), the values of fluid pressure are much closer to the responses correspondent to an incompressible fluid, as expected.

As fluid compressibility is increased (lower fluid bulk modulus), the fluid pressure dissipation through time is much slower. As already said, initially the imposed load goes directly to the fluid. Over time, this stress is transferred to the solid matrix, which strains (pore closing). For a fully saturated sample, such as the analyzed in this case, the void volume changes represent fluid volume variation within the porous medium.

If the fluid is considered incompressible, there are no changes in the volume of fluid and the strains of the solid matrix imply fluid flow. However, if the compressibility of the fluid is significant, the volume of fluid varies over time. This means the pore closing causes fluid compression, resulting in mass storage within the porous medium.

Specifically for the used parameters and imposed conditions in the performed simulations, it can be noticed that from a specific value of fluid bulk modulus (k_f = 3,7x10^6 kPa), the fluid pressure starts to be influenced.

There are few studies related to the fluid compressibility subjected in literature. There are some results of comparison of the evolution of fluid pressure over time using different fluid compressibility values in the research proposed by Jha (2005).

The tendency of behavior of the porous medium in terms of fluid pressure presented by Jha (2005) is similar to the results achieved in these simulations, with the same delay of fluid pressure dissipation here observed.

To illustrate how the stress state of the sample evolves, the stress paths for this simulation are shown in Figure 5.5, for the incompressible fluid (k_f = 1,0x10^{12} kPa) and in Figure 5.6 for the fluid with highest compressibility in this case (k_f = 5,0x10^2 kPa).

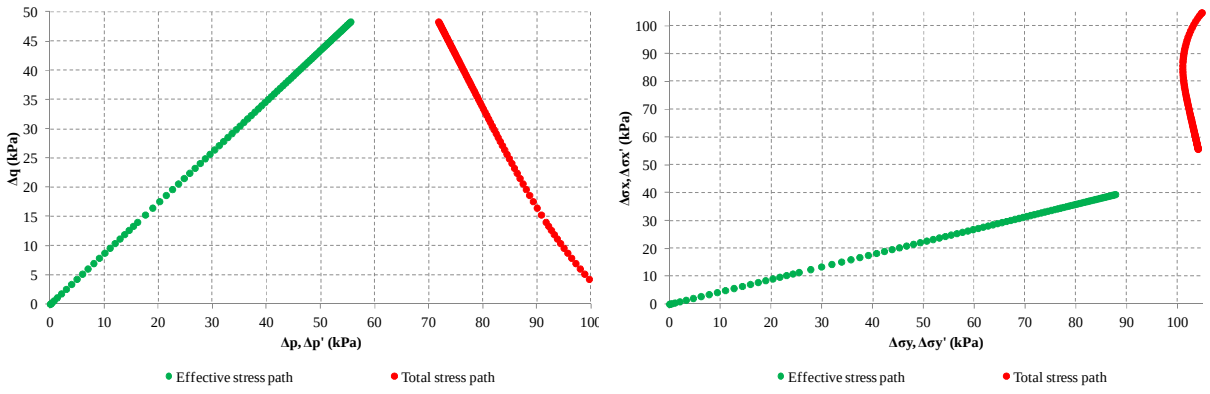

(a) (b)

Figure 5.5 - Stress paths for 100 kPa load simulation (k_f = 1,0x10^{12} kPa - lin. elastic model).

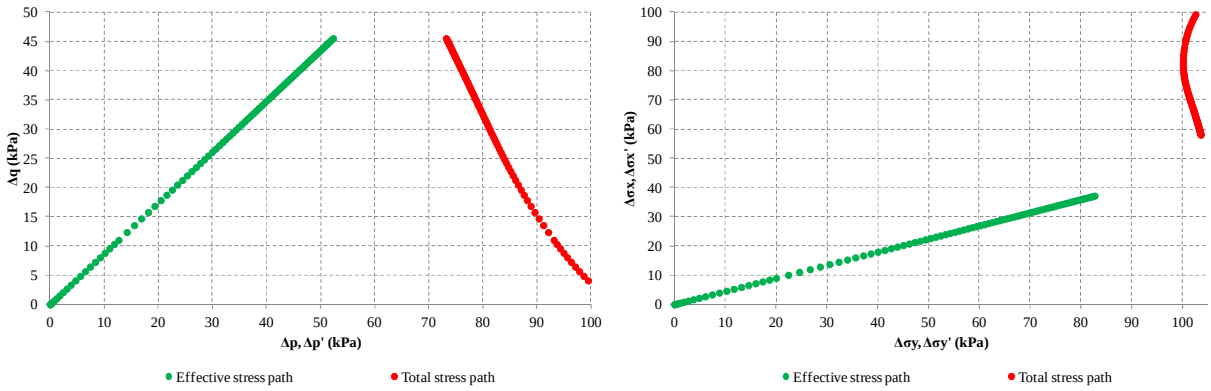

(a) (b)

Figure 5.6 - Stress paths for 100 kPa load simulation (k_f = 5,0x10^2 kPa - linear elastic model).

As expected, effective stress increases over time, as fluid pressure dissipates, as shown in Figure 5.5 (a) and Figure 5.6 (a). Also, it can be noticed that if the simulation was made to a longer period of time, the effective stress sample would tend to reach the same value of the total stress. This can be seen in Figure 5.5 (b) and Figure 5.6 (b). At that stage, fluid pressure would have dissipated completely. These behavior tendencies are similar for incompressible and compressible fluid simulations.

A complementary analysis is made with the evaluation of changes in fluid density for different values of load, presented in Figure 5.7.

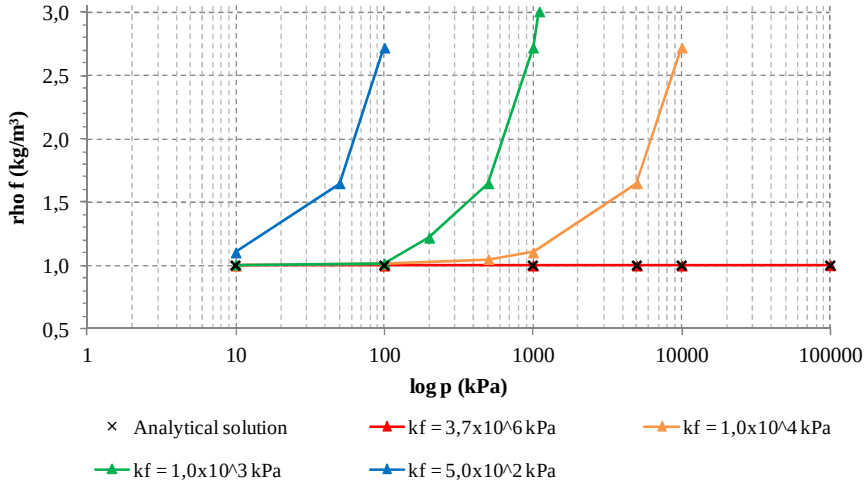

Figure 5.7 - Changes in fluid density for different values of fluid compressibility.

The value of fluid density increases for greater values of fluid compressibility (lower k_f), as expected. However, k_f =5,0x10^2 kPa is the limit value for the bulk modulus of the fluid for simulations with the used parameters, even though it does not represent a real fluid bulk modulus value.

In the formulation proposed in this research, as fluid bulk modulus increases, the values of the mass matrix increase greatly, with large storage of fluid mass. In these cases, flow does not take place. The solution of the system of equations becomes numerically unstable and it may not be representative for the study.

The following analysis was performed in order to evaluate the degree of influence of the stress state in fluid pressure results for the same fluid compressibility value. The results were taken only for time factors T=0,05; 0,5; 0,8 and they are shown in Figure 5.8.

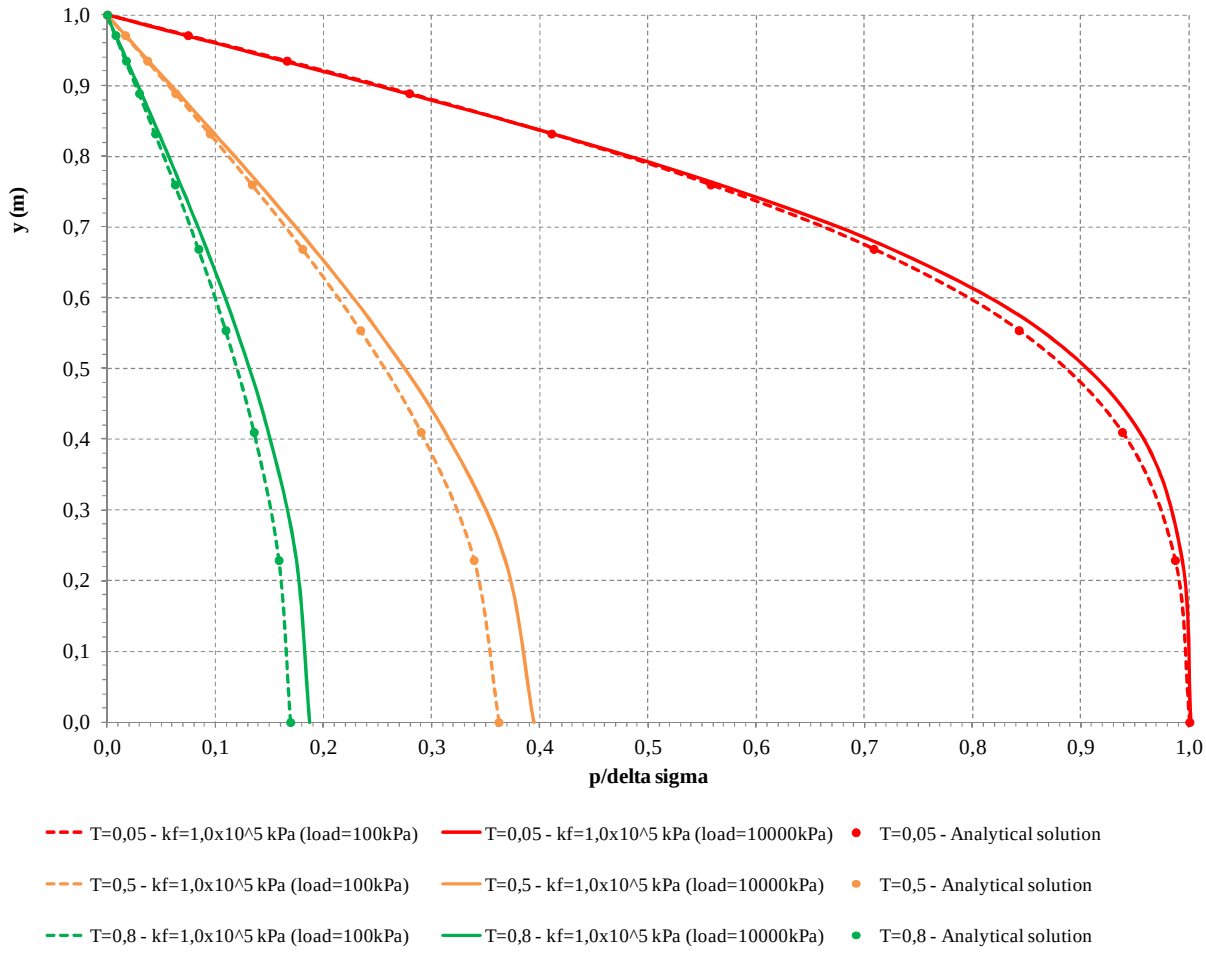

Figure 5.8 - Fluid compressibility influence in results of fluid pressure for different stress levels (linear elastic model).

Fluid compressibility does not influence the responses for a 100 kPa load. The results for this simulation are similar to the analytic response of the one-dimensional consolidation problem proposed by Terzaghi. There is no delay in dissipation of fluid pressure provoked by the effect of fluid compressibility during the consolidation of this sample.

On the other hand, for a 10000 kPa load, the fluid compressibility has a large influence in fluid pressure results, with values 10% greater than the predicted in cases where the effect of fluid compressibility is not significant. In this case, the effect of fluid compressibility is remarkable. The delay in dissipation of fluid pressure in the consolidation of the sample is clear. So, it may be stated that greater loads increase the effect of fluid compressibility, with consequent higher values of fluid pressure.

This analysis is extremely important for reservoir geomechanics. Oil reservoirs are often located at great depths, being subjected to high stress levels. In these cases, the compressibility of the fluid is proven to be significant. The expected values of fluid pressure are largely increased by considering the fluid compressibility influence.

5.1.1.2 MODIFIED CAM-CLAY MODEL RESPONSES

The analyses performed with this model use the parameters shown in Table 5.3. Other parameters required for the simulations are defined later, given the necessity of varying them to the sensitivity analysis.

Table 5.3 - Parameters of modified Cam-clay model for one-dimensional consolidation problem (fluid compressibility sensitivity analysis).

M		1
p_0	For $\Delta\sigma = 100$ kPa	50 kPa
	For $\Delta\sigma = 10000$ kPa	5000 kPa
Overconsolidation ratio (OCR)		0,20
λ	For $\Delta\sigma = 100$ kPa	0,00500
	For $\Delta\sigma = 10000$ kPa	0, 13720
κ	For $\Delta\sigma = 100$ kPa	0,00050
	For $\Delta\sigma = 10000$ kPa	0,01372
Initial void ratio (e_0)		0,90
Poisson coefficient (ν)		0,31
Solids density (ρ_s)		2,65 kg/m³
Fluid density (ρ_f)		1,00 kg/m³
Permeability (*k*)		$1{,}0 \times 10^{-6}$ m/s

In the first analysis, the influence of fluid compressibility in the hydro-mechanical behavior of the porous medium is evaluated with the results of fluid pressure. The evolution

of the fluid pressure during the simulation of the consolidation process is monitored for specific time factors (T=0; 0,2; 0,5 e 0,8). They are presented in Figure 5.9.

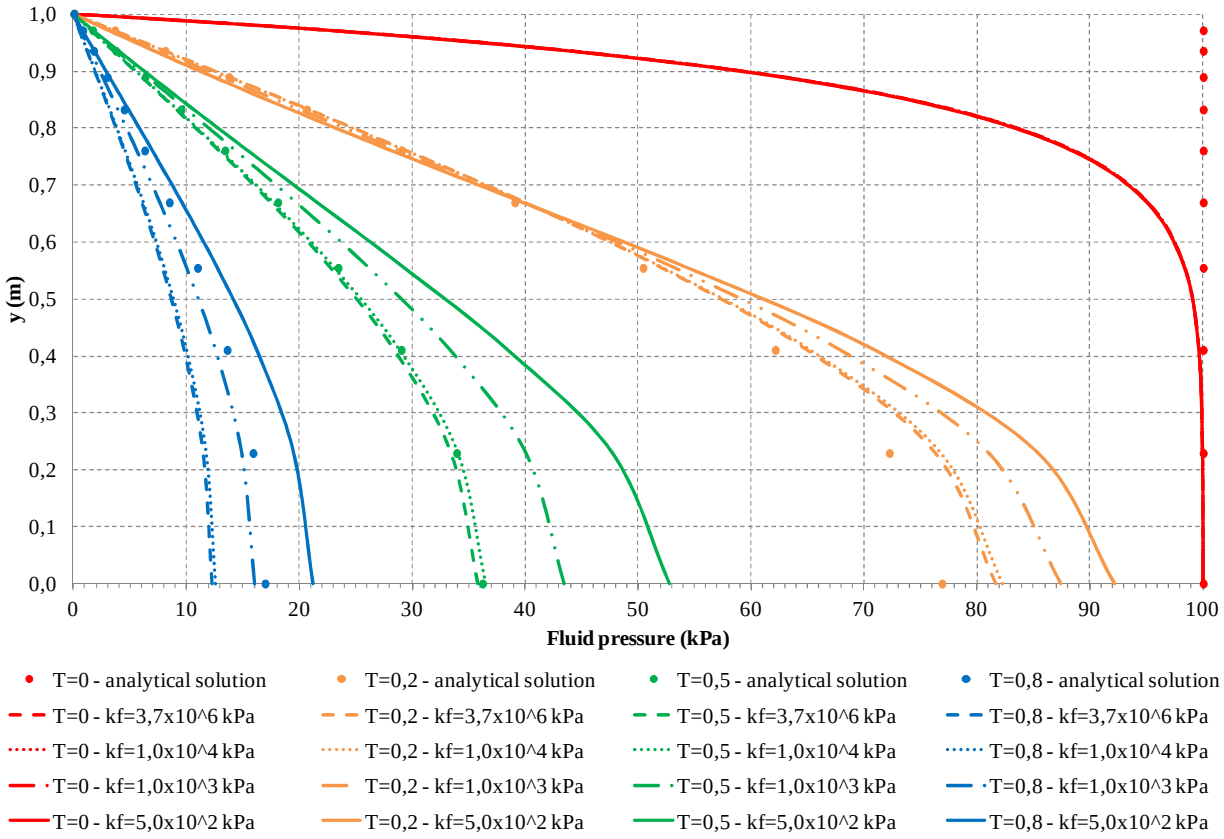

Figure 5.9 - Results of fluid pressure for 100 kPa load in soil column (fluid compressibility analysis – modified Cam-clay model).

The interpretation of these results is similar to the achieved with the linear elastic model. The tendency of behavior is the same in both cases. For the time factor T=0, all curves are overlap, indicating the immediate transmission of the load to the fluid at this first stage.

Gradually, over time, fluid pressure starts to dissipate with the transference of the pressure of the fluid to stress to the solid matrix. Depending on the influence of fluid compressibility, this process of dissipation may occur more rapidly (low fluid compressibility influence) or quicker (great fluid compressibility influence).

For values greater than $3{,}7x10^6$ kPa for fluid bulk modulus, it may be observed that the fluid pressure dissipation is much slower. This process is explained by the variation of fluid volume due to its compressibility, as explained before. The delay of fluid pressure dissipation is shown in Figure 5.9.

Another important analysis is related to the significant differences observed between the analytical solution, with a linear elastic constitutive model, and the responses achieved with the modified Cam-clay model.

It can be noticed that there is significant difference between the results of fluid pressure when using these two constitutive models. This can be explained by premises of stress-strain relation of each model.

In the linear elastic model, stress and strain have a linear relation. On the other hand, in the modified Cam-clay model, the stress-strain relation is non-linear for plastic strains. Thus, the predictions of expected strains for a porous medium differ depending on which model is applied during the simulations.

In cases in which the Young modulus for the elastoplastic model is obtained by a secant going from the origin to the point of maximum stress, as shown in Figure 5.10, this interpretation can be easily made.

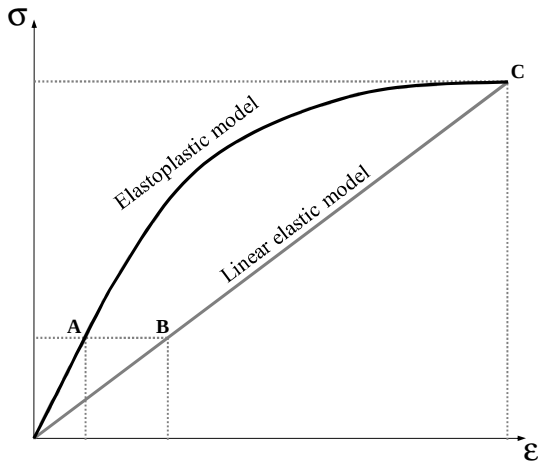

Figure 5.10 - Comparison between elastoplastic and linear elastic models.

Comparing the points A and B in Figure 5.10, it can be observed that for the same stress value, the strains achieved with the linear elastic model are greater than with the elastoplastic model. The differences between values of strain for a same stress value may be verified until the stress-strain curves for both models meet, at point C.

In a coupled hydro-mechanical phenomenon such as the simulated, the behavior of the solid matrix influences directly the hydraulic responses of the medium. Therewith, one can infer that with an elastoplastic model, like modified Cam-clay, the transference of fluid pressure to the solid matrix will occur in a different manner than the expected for the linear elastic model.

Again, to illustrate how the stress state of the sample evolves, the stress paths for this simulation are shown in Figure 5.11, for the incompressible fluid (k_f = 1,0x10^{12} kPa) and in Figure 5.12 for the fluid with highest compressibility in this case (k_f = 5,0x10^{2} kPa).

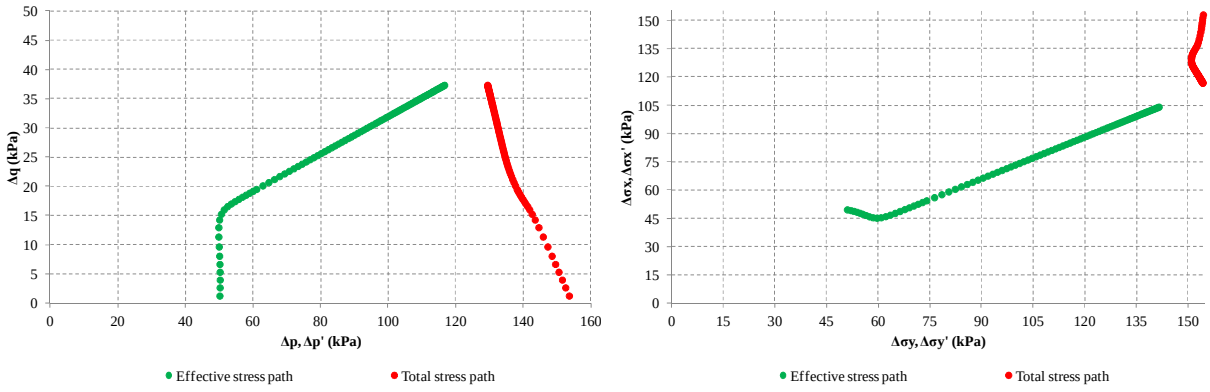

(a) (b)

Figure 5.11 - Stress paths for 100 kPa load simulation (k_f = 1,0x10^{12} kPa – modified Cam-clay model).

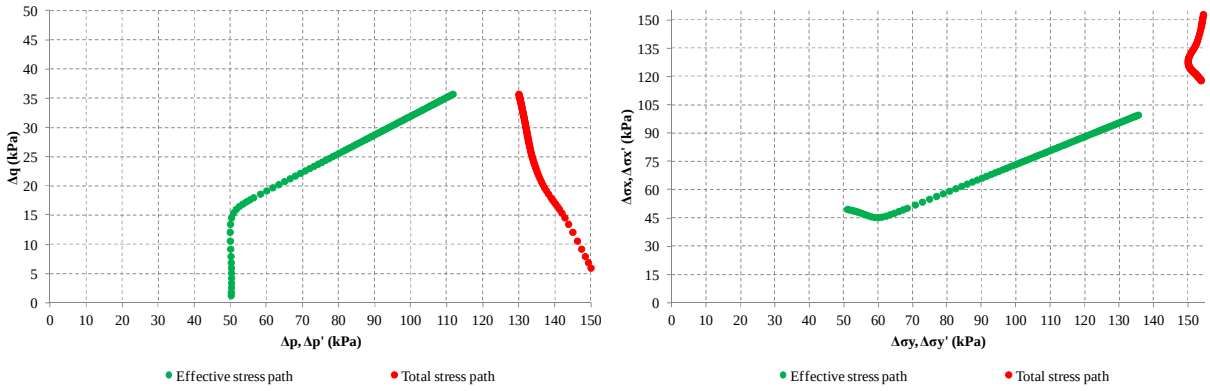

(a) (b)

Figure 5.12 - Stress paths for 100 kPa load simulation (k_f = 5,0x10^{2} kPa – mod. Cam-clay model).

In this case, effective stress also increases over time with fluid pressure dissipation (Figure 5.11 (a) and Figure 5.12 (a)). For that reason, it is observed the same behavior tendency of the soil sample in these simulations as the ones performed with the linear elastic model. The effective stress tends to reach the total stress value after a longer period of time, with complete dissipation of fluid pressure. This tendency can be seen in Figure 5.11 (b) and Figure 5.12 (b). Again, the results are similar for incompressible and compressible fluid simulations.

Finally, a complementary analysis is presented, in order to show the effects of stress level in fluid pressure results for the same value of fluid bulk modulus. The comparison between the consolidation process of the soil column for two different loads, 100 kPa and 10000 kPa, is shown in Figure 5.13 for time factors T=0,05; 0,5; 0,8.

For a 100 kPa load, the simulation results tend to be proximate to the analytical solution, even though the used constitutive model does not represent the conditions fixed by Terzaghi.

At time factor T=0,05, the values of fluid pressure follow the same tendency of the analytical solution, regardless the stress level. Due to simulation short elapsed time, this stage still represents an undrained load situation, with almost no fluid pressure dissipation.

For the following time factors, it may be noticed that fluid pressure dissipates faster for a 10000 kPa, the opposite of the observed with the linear elastic model.

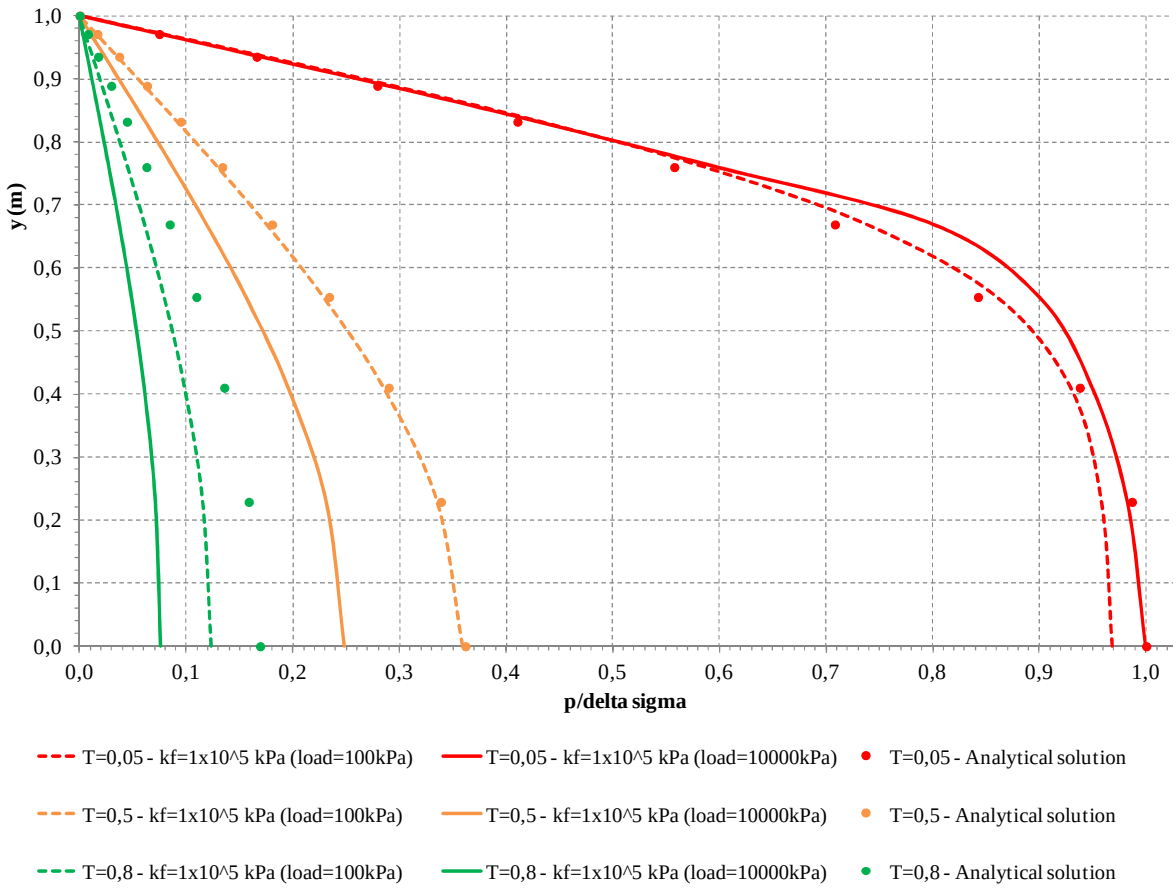

Figure 5.13 - Fluid compressibility influence in results of fluid pressure for different stress levels (modified Cam-clay model).

The modified Cam-clay model captures the stress and strain changes of the porous medium more accurately than the linear elastic model and, for this reason, it adequately represents pore closing for a 10000 kPa load simulations. These volume changes may influence the fluid behavior, inducing fluid flow. It can be observed in this simulation that the 10000 kPa load induced flow, making the values of fluid pressure lower. The effect of fluid compressibility, even though it is proved to affect the hydro-mechanical behavior of the porous medium at this stress level, could not compensate this flow induction.

Specifically in terms of reservoir geomechanics, this phenomenon is named compaction drive. As mentioned in chapter 2, the compaction drive mechanism is the increase in oil flow out of the reservoir due to pore volume changes. This explains the observed decrease in fluid pressure for a higher stress level. The fluid compressibility effect could not be observed and analyzed for these simulation conditions.

5.1.2 SENSITIVITY ANALYSIS FOR THE SOLIDS COMPRESSIBILITY

Similarly to the performed analyses for the fluid compressibility, the influence of the solids compressibility in the hydro-mechanical behavior of porous media is evaluated. The simulations were also divided in two parts:

- Verification of the influence of solids compressibility;
- Verification of the influence of stress state in fluid pressure results for the same solids compressibility value.

Again, for a 100 kPa load, the values of compressibility of the solids were varied, as shown in Table 5.4. Based on the achieved results, it has been demonstrated the need for making this simulation also for a 10000 kPa load. Thus, the effects of solids compressibility may be clearly observed. For this analysis, the parameters are shown in Table 5.5.

The chosen values for solids compressibility were selected based on the fixed value of fluid compressibility. It is admitted that fluid compressibility could not be greater than solids compressibility, so the chosen values should fulfill this requirement. The solids bulk modulus values are in Table 5.4 and Table 5.5, for 100 kPa and 10000 kPa simulations, respectively.

Another determinant aspect for the choice of the fluid compressibility was the analyses already performed. It was proved that for similar conditions of stress state, a value of fluid compressibility of $1x10^5$ kPa did not influence the results of fluid pressure in comparison to the responses for an incompressible fluid (section 5.1.1).

The values of solids bulk modulus vary from the simulation with a 100 kPa load to the 10000 kPa load. These values were carefully chosen to avoid any numerical instabilities of the model which could interfere on the results of the simulations.

Table 5.4 - Parameters for simulation of solids compressibility influence (100 kPa load).

Solids bulk modulus (k_s)	$5{,}0\text{x}10^{7}$ kPa
	$1{,}0\text{x}10^{7}$ kPa
	$5{,}0\text{x}10^{6}$ kPa
	$1{,}0\text{x}10^{6}$ kPa
Fluid bulk modulus (k_f)	$1{,}0\text{x}10^{5}$ kPa

Table 5.5 - Parameters for simulation of solids compressibility influence (10000 kPa load).

Solids bulk modulus (k_s)	$1{,}0\text{x}10^{10}$ kPa
	$1{,}0\text{x}10^{9}$ kPa
	$1{,}0\text{x}10^{8}$ kPa
	$5{,}0\text{x}10^{7}$ kPa
Fluid bulk modulus (k_f)	$1{,}0\text{x}10^{5}$ kPa

In order to verify the influence of stress state in fluid pressure results for a solids compressibility specific value, a comparison between results of the simulations for a 100 kPa and 10000 kPa was made. The compressibility of the solids was kept constant through the tests ($k_s = 5\text{x}10^{7}$ kPa) and the results were evaluated to time factors T=0,05; 0,5; 0,8.

It is important to state the time factors presented in these results correspond to those calculated with the premises of classic consolidation theory (section 5.1.1). They are kept constant for all simulations, permitting a comparison of results at the same stage of analysis.

5.1.2.1 LINEAR ELASTIC MODEL RESPONSES

The used parameters are the same of fluid compressibility simulations with the linear elastic model. The model parameters are shown in Table 5.2.

The influence of solids compressibility is evaluated with the results of fluid pressure in the first analysis. The evolution of the fluid pressure during the simulation of the consolidation process is monitored for specific time factors (T=0; 0,2; 0,5 e 0,8). The results for a 100 kPa and 10000 kPa loads are presented in Figure 5.14 and Figure 5.15, respectively.

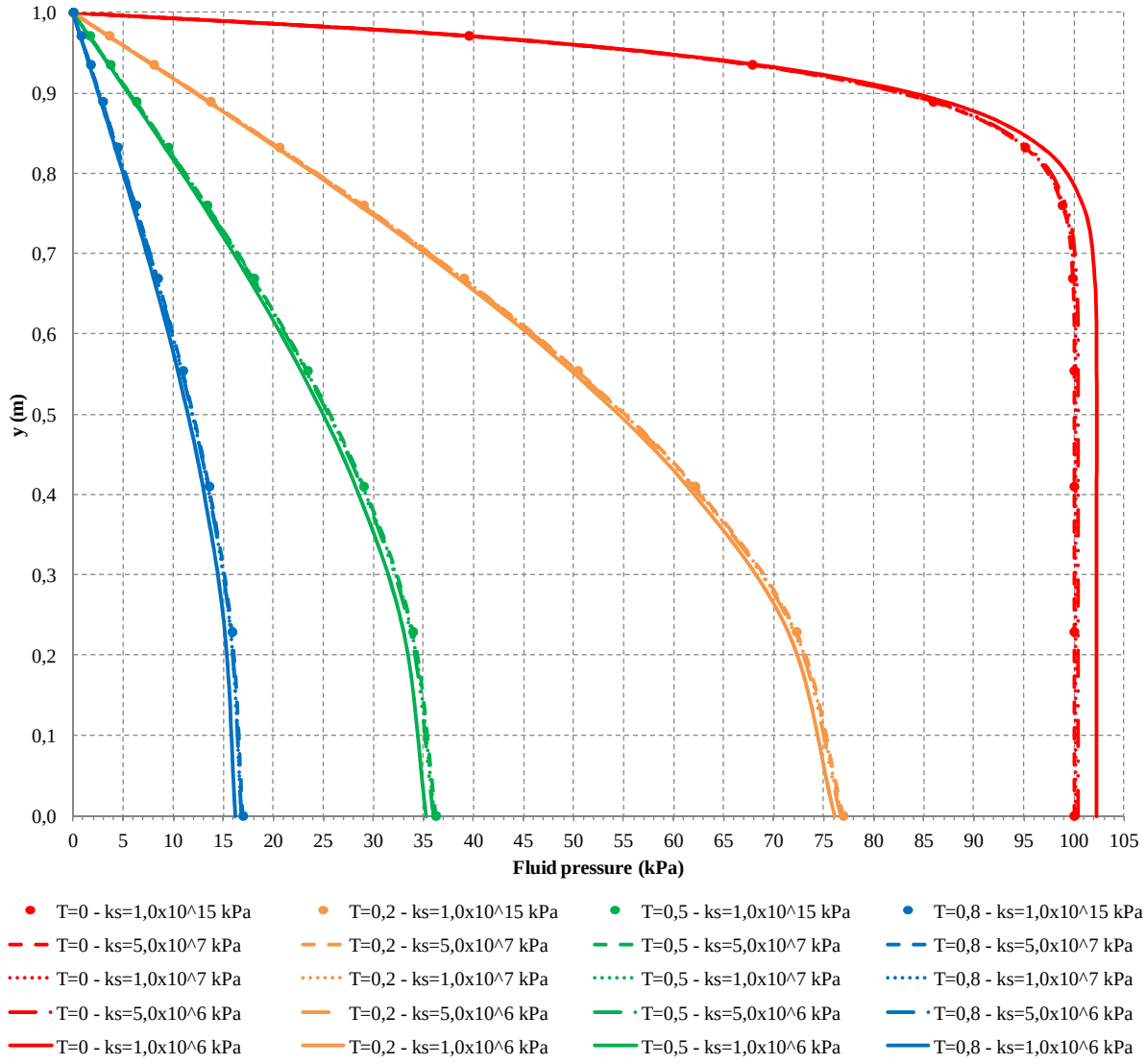

Figure 5.14 - Results of fluid pressure for 100 kPa load in soil column (solids compressibility analysis – linear elastic model).

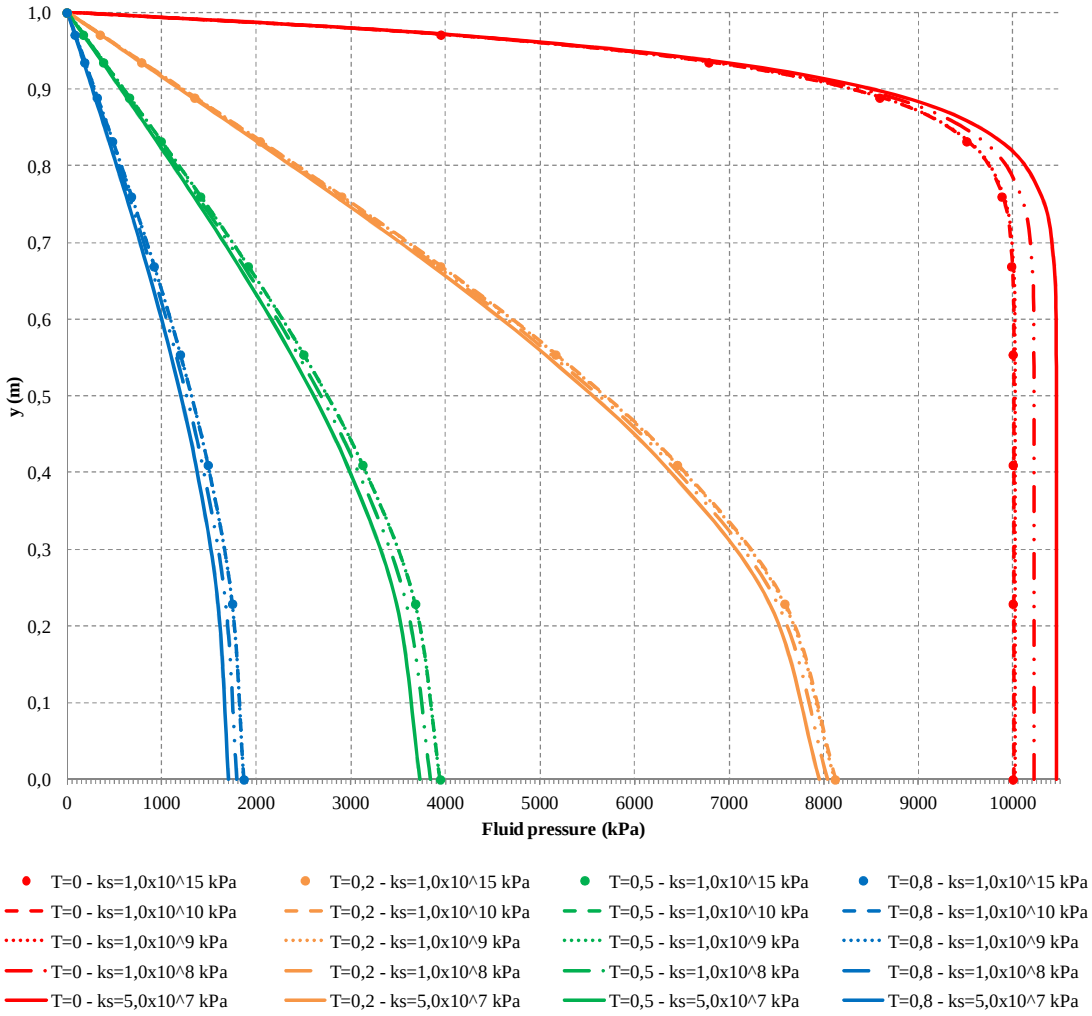

Figure 5.15 - Results of fluid pressure for 10000 kPa load in soil column (solids compressibility analysis – linear elastic model).

The results for both loads show the same tendency of behavior of the medium. For the first analyzed time factor (T=0), it can be observed some numerical instability. This instability could be explained by a more significant interference from the advective term in the flow matrix due to the lower values of solids bulk modulus.

The expected behavior for this first time stage is that the total imposed load goes directly to the fluid due to the short elapsed time. So, the values of fluid pressure are equal at T=0, regardless the solids compressibility. These curves should have been overlap.

For all other time stages (T=0,2; T=0,5; T=0,8), the fluid pressure decreases for higher values of solids compressibility (k_s decrease). When the solid matrix is more compressible, it is easier for it to deform, absorbing the effect of stress increase over the porous medium. Therewith, the transference of the load to the solid matrix occurs more rapidly than if the solids compressibility was not taken into account, being registered lower values of fluid

pressure, as observed in Figure 5.14 and Figure 5.15. However, it is fair to say that the solids compressibility effect is not expressive, considering that the difference between the incompressible and compressible conditions are not very significant.

A relevant aspect is the relation between solids and fluid compressibility. In the performed simulations, the fluid bulk modulus is fixed at $1{,}0x10^5$ kPa. When the value of solids bulk modulus is lowered, getting closer to $1{,}0x10^5$ kPa, solids and fluid bulk modulus have the same magnitude. Thus, the effects of fluid compressibility are diminished or not as significant. This means the effect of increase in fluid pressure due to fluid compressibility (section 5.1.1) is annulled, making the values of fluid pressure lower than the expected for this fluid compressibility in this stress level.

In order to complement the studies of stress state on the soil sample, the stress paths for these simulations are shown in Figure 5.16 and Figure 5.17 for the incompressible solids (k_s = $1{,}0x10^{15}$ kPa) and in Figure 5.18 and Figure 5.19 for the solids with highest compressibility (k_s = $1{,}0x10^6$ kPa and k_s = $5{,}0x10^7$ kPa), for a 100 kPa and 10000 kPa, respectively.

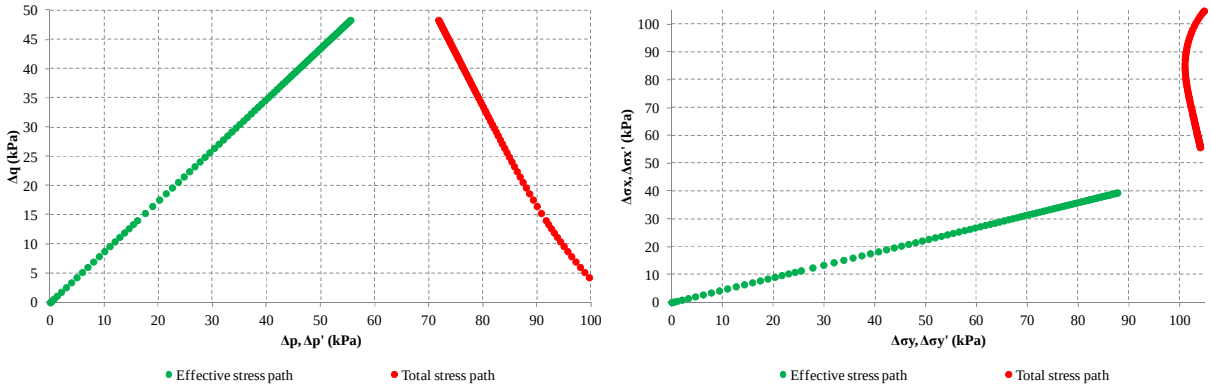

(a) (b)

Figure 5.16 - Stress paths for 100 kPa load simulation (k_s = $1{,}0x10^{15}$ kPa - lin. elastic model).

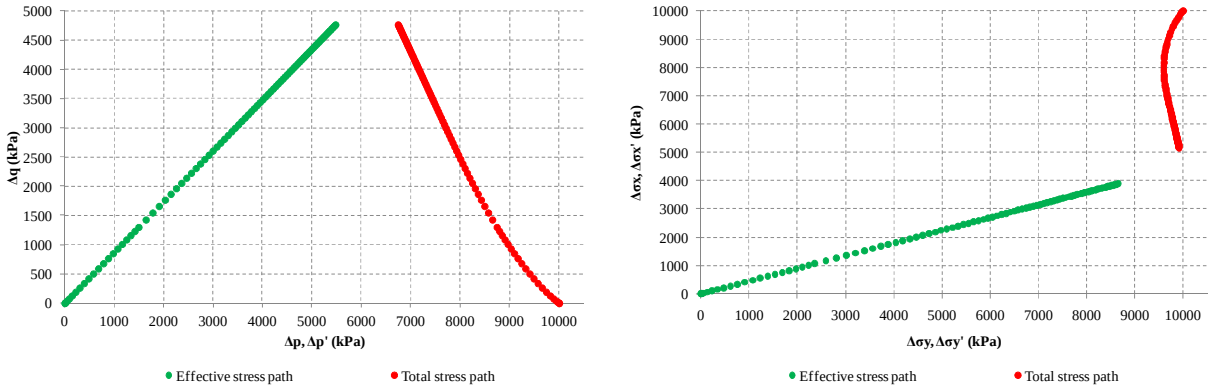

(a) (b)

Figure 5.17 - Stress paths for 10000 kPa load simul. (k_s = $1{,}0x10^{15}$ kPa - lin. elast. model).

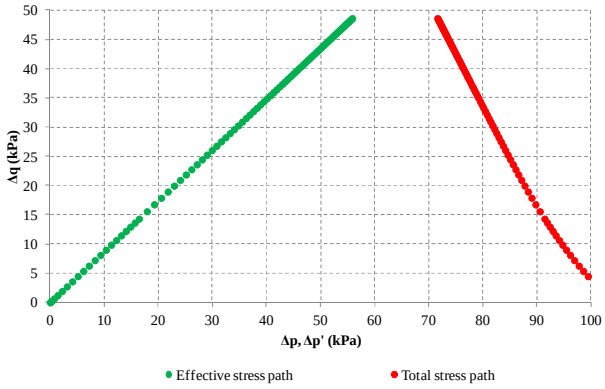

(a)

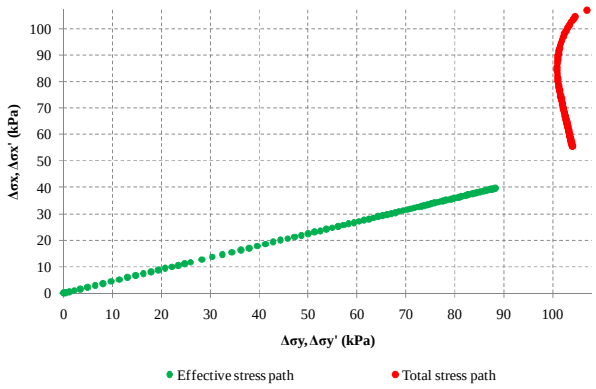

(b)

Figure 5.18 - Stress paths for 100 kPa load simul. (k_s = 1,0x10^6 kPa - linear elastic model).

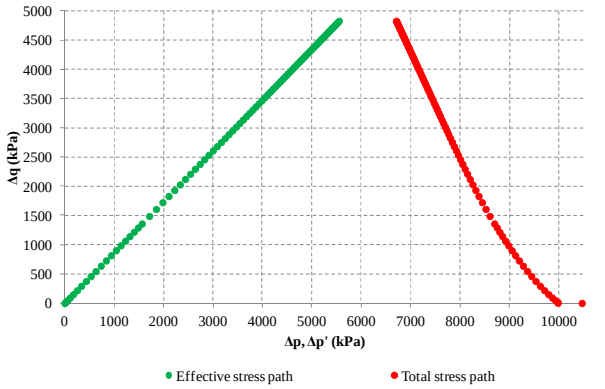

(a)

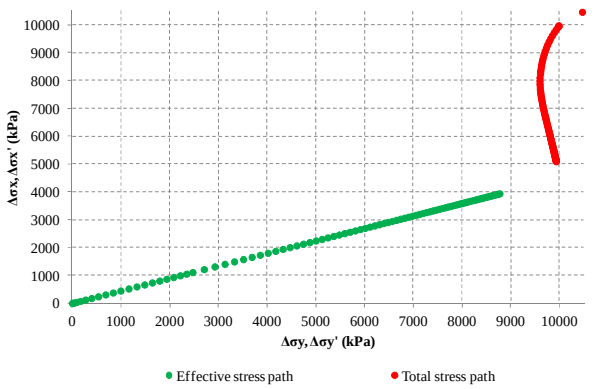

(b)

Figure 5.19 - Stress paths for 10000 kPa load simulation (k_s = 5,0x10^7 kPa - lin. elast. model).

The stress paths for these simulations follow the same behavior tendency seen in fluid compressibility simulations. It has been established that the effect of solids compressibility was not so expressive in these simulations. So, there is also no evidence of influence of solids compressibility in the stress paths. Again, effective stress increases over time, as fluid pressure dissipates, as shown in Figure 5.16 (a), Figure 5.17 (a), Figure 5.18 (a) and Figure 5.19 (a). Also, it can be inferred that if the simulation was made to a longer period of time, the effective stress sample would tend to reach the same value of the total stress, as shown in Figure 5.16 (b), Figure 5.17 (b), Figure 5.18 (b) and Figure 5.19 (b). At that stage, fluid pressure would have dissipated completely. These behavior tendencies are similar for incompressible and compressible solids simulations.

Another important analysis can be made relating fluid compressibility and the stress state imposed in each simulation. The fluid compressibility, as said, is fixed at 1,0x10^5 kPa. As shown in previous results (section 5.1.1), for a 100 kPa load, this value of fluid

compressibility does not influence significantly the fluid pressure responses of the model. Therefore, one can conclude that this fluid behaves as an incompressible fluid for this load. On the other hand, for a 10000 kPa load, the same value of fluid compressibility influences significantly fluid pressure responses. For a higher load, the same fluid can be referred to as being compressible. This should be considered when analyzing the responses the model provides. This effect can be seen when comparing Figure 5.14 and Figure 5.15. The values of fluid pressure for a 10000 kPa load are proportionally higher than for the 100 kPa simulation and this effect is associated with fluid compressibility.

Then, the following analysis was performed in order to evaluate the degree of influence of the stress state in fluid pressure results for the same solids compressibility value. Based on the previous analyses, the limit value of solids bulk modulus is $5{,}0x10^7$ kPa, so the analysis was performed for this value. The results were taken only for time factors T=0,05; 0,5; 0,8 and they are shown in Figure 5.20.

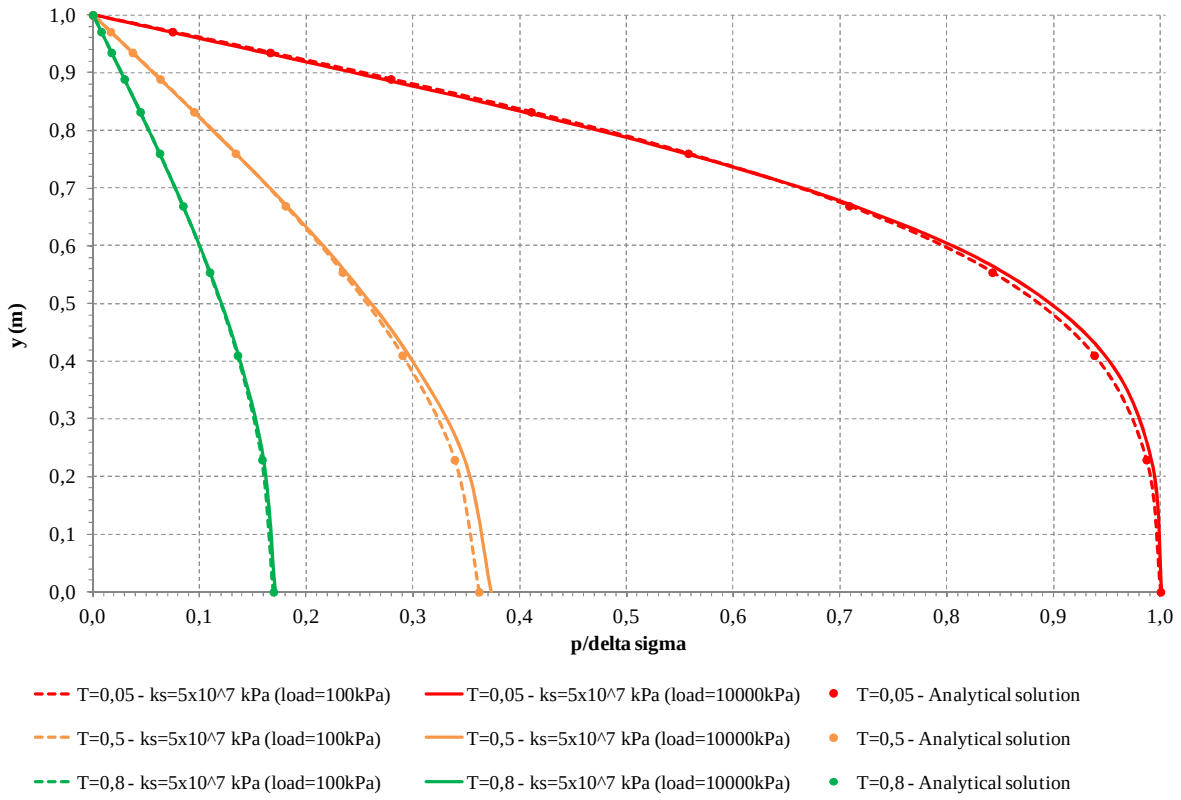

Figure 5.20 - Solids compressibility influence in results of fluid pressure for different stress levels (linear elastic model).

The results of fluid pressure show that the influence of the stress level in fluid pressure results for the same solids compressibility value is insignificant. It does not affect or

influence porous medium behavior. The results for this simulation are similar to the analytic response of the one-dimensional consolidation problem proposed by Terzaghi, regardless the stress level or the solids compressibility.

Thus, one possible interpretation is that the compressibility of the solid matrix is not so significant in the physical behavior of the porous media. The solids compressibility consideration could be neglected without major losses in terms of representativeness of the numerical model.

5.1.2.2 MODIFIED CAM-CLAY MODEL RESPONSES

The analyses performed with this model use the parameters shown in Table 5.6. Other parameters required for the simulations are defined later, given the necessity of varying them to the sensitivity analysis.

Table 5.6 - Parameters of modified Cam-clay model for one-dimensional consolidation problem (solids compressibility sensitivity analysis).

M		1
p_0	For $\Delta\sigma = 100$ kPa	50 kPa
	For $\Delta\sigma = 10000$ kPa	5000 kPa
Overconsolidation ratio (OCR)		0,20
λ	For $\Delta\sigma = 100$ kPa	0,0050
	For $\Delta\sigma = 10000$ kPa	0,0030
κ	For $\Delta\sigma = 100$ kPa	0,0005
	For $\Delta\sigma = 10000$ kPa	0,0003
Initial void ratio (e_0)		0,90
Poisson coefficient (ν)		0,31
Density of the solids (ρ_s)		2,65 kg/m³
Density of the fluid (ρ_f)		1,00 kg/m³
Permeability (*k*)		$1{,}0 \times 10^{-6}$ m/s

In the first set of performed simulations, it was tested the influence of solids compressibility in the responses for the one-dimensional consolidation case. The evolution of the fluid pressure during the simulation of the consolidation process is monitored for specific time factors (T=0; 0,2; 0,5 e 0,8). The results for a 100 kPa load and 10000 kPa are presented in Figure 5.21 and Figure 5.22, respectively.

The results for both loads show the same tendency of behavior of the medium already analyzed for the linear elastic model. For the first analyzed time factor (T=0), it can be observed some numerical instability, as already mentioned. For this first time stage, it is expected that the total imposed load goes directly to the fluid due to the short elapsed time. Therefore, the values of fluid pressure, regardless the solids compressibility, are equal at T=0 and the curves should have been overlap.

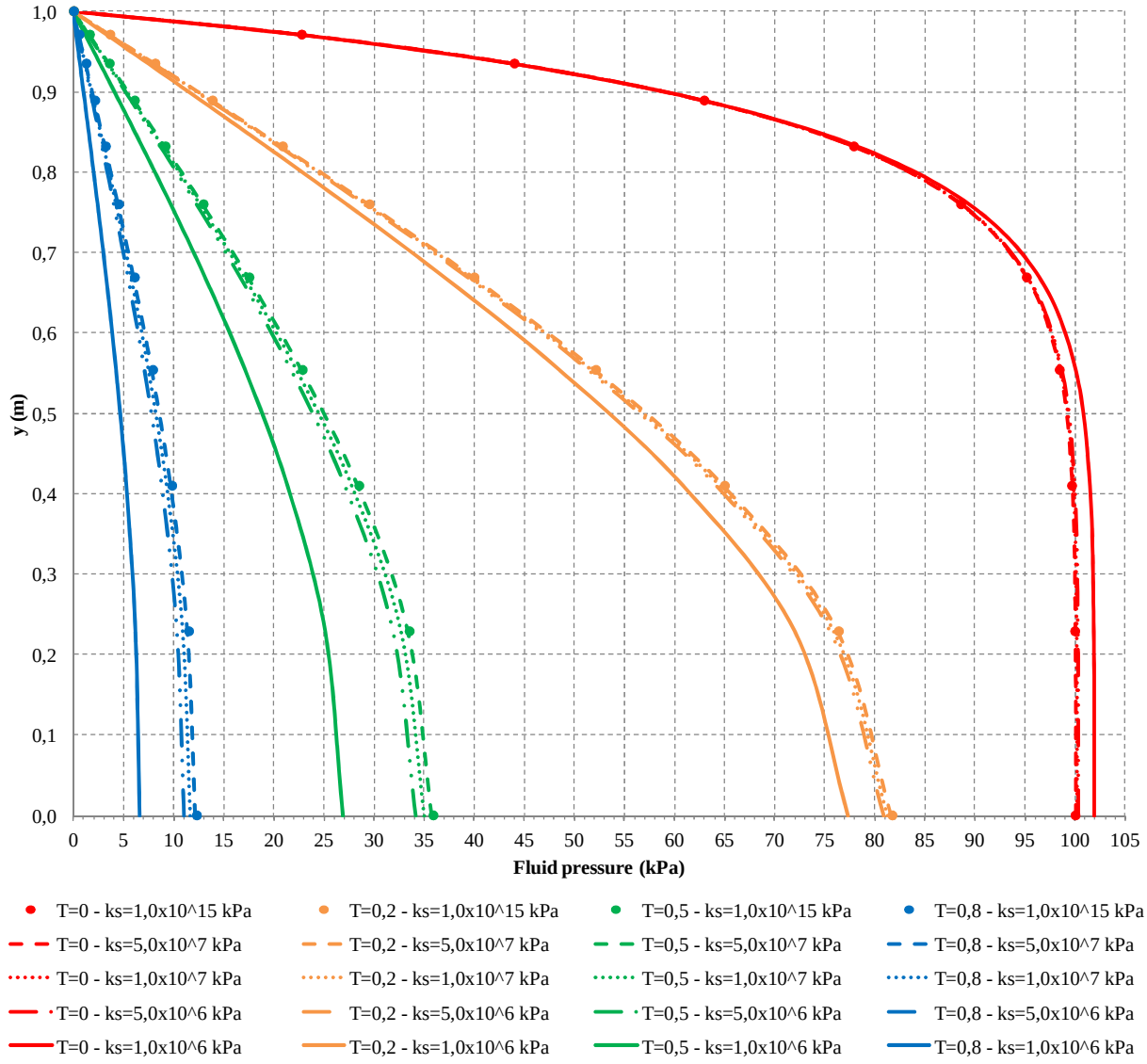

Figure 5.21 - Results of fluid pressure for 100 kPa load in soil column (solids compressibility analysis – modified Cam-clay model).

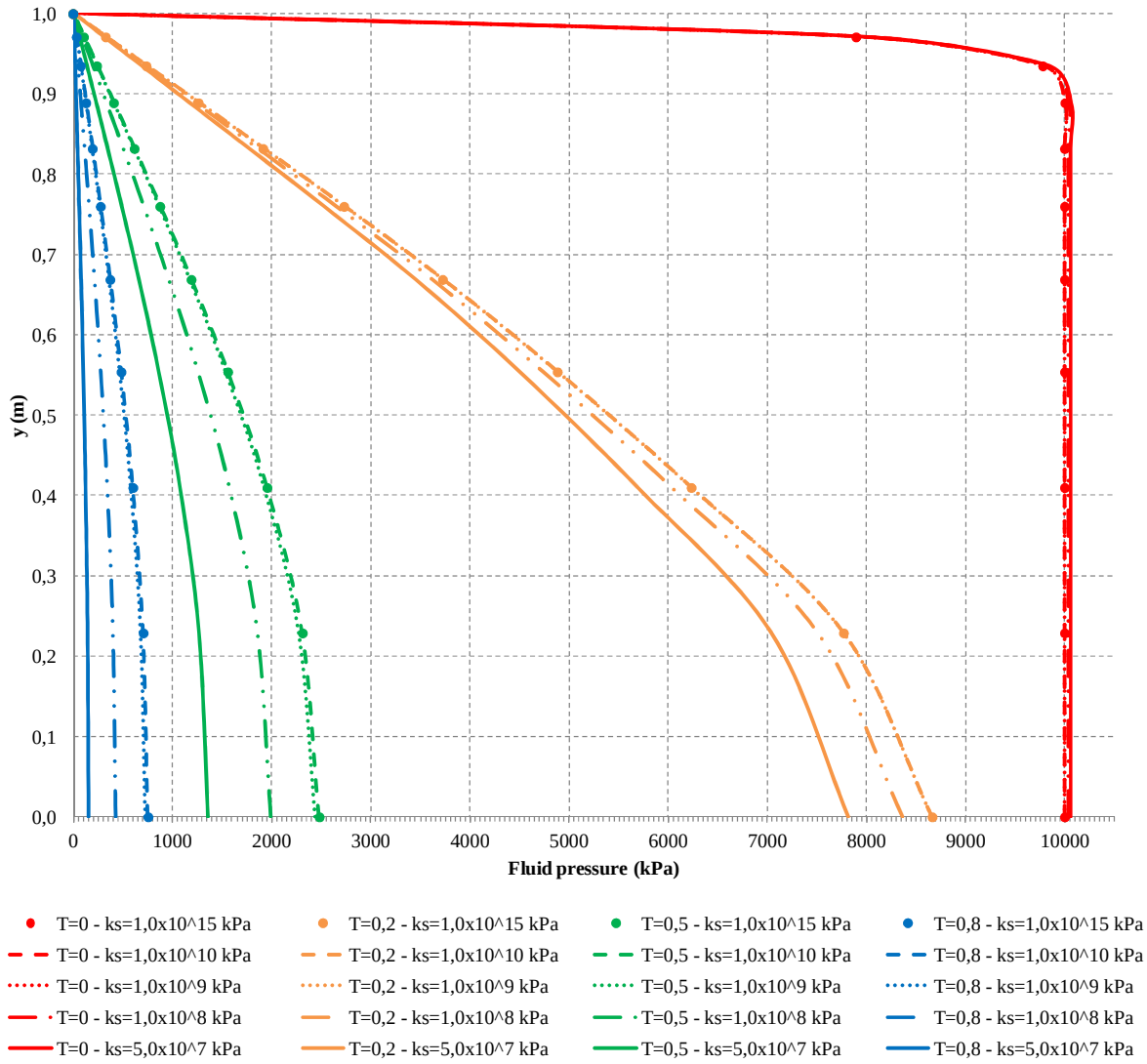

Figure 5.22 - Results of fluid pressure for 10000 kPa load in soil column (solids compressibility analysis – modified Cam-clay model).

For all other time stages (T=0,2; T=0,5; T=0,8), the fluid pressure decreases for higher values of solids compressibility (k_s decrease). When solid matrix is more compressible, it is easier for it to deform, absorbing the effect of stress increase over the porous medium. Thus, the pressure over the fluid tends to decrease, due to the fact that the transference of the load to the solid matrix would occur more rapidly than if the solids compressibility was not taken into account. This can be observed in Figure 5.21 and Figure 5.22.

Comparing the results achieved with the linear elastic model and the modified Cam-clay model, it can be noticed that the referred elastoplastic model is much more willing to variation of fluid pressure responses for different applied loads than the linear elastic model.

Given its features, the elastoplastic model captures the stress and strain changes of the porous medium more accurately than the linear elastic model. Therewith, it is fair to state that

the fluid pressure results are significantly affected by the constitutive model employed. The modified Cam-clay model simulation results may portray the effects of solids compressibility in a more realistic way, representing the porous medium response more effectively.

Another important aspect is the relation between solids and fluid compressibility. In the performed simulations, the fluid bulk modulus is fixed at $1{,}0x10^5$ kPa. When the value of solids bulk modulus is lowered, getting closer to $1{,}0x10^5$ kPa, the effects of fluid compressibility are diminished or not as significant. This means the effect of increase in fluid pressure due to fluid compressibility (section 5.1.1) is annulled, making the values of fluid pressure lower than the expected for this fluid compressibility in this stress level.

The evolution of stress in the sample is represented by the stress paths for these simulations, shown in Figure 5.23 and Figure 5.24 for the incompressible solids (k_s = $1{,}0x10^{15}$ kPa) and in Figure 5.25 and Figure 5.26 for the solids with highest compressibility ($k_s = 1{,}0x10^6$ kPa and $k_s = 5{,}0x10^7$ kPa), for a 100 kPa and 10000 kPa, respectively.

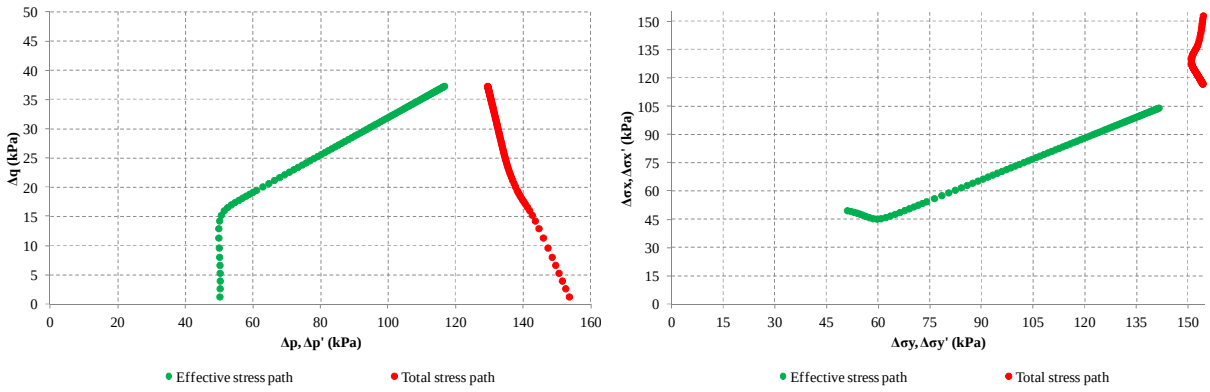

(a) (b)

Figure 5.23 - Stress paths for 100 kPa load sim. (k_s = $1{,}0x10^{15}$ kPa - mod. Cam-clay model).

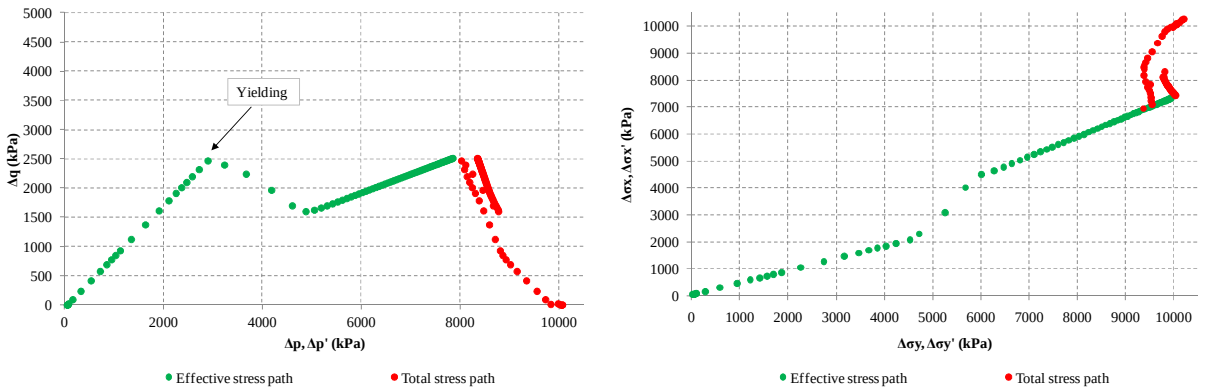

(a) (b)

Figure 5.24 - Stress paths for 10000 kPa load simulation (k_s = $1{,}0x10^{15}$ kPa - mod. Cam-clay model).

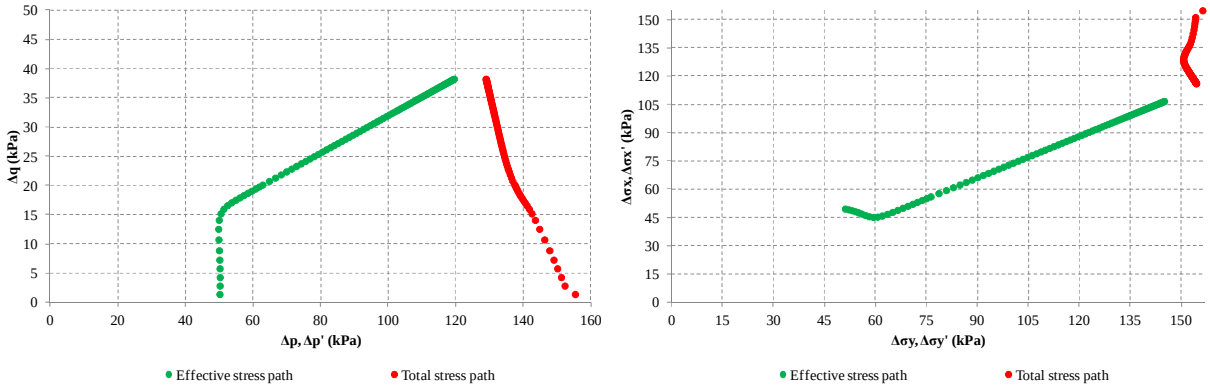

(a) (b)

Figure 5.25 - Stress paths for 100 kPa load simul. (k_s = 1,0x10^6 kPa - mod. Cam-clay model).

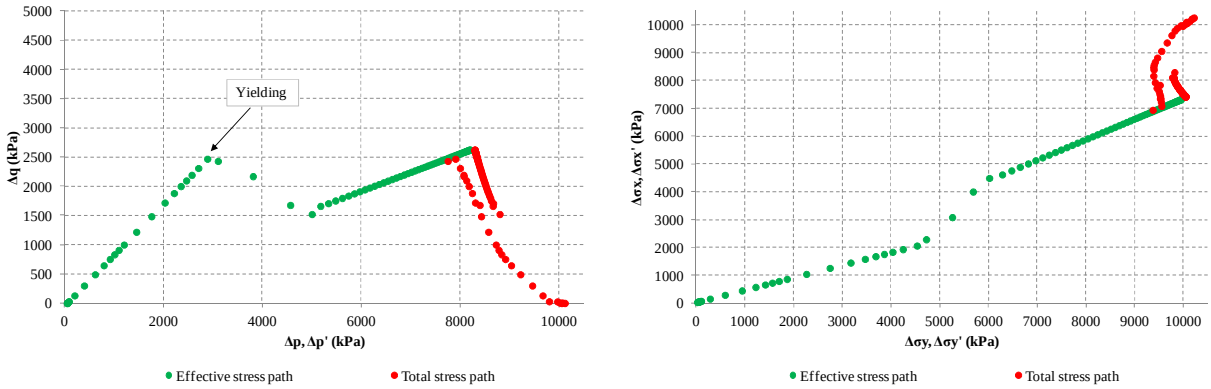

(a) (b)

Figure 5.26 - Stress paths for 10000 kPa load simulation (k_s = 5,0x10^7 kPa - mod. Cam-clay model).

As observed in the simulations, the effect of solids compressibility was not so expressive. Again, there is also no evidence of influence of solids compressibility in the stress paths. Effective stress increases over time due to fluid pressure dissipation, as shown in Figure 5.23 (a), Figure 5.24 (a), Figure 5.25 (a) and Figure 5.26 (a). Also, it is interesting to notice that yielding is reached in the 10000 kPa load simulations, as indicated in Figure 5.24 (a) and Figure 5.26 (a). These behavior tendencies are similar for incompressible and compressible solids simulations.

One important conclusion is related to the effect of fluid compressibility in different stress levels. As explained, for a 100 kPa load, a 1,0x10^5 kPa fluid compressibility does not influence significantly the fluid pressure responses of the numerical model. Therefore, one can conclude that this fluid is incompressible for this load. On the other hand, for a 10000 kPa load, the same value of fluid compressibility influences significantly fluid pressure

responses. For a higher load, the same fluid behaves as a compressible fluid. This should be considered when analyzing the responses the model provides. This effect can be seen when comparing Figure 5.21 and Figure 5.22. The values of fluid pressure for a 10000 kPa load are proportionally higher than for the 100 kPa simulation.

The following analysis is used to evaluate the influence of the stress state in fluid pressure results for the same solids compressibility value. Based on previous analyses, the limit value of solids bulk modulus is $5{,}0x10^7$ kPa for the stress level used in these simulations. Values of solids bulk modulus lower than this can induce numerical instability. This influences fluid pressure responses, making the evaluation not appropriate for comparison of results achieved with the model. The results were taken only for time factors T=0,05; 0,5; 0,8 and they are shown in Figure 5.27.

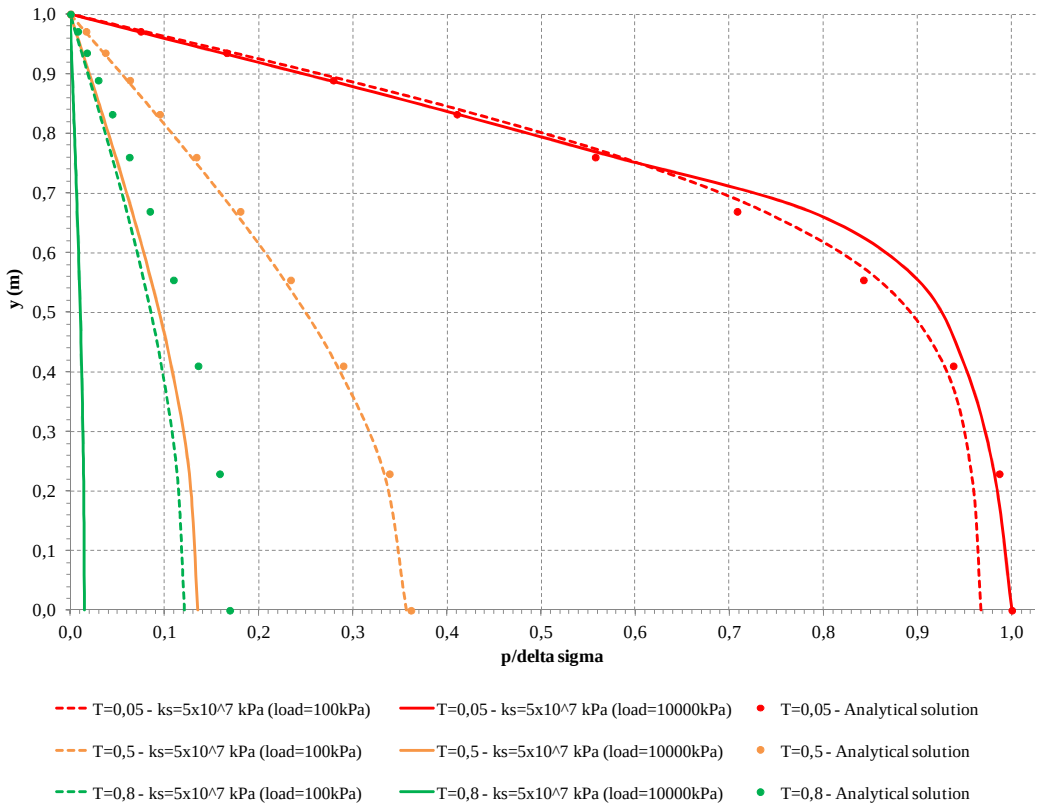

Figure 5.27 - Solids compressibility influence in results of fluid pressure for different stress levels (modified Cam-clay model).

For a 100 kPa load, it can be observed the results for this simulation are similar to the analytic response of the one-dimensional consolidation problem proposed by Terzaghi.

For a 10000 kPa load, the solids compressibility influences the results of fluid pressure. The values of fluid pressure are lower than the predicted in cases with no solids compressibility consideration. Again, a possible effect is compaction drive due to the 10000

kPa load. This loading induces pore closing and, consequently, fluid flow. Considering this, the solids compressibility does not influence the observed results.

A complementary analysis was made with the results in order to verify the effect of consideration of solids compressibility. This effect could be measured by the Biot parameter, already defined in chapter 3 and expressed by the Eq. (5.4):

$$\alpha_b = 1 - \frac{\{m\}^T \left[D^{ep} \right] \{m\}}{9k_s} \tag{5.4}$$

where: $\{m\}^T = \{1 \quad 1 \quad 1 \quad 0 \quad 0 \quad 0\}$ for a 3D analysis, [D^{ep}] is the constitutive matrix and k_s is the solids bulk modulus.

For isotropic, homogeneous and linear elastic media, the Biot parameter is defined as $\alpha_b = 1$. This suggests that the compressibility of the solid matrix does not interfere in the porous medium behavior in these conditions.

However, this parameter is used in the formulation proposed in this dissertation and it influences all matrixes of the solution of the mass conservation equation. Therefore, defining the degree of influence of this parameter in the results may be the basis for evaluating the necessity of calculating Biot parameter for each simulation.

For the same simulations already performed, the results of the Biot parameter for different values of solids bulk modulus are shown in Figure 5.28, for a 100 kPa load, and in Figure 5.29, for a 10000 kPa load.

The values of Biot parameter (α_b) presented in these graphics are for simulations with the linear elastic model (*alpha LE*) and with the modified Cam-clay model (*alpha CC*).

The value of α_b is constant for all stages of time for simulations with the linear elastic model. On the other hand, the values of α_b for modified Cam-clay model simulations change over time. Defining a specific value adequate for representing each simulation could not be truly representative, so it has been established that the minimum and maximum values of α_b would be plotted in the graphics. Also, an average value of α_b was determined for each modified Cam-clay simulation, with its calculation weighted by the frequency of occurrence of each value of α_b. The values of α_b were then used in the definition of the curve of average values of α_b for the modified Cam-clay model (*alpha CC average*).

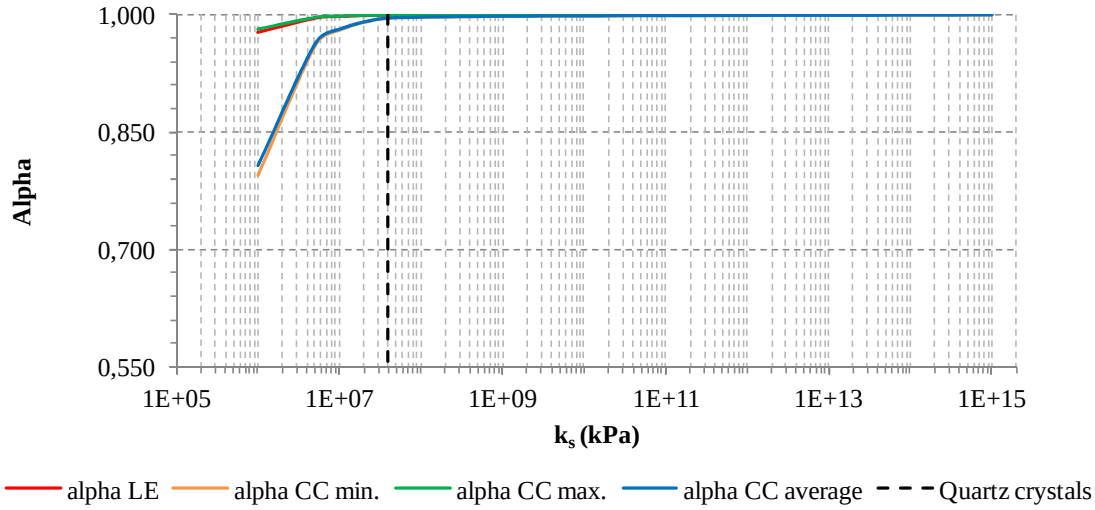

Figure 5.28 - Changes in Biot parameter for a 100 kPa load.

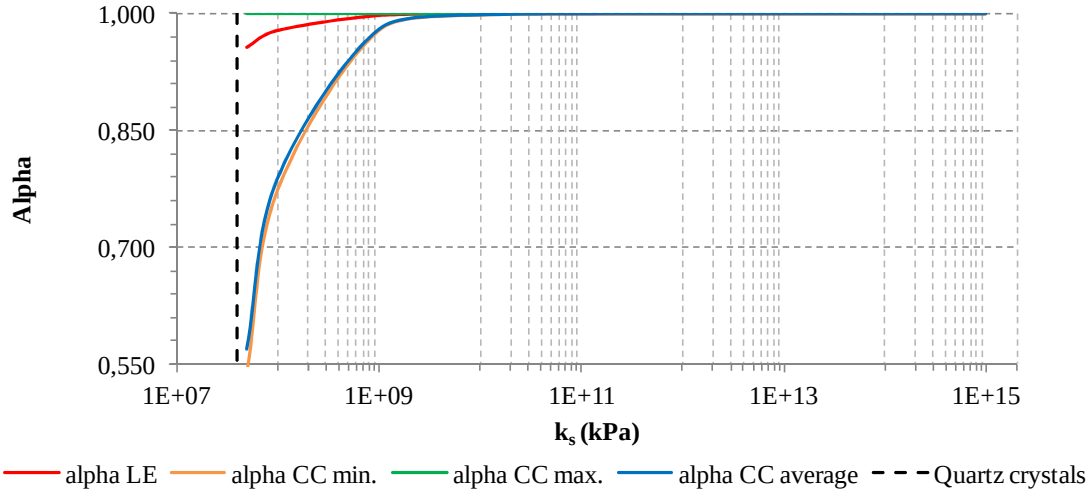

Figure 5.29 - Changes in Biot parameter for a 10000 kPa load.

It can be noticed from both graphics that the value of α_b is not significantly altered for values of solids bulk modulus higher than $1x10^7$ kPa for a 100 kPa load and $1x10^9$ kPa for a 10000 kPa. For values lower than that, the values of α_b start to vary more noticeably.

Considering that this parameter represents the effect of solids compressibility on the sample, it is fair to say that the verification of influence of the stress state of a sample in Biot parameter reveals its importance to evaluate porous media physical behavior.

In real cases, the values of solids bulk modulus for most soils and rocks are around these limits, with $4x10^7$ kPa for quartz crystals (Figure 5.28 and Figure 5.29), for instance (Richardson et al., 2002). Therewith, it may be remarked that the solids compressibility does not influence the responses of the porous medium significantly for lower loads (100 kPa).

This type of analysis permits to infer that this effect of solids compressibility could be neglected in these cases, simplifying the performed simulations.

However, for greater loads (10000 kPa), α_b varies considerably for real values of solids bulk modulus. Considering solids compressibility may be important in cases such as petroleum reservoir simulations, in which the level of stress imposed to the porous medium is higher.

5.2 TWO-DIMENSIONAL CONSOLIDATION PROBLEM

The second case is a two-dimensional consolidation problem. An infinitely deep layer of soil is analyzed in a plane-strain situation, with *x*, *z* as the in-plane axes.

The porous medium hydro-mechanical behavior is analyzed with the application of an uniform load, infinite in one direction (*y*) and limited on the other (from $x = -b$ to $x = b$), as shown in Figure 5.30. The soil is considered totally saturated and it is subjected to a geostatic initial stress state. Also, the fluid is assumed to escape freely at the surface. This case is also based on simulations performed by Farias (1993) and Cordão Neto (2005).

The studied domain is discretized in 200 three-dimensional 8-noded elements (Figure 5.2), making up a mesh with a total of 462 nodes. The division of the domain follows an exponential distribution in both directions (*x* and *y*). The configuration of the finite element mesh is shown in Figure 5.30.

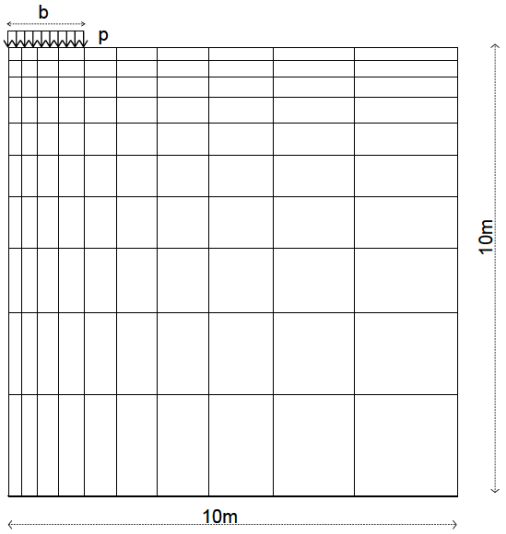

Figure 5.30 - Two-dimensional consolidation problem (modified Cordão Neto, 2005).

The formulation implemented on ALLFINE is tested for this case in terms of fluid compressibility sensitivity. The validation of the proposed formulation is done by the

comparison of the results achieved with ALLFINE and the analytical solution for the problem.

When the fluid bulk modulus is large enough (comparing to solids bulk modulus), the fluid is considered incompressible. So, using values for these parameters correspondent to the condition of incompressibility, the results should match the analytical solution of the problem, proposed by Biot (1940).

These results are presented in terms of normalized displacements. This normalization is made by dividing the surface displacements results by w_{inf} (Eq. (3.1)), correspondent to the initial uniform displacement the surface would suffer if the load extended from $x = -\infty$ to $x = \infty$.

$$w_{\inf} = \frac{apl}{4\sqrt{\pi}} \tag{5.5}$$

where: w_{inf} is the initial uniform displacement, p is the load and l is the double of the extension in which the load is applied ($l=2b$).

In Equation (5.5), a is defined as:

$$a = \frac{(1-2\nu)(1+\nu)}{E(1-\nu)} \tag{5.6}$$

where: E is the Young modulus and ν is the Poisson coefficient.

For other conditions, such as fluid compressibility consideration, the values of displacements are not normalized. The initial uniform displacement (w_{inf}) is calculated for a linear elastic model response, with incompressible fluid. Therefore, using the normalization procedure for compressible fluids does not have any physical for the proposed sensitivity analysis.

Again, the time factors for which the results are presented correspond to those based on classic consolidation theory (section 5.1.1). The value of the time factor is maintained constant for all simulations, permitting a comparison of results at the same stage of analysis.

The presented results permit an evaluation of the hydro-mechanical behavior of the porous medium in a consolidation analysis, verifying the applicability of the enhanced version of ALLFINE, with the compressibility hypothesis considered.

5.2.1 SENSITIVITY ANALYSIS FOR THE FLUID COMPRESSIBILITY

The analyses performed for these tests of fluid compressibility are for a two-dimensional consolidation condition. They are divided in two parts:

- Validation of the proposed formulation;
- Comparison of results for different fluid bulk modulus values.

The formulation is tested with the responses obtained with the simulation of a case in which the fluid is incompressible (k_f =1,0x10^{12} kPa). The results of these simulations are compared to the analytical solution of this problem.

The tests are made for both linear elastic and modified Cam-clay models. When the linear elastic model simulations are performed, the mechanical parameters used are the same as the established for the analytical solution of the problem. In this case, the results are expected to being similar to the analytical response.

However, for the modified Cam-clay model, the mechanical parameters are not the same as the used for an analytical solution, given the differences between an elastoplastic and an elastic model. Furthermore, it is not likely that the results achieved when using the modified Cam-clay model are close to the analytical response. Also, the value of displacement for *x=0* for the last evaluated time stage is expected to match the linear elastic response. This is used for calibration of the modified Cam-clay model.

The results are presented for five different time factor values, T=1/8, 2/8, 3/8, 4/8 and 5/8, in terms of vertical displacements. Again, these time factors refer to the analytical solution of Terzaghi's consolidation problem analysis. These time factors are only employed in order to facilitate the visualization of the results for each simulation over time.

5.2.1.1 LINEAR ELASTIC MODEL RESPONSES

Firstly, the simulation for the validation of the formulation was performed for the studied case with a linear elastic model. For an incompressible fluid (k_f =1,0x10^{12} kPa), the results achieved with ALLFINE are presented in Figure 5.31. It is important to state that the presented results are the values of displacements for each time stage (T=1/8 to 5/8) with deduction of the values of displacement for the initial time stage (T=0). The values of displacement to the initial time stage correspond to an undrained behavior of the soil, not being representative of the consolidation phenomenon. The results have been normalized by the initial uniform displacement w_{inf} (Eq. (3.1)).

The parameters required for the calculation of the initial uniform displacement are related in Table 5.7 and the parameters used for the simulation are disposed in Table 5.8.

Table 5.7 - Parameters for calculating the initial uniform displacement w_{inf}.

a	0,0001 kPa^{-1}
Load (*p*)	100 kPa
Extension of application of the load (*b*)	1,68 m
l (*l=2b*)	3,36 m

Table 5.8 - Parameters for two-dimensional consolidation problem (linear elastic model).

Young modulus (*E*)	10000 kPa
Poisson coefficient (ν)	0
Initial void ratio (e_0)	0,90
Density of the solids (ρ_s)	2,65 kg/m³
Solids bulk modulus (k_s)	$1,0x10^{15}$ kPa
Density of the fluid (ρ_f)	1,00 kg/m³
Fluid bulk modulus (k_f)	$1,0x10^{12}$ kPa $3,7x10^{6}$ kPa $1,0x10^{3}$ kPa $5,0x10^{2}$ kPa
Permeability (*k*)	$1,0x10^{-6}$ m/s

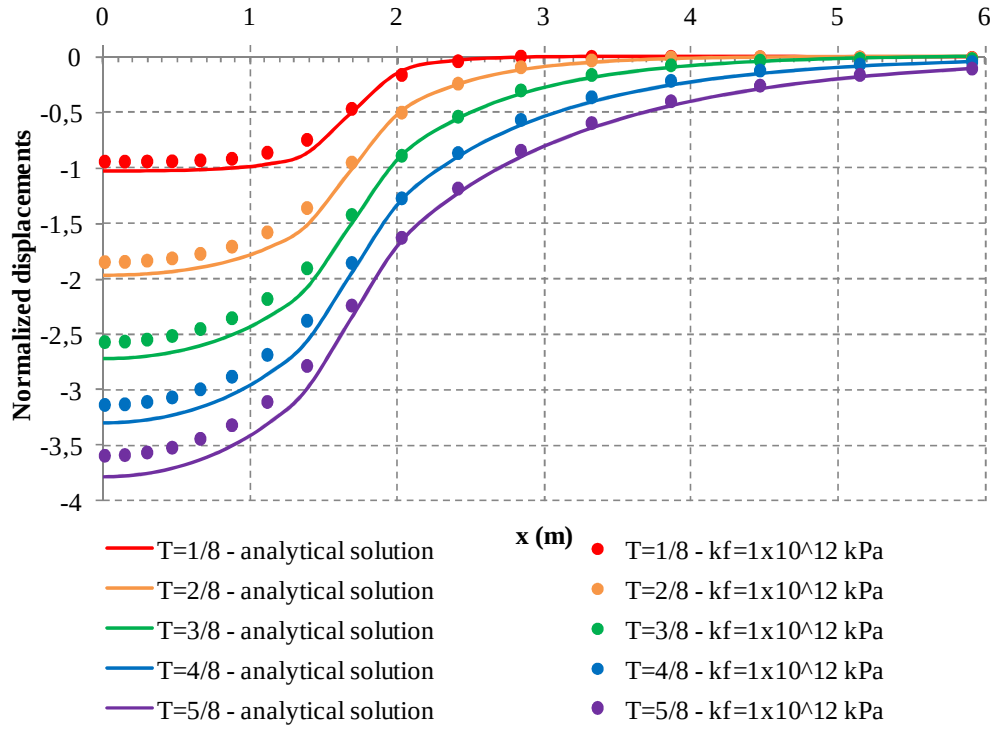

Figure 5.31 - Comparison between analytical solution and results of simulation with ALLFINE for a two-dimensional consolidation problem (linear elastic model).

It may be noticed that the responses achieved with ALLFINE are satisfyingly close to the analytical solution for the problem, with minimum error associated to the numerical solution.

The difference between the responses of analytical solution and simulation may be explained by considerations made in the numerical modeling. In this case, the domain of the problem is finite, limited in all directions, *x*, *y* and *z*, differently than the conditions of the analytical solution, which preview an infinite semi-space. This induces the simulations results to values not so close to the analytical solution as they could be.

Also, the discretization made on the domain of the numerical solution requires boundary conditions which contribute to the noticed difference between the model results and the analytic response of the problem.

After validating the proposed formulation for the two-dimensional consolidation case, the simulations are performed for different values of fluid bulk modulus, in order to evaluate the effects of fluid compressibility in results of vertical displacement in the porous medium. These values of displacement are not normalized, but the displacement referent to the undrained loading condition (initial stage, T=0) is deducted.

The results of the simulations are shown in Figure 5.32. The values of fluid bulk modulus employed in the simulations are presented in Table 5.8.

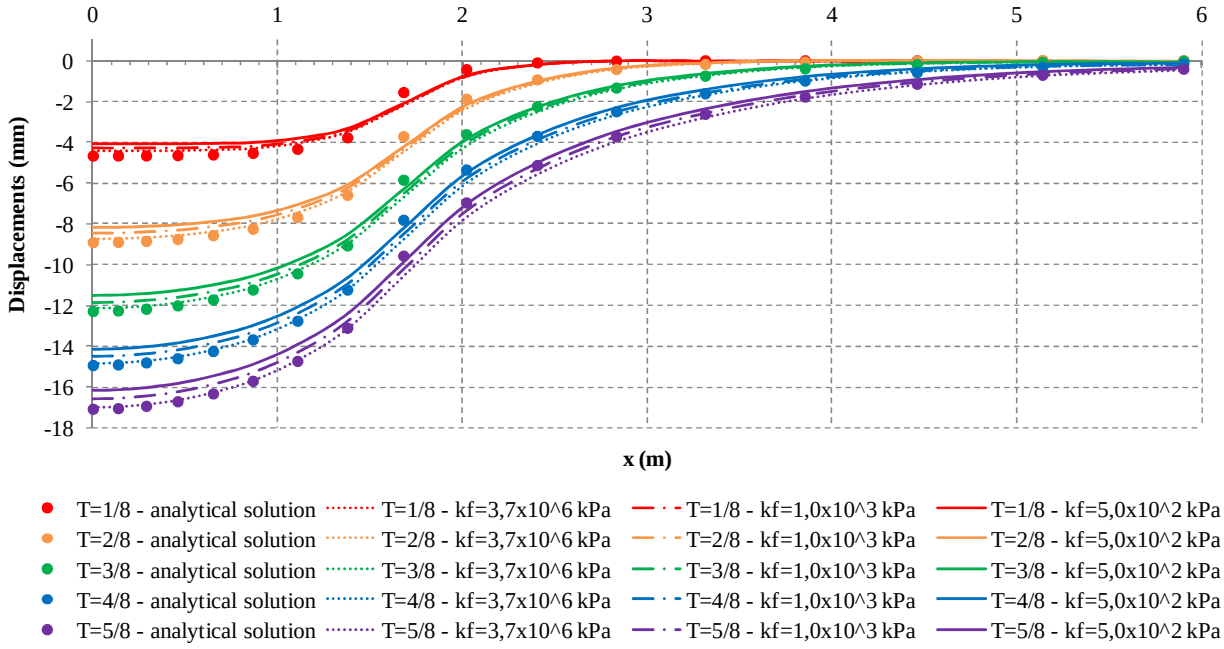

Figure 5.32 - Results of displacements for different fluid bulk modulus (linear elastic model).

The values for fluid bulk modulus can be increased from the totally incompressible condition (k_f =1,0x10^{12} kPa) to the value already stated as limit for the fluid compressibility starts to influence the porous medium physical behavior. It can be noticed that for this limit value, the results achieved with ALLFINE simulations do not differ significantly from the analytical response.

When fluid compressibility is increased over this limit value (k_f decrease), it can be noticed the results of vertical displacements are influenced. The surface displacements decrease for fluids with higher compressibility, considering the same time factor.

This could be interpreted as the effect of fluid pressure increasing already remarked in one-dimensional consolidation analysis (section 5.1). Instantaneously after load application, the fluid receives the entire load, increasing fluid pressure to a maximum value. Over time, the fluid pressure tends to dissipate, as load is gradually transferred to solid matrix. This stress transference is more expressive with incompressible fluids.

However, in a case in which the fluid compressibility is significant, the transference of stress from the fluid to the solid matrix is delayed. The initial increase of fluid pressure makes the fluid have its volume reduced. Thus, fluid pressure increases more than with incompressible fluids, justifying the higher values of fluid pressure registered for compressible fluid during a consolidation process.

This delay in fluid pressure dissipation makes the effective stress to which the porous medium is subjected lower (fluid pressure is higher). Therewith, one can deduce that the stress-strain relations of the porous medium are affected. For lower stress, the strain rate of the soil is lower as well, justifying the decrease in the values of vertical displacement as fluid compressibility is increased.

5.2.1.2 MODIFIED CAM-CLAY MODEL RESPONSES

Firstly, the simulation for the validation of the formulation was performed for the studied case with the modified Cam-clay model. For an incompressible fluid (k_f =1,0x10^{12} kPa), the results achieved with ALLFINE are shown in Figure 5.33.

Differently than the results presented for the linear elastic model, the values of displacement in this graphic have no deduction of the values of displacement to the initial time stage. This consideration might seem inadequate, given the physical significance of the initial time displacements, given in an undrained condition of loading which does not represent the consolidation phenomenon. For that reason, the results of the simulation are compared with the analytical solution also with no discount of this initial stage

displacements. This consideration is made in order to better adjust the modified Cam-clay model parameters (Table 5.9), calibrating it properly, permitting the responses to being adequate to represent the studied phenomenon.

Table 5.9 - Parameters for two-dimensional consolidation problem (modified Cam-clay model).

M	1
***p₀* (for $\Delta\sigma = 100$ kPa)**	50 kPa
Overconsolidation ratio (OCR)	0,20
λ	0,050
κ	0,005
Initial void ratio (e_0)	0,90
Poisson coefficient (ν)	0
Density of the solids (ρ_s)	2,65 kg/m³
Density of the fluid (ρ_f)	1,00 kg/m³
Permeability (*k*)	$1{,}0\text{x}10^{-6}$ m/s

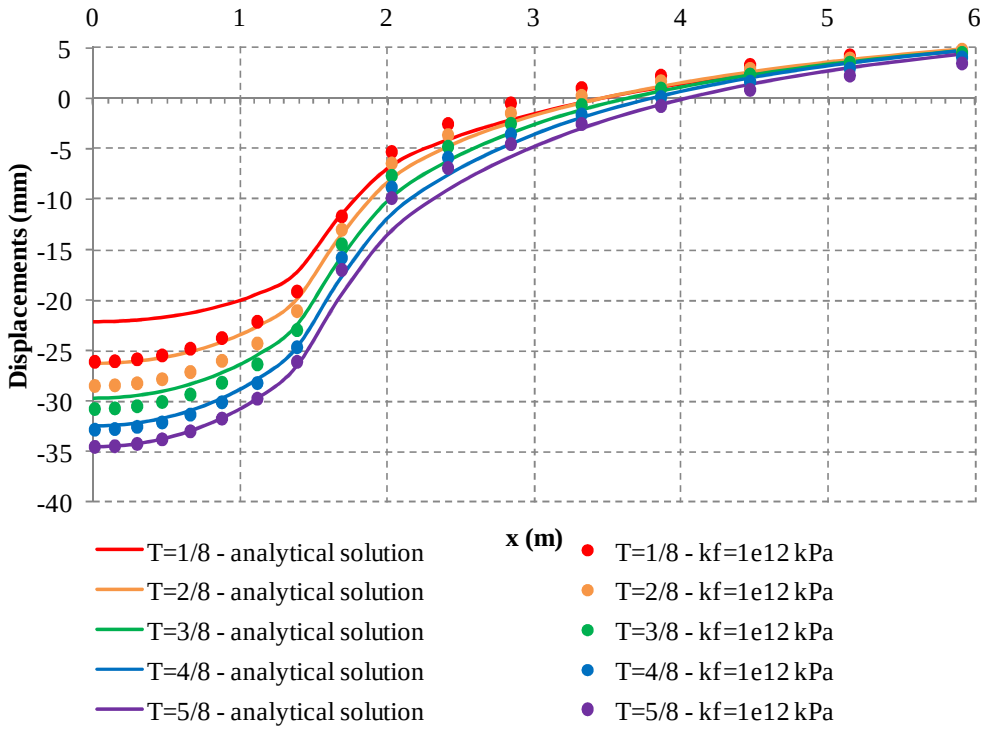

Figure 5.33 - Comparison between analytical solution and results of simulation with ALLFINE for a two-dimensional consolidation problem (modified Cam-clay model).

The results of the numerical solution of the problem with the modified Cam-clay model and its analytical solution are shown in Figure 5.33. The calibration of modified Cam-clay model parameters was based on the values of displacement for the final stage of analysis (T=5/8). The results achieved with the numerical solution should match adequately the expected displacements with the analytical solution.

For more advanced time stages (T=3/8; 4/8; 5/8), the accordance of the numerical and analytical solution results is satisfying. Again, any difference observed between these responses may be explained by considerations made for performing numerical simulation, such as defining a finite domain for the analysis or even the mesh used for element discretization.

However, for the first time stages (T=1/8; 2/8), the responses do not adequately match the behavior previewed by the analytical solution. This could be explained by different characteristics of the constitutive models.

As explained before (section 5.1.1), the stress-strain relation is linear for a linear elastic model and it is non-linear for an elastoplastic model, such as modified Cam-clay.

In cases in which the Young modulus for the elastoplastic model is obtained by a secant going from the origin to the point of maximum stress, this interpretation can be easily made. For a same stress value, the strains achieved with the linear elastic model are greater than with the elastoplastic model. The differences between values of strain for a same stress value may be verified until the stress-strain curves for both models meet (Figure 5.10).

This interpretation for the difference on stress-strain relation between these models justifies the observed behavior in this case. For the first time stages, the effective stress to which the solid matrix is subjected is not sufficient to reach the point when both linear and elastoplastic model stress-strain curves meet, explaining the differences between the responses.

In the second analysis made for this set of simulation, the influence of fluid compressibility is evaluated. The comparison of vertical displacements results for different fluid bulk moduli using the modified Cam-clay model reveal the same tendency of behavior observed in linear elastic simulations. Porous media which the fluid within is significantly compressible are more likely to present lower strain rates, given the increase of fluid pressure already verified with other analysis (section 5.1.1). Thus, the displacements observed in the porous medium are lower when the fluid within is compressible than in situation in which the fluid may be considered incompressible. This can be observed in Figure 5.34.

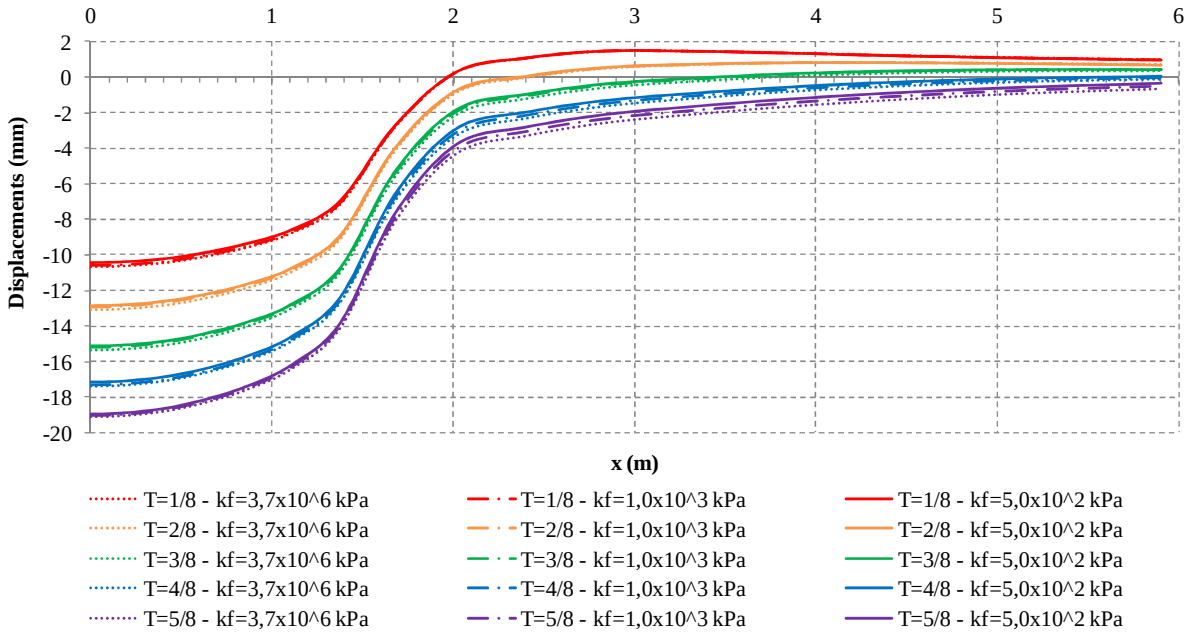

Figure 5.34 - Results of displacements for different fluid bulk modulus (modified Cam-clay model).

The results achieved with linear elastic and modified Cam-clay models show that the influence of the compressibility of the fluid is minimum for this case. In standard geotechnical problems, such as this example, this kind of approach is not relevant. The level of stress and strains porous media suffer is not in the same magnitude order as the reservoir geomechanics problems. Thus, the results are not much influenced by the consideration of fluid compressibility.

5.3 SUMMARY

In this chapter, aspects regarding the mechanical parameters of the studied phenomenon have been discussed. The influence of fluid and solids compressibility on a porous medium has been analyzed with the simulation of one-dimensional and two-dimensional consolidation cases for the linear elastic and modified Cam-clay models.

Firstly, the adequacy of the formulation proposed in this dissertation was tested, with comparison of the results of the simulation, considering fluid and solids incompressible, to the analytical solution of each problem.

The next procedure was to evaluate the degree of influence of fluid compressibility. This was verified with the variation of fluid bulk modulus in each case, with same conditions of load, permeability, fluid and solids density and void ratio of the porous medium. This analysis was performed for both one-dimensional and two-dimensional consolidation cases.

The influence of fluid compressibility is quite significant. The results for the one-dimensional case show that when the fluid is more compressible, the tendency is to observe a delay in fluid pressure dissipation. This is explained by the volume changes the fluid suffers when load is applied in the soil (or rock).

In the two-dimensional case, it was possible to observe less displacement of the soil surface when the fluid is more compressible. This is explained by the reduction of effective stress (due to fluid pressure increase). Consequently, the soil straining observed is much less significant, resulting in less vertical displacement.

In order to evaluate the influence of stress level (different loading conditions) in the results of fluid pressure, simulations were performed in order to compare the response for a same value of fluid bulk modulus. This analysis was made only for the one-dimensional consolidation problem.

For the linear elastic model, the results show that for a higher level of stress, the fluid compressibility is more significant. The analyses of petroleum reservoirs are greatly influenced by this aspect, given the high levels of stress to which the reservoir may subjected at great depths.

For the modified Cam-clay model, however, fluid pressure dissipates faster for a 10000 kPa, the opposite of the expected behavior in these analyses.

This can be explained by the specific features of this constitutive model. The volume changes of the porous medium are better captured with this model. Therewith, two possible phenomena can occur. The fluid within the porous medium can be trapped in the voids or fluid flow can be induced. In the simulations results, it can be observed that the 10000 kPa load induced flow, making the values of fluid pressure lower.

Specifically for reservoir geomechanics, this phenomenon is characterized as compaction drive mechanism, when oil flow is induced due to pore volume changes. This explains the observed decrease in fluid pressure for a higher stress level.

Then, the simulations for sensitivity analysis for solids compressibility were performed, only for the one-dimensional consolidation case.

The simulations were made for two different loads, 100 kPa and 10000 kPa, in order to compare and verify if there could be noticed any behavior tendency differences between them. A comparison of the influence of stress level was also performed and finally, values of Biot's coefficient (α_b) were verified.

These results showed that the influence of solids compressibility is not significant for the numerical solution of the problem. This effect could be neglected without great interference in model response.

Biot's coefficient (α_b) may vary significantly for lower solids bulk modulus values. When comparing the real values of solids bulk modulus to the performed simulations, depending on the stress level to which the porous medium is subjected, the values of α_b may be much lower than 1. In terms of physical behavior of the medium, this could represent the solid matrix compressibility influences more the results for higher levels of stress.

An interesting aspect of these analyses was the verification of the difference of results achieved when performing the simulations with linear elastic or modified Cam-clay models, either for fluid and solids compressibility.

The comparison of the results show there is some difference for initial time stages of the simulation. Over time, this difference decreases until it is practically null. This can be explained by the difference in concept between linear elastic and elastoplastic models.

A linear elastic model has a linear stress-strain relation, as an elastoplastic model has a non-linear stress-strain relation. Thus, for certain stress levels, the straining for the linear elastic model is higher than for the elastoplastic model. However, for a determined value of stress, the curves which represent each model behavior meet, indicating that the value of strain for that level of stress is the same for both models.

The analyses reported in this chapter were essential to visualize the behavior of a porous medium in a consolidation case, a similar situation to the compaction of oil reservoirs. The conclusions here presented help understanding the influence of fluid compressibility in soils and rocks behavior, facilitating the comprehension of certain aspects of the involved phenomena.

The numerical tool developed, validated and calibrated so far shows great potential of enhancing the quality of numerical simulation of petroleum reservoirs.

6 SENSITIVITY ANALYSIS FOR HYDRAULIC PARAMETERS

Similarly to the performed simulations presented in chapter 5, aspects regarding hydraulic parameters, specifically permeability, are discussed in this part of the research.

For the evaluation of permeability features during the simulation of soil consolidation (or reservoir compaction, in reservoir geomechanics), the study case is the same used in the one-dimensional analysis in chapter 5. It is a laterally confined column of soil during consolidation process.

The permeability is defined as function of void ratio of the porous medium, and the simulations are performed for three different configurations of this function. Also, the fluid compressibility is varied for the simulations, in order to being verified the combined effect of compressibility and permeability changes.

These analyses are repeated for linear elastic and modified Cam-clay models for the solid matrix. The specific parameters of each are adequately described on its corresponding sections throughout this chapter.

6.1 ONE-DIMENSIONAL CONSOLIDATION PROBLEM

This case is the same already presented in chapter 5 (section 5.1). It consists of a laterally confined column of soil, 1 meter high and supporting an uniform load of a 10000 kPa. The soil is assumed to be totally saturated and fluid flow is laterally restricted, but it can occur at the top surface. The discretization is made in three-dimensional 8-noded elements.

6.2 PERMEABILITY FUNCTIONS

In some cases, the permeability of a porous medium is considered constant during consolidation. However, due to the mechanical and hydraulic phenomena which take place, one can deduce this is not an accurate assumption. The solid matrix suffers stress changes and straining during this process, implying on pore closing.

The observed reduction in pore volume influences permeability and these two soil characteristics may be related by the following expression:

$$k = A\frac{\exp(Be)}{\exp(BC)} \tag{6.1}$$

where: k is the porous medium permeability, e is the void ratio, A, B and C are the function parameters.

Initially, the permeability sensitivity analysis would be performed for the one-dimensional consolidation case for a 100 kPa load. However, the results achieved with both linear elastic and modified Cam-clay models showed that the variation in void ratio values was too small.

Given the importance of more significant void ratio changes for permeability analysis, the simulations were performed for a 10000 kPa load. Even though the void ratio variation was not as expressive in these simulations, the results were more visible, making the analysis of the phenomenon clearer.

For this study, three different permeability functions were defined for the simulations with the calibration of parameters *A*, *B* and *C*. In literature, references to adequate parameters for permeability functions are rarely reported. For this reason, a methodology of calibration for these functions was developed in this study.

The parameter *A* corresponds to the initial permeability value (k_0) for the porous medium. The parameter *C* is equivalent to a reference void ratio value and, specifically, in this case, it corresponds to initial void ratio value (e_0). The parameter *B* was calibrated considering the void ratio variation range. With this parameter, the function reaches constant values of permeability (function k_1), values 10 times lower than the initial (function k_2) or values 100 times lower than the initial (function k_3) when the porous medium reaches the smallest final void ratio for the simulations (0,876). The values of each parameter are presented in Table 6.1 and its corresponding permeability functions are shown in Figure 6.1.

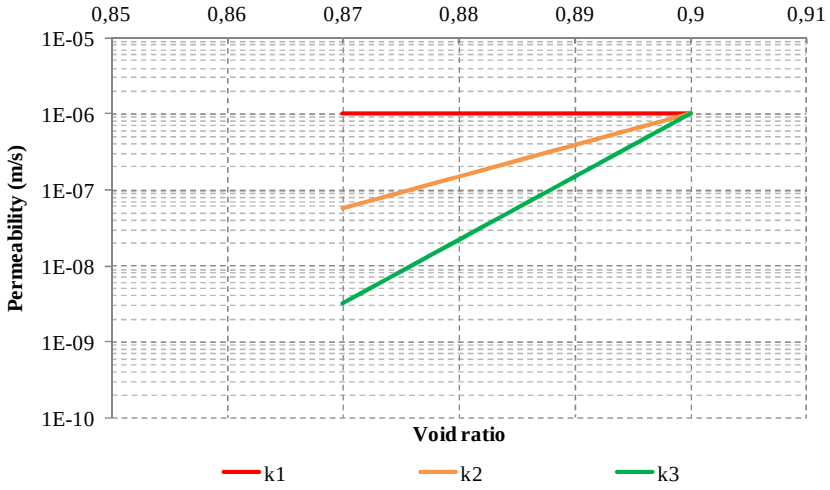

Figure 6.1 - Permeability functions.

Table 6.1 - Calibration parameters for the permeability function.

A		$1,0x10^{-6}$
B	For function k_1	0,0
	For function k_2	95,8
	For function k_3	191,9
C		0,90

These permeability functions are used in simulations with incompressible (k_f =$1x10^{12}$ kPa) and compressible fluids (k_f =$1x10^5$ kPa), for linear elastic and modified Cam-clay models. Thus, the effect of fluid compressibility with permeability variation is evaluated. With different permeability functions, any evidence of interference in the physical behavior of the porous medium should be remarked in the proposed simulations. The results are presented in sections 6.3 and 6.4.

6.3 LINEAR ELASTIC MODEL RESPONSES

The analyses performed with this model use the parameters shown in Table 6.2. The values of permeability vary according to the permeability functions defined in section 6.2.

Table 6.2 - Parameters of linear elastic model for one-dimensional consolidation problem.

Young modulus (*E*)	2500000 kPa
Poisson coefficient (ν)	0,31
Initial void ratio (e_0)	0,90
Density of the solids (ρ_s)	2,65 kg/m³
Solids bulk modulus (k_s)	$1,0x10^{15}$ kPa
Density of the fluid (ρ_f)	1,00 kg/m³

For the linear elastic model analyses, the final void ratio is 0,895, regardless the permeability function used. The volume change is small, but the effects of permeability variation can be noticed in fluid pressure results. The evolution of the fluid pressure during the simulation of the consolidation process is monitored for specific time factors (T=0; 0,2; 0,5 e 0,8). The results for incompressible and compressible fluid analysis are presented in sections 6.3.1 and 6.3.2, respectively.

6.3.1 INCOMPRESSIBLE FLUID

The simulations with incompressible fluid (k_f =1x10^{12} kPa) were performed for the three permeability functions, k_1, k_2 and k_3. The fluid pressure results for each time factor (T=0; 0,2; 0,5 e 0,8) are presented in Figure 6.2, Figure 6.3, Figure 6.4 and Figure 6.5.

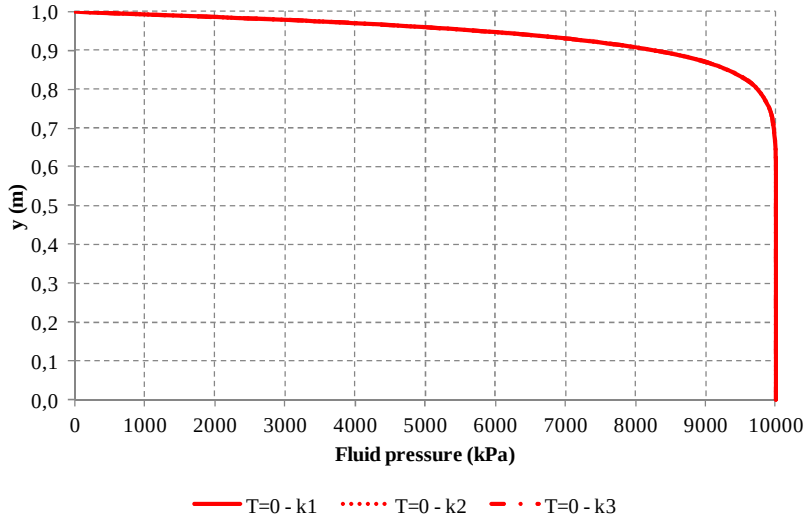

Figure 6.2 - Results of fluid pressure for linear elastic model - incompressible fluid (T=0).

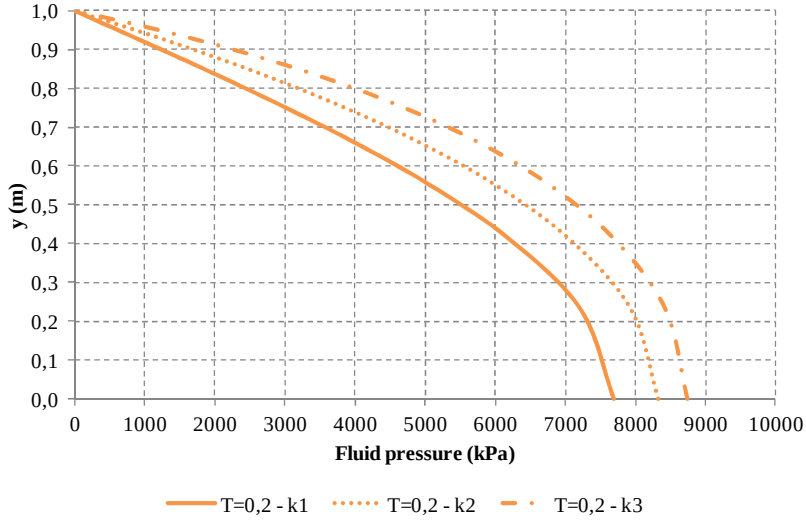

Figure 6.3 - Results of fluid pressure for linear elastic model - incompressible fluid (T=0,2).

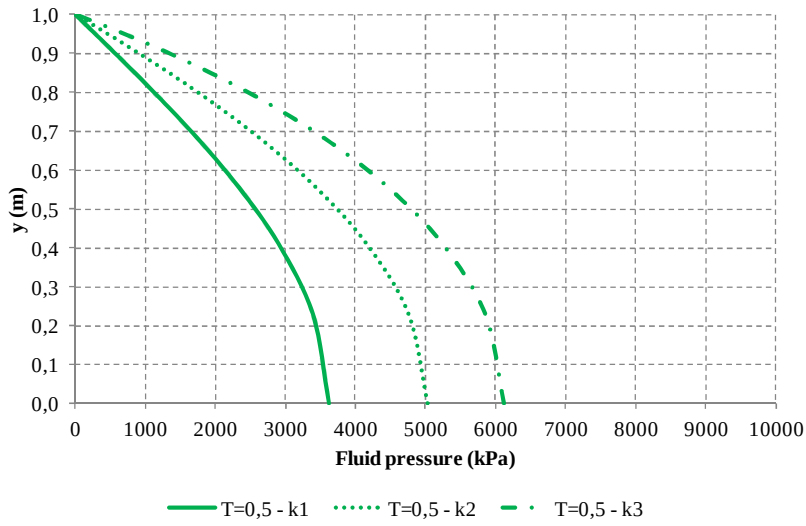

Figure 6.4 - Results of fluid pressure for linear elastic model - incompressible fluid (T=0,5).

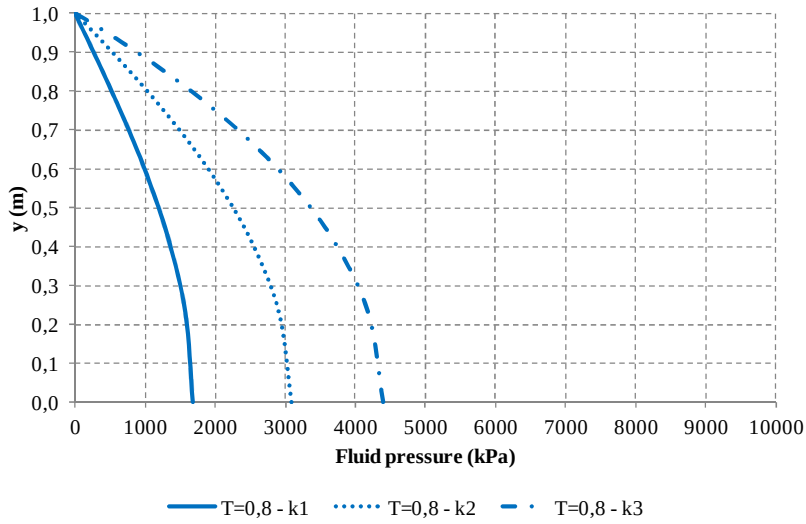

Figure 6.5 - Results of fluid pressure for linear elastic model - incompressible fluid (T=0,8).

For the first time stage (T=0), there is no fluid flow, so the fluid pressure is the same for all permeability functions, corresponding only to the load applied on the soil.

For the following time stages, the effect of varying permeability due to void ratio changes can be noticed in fluid pressure results, because it dissipates faster over time when the medium is more permeable. Thus, the values of fluid pressure decrease more rapidly for the constant permeability function (k_1 function) and slower for the function which reaches a permeability value 100 times lower than the initial value (k_3 function).

It can be noticed that the results of fluid pressure are influenced by permeability, even for low void ratio variation. However, it is important to highlight that the linear elastic model is not adequate for representing the volume changes in porous media solid matrix. The

mechanical behavior results with this constitutive model are not as accurate as the results achieved with an elastoplastic model. The analyses with the modified Cam-clay allow a better understanding of permeability function influence in porous medium behavior. They are presented in section 6.4.

In order to complement this analysis, the void ratio and permeability profiles for functions k_2 and k_3 of this soil sample are shown in Figure 6.6, Figure 6.7 and Figure 6.8, respectively.

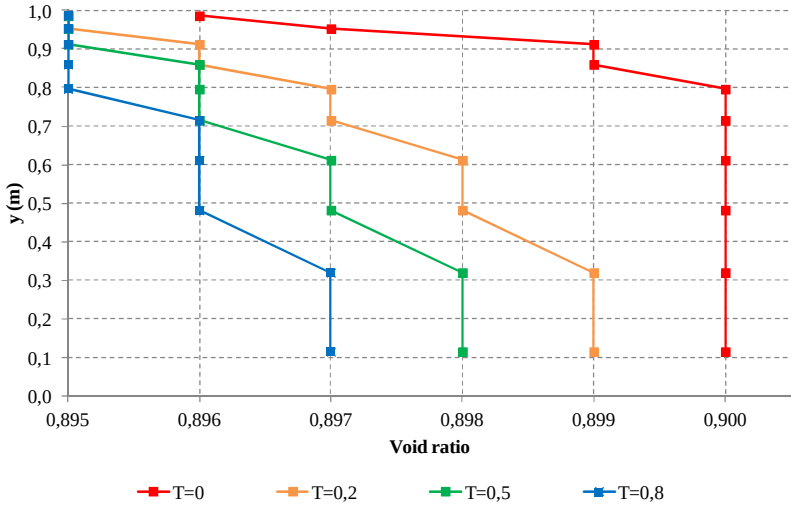

Figure 6.6 - Void ratio profile (incompressible fluid - linear elastic model).

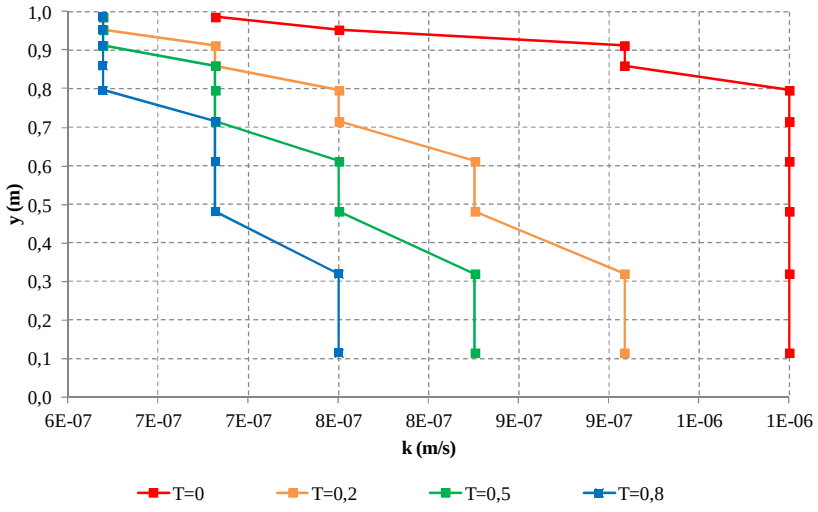

Figure 6.7 - Permeability profile for function k_2 (incompressible fluid - linear elastic model).

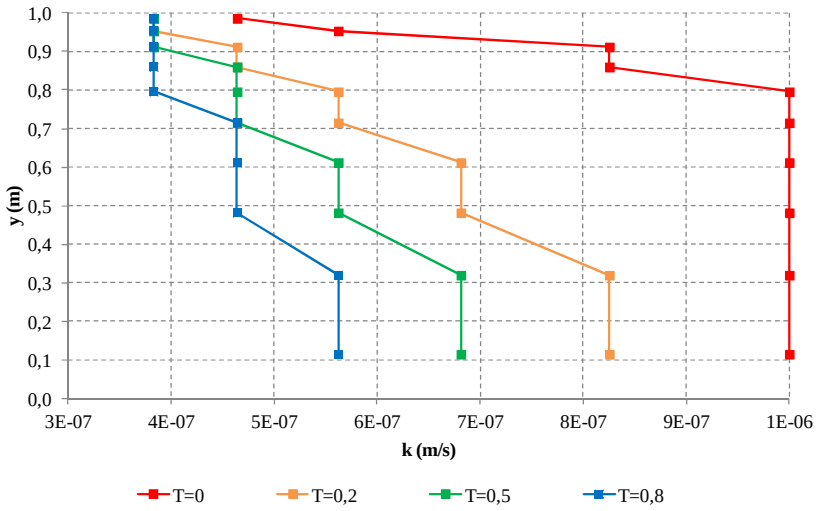

Figure 6.8 - Permeability profile for function k_3 (incompressible fluid - linear elastic model).

6.3.2 COMPRESSIBLE FLUID

The simulations with compressible fluid (k_f =1x10^5 kPa) were performed for the three permeability functions, k_1, k_2 and k_3. The fluid pressure results for each time factor (T=0; 0,2; 0,5 e 0,8) are presented in Figure 6.9, Figure 6.10, Figure 6.11 and Figure 6.12.

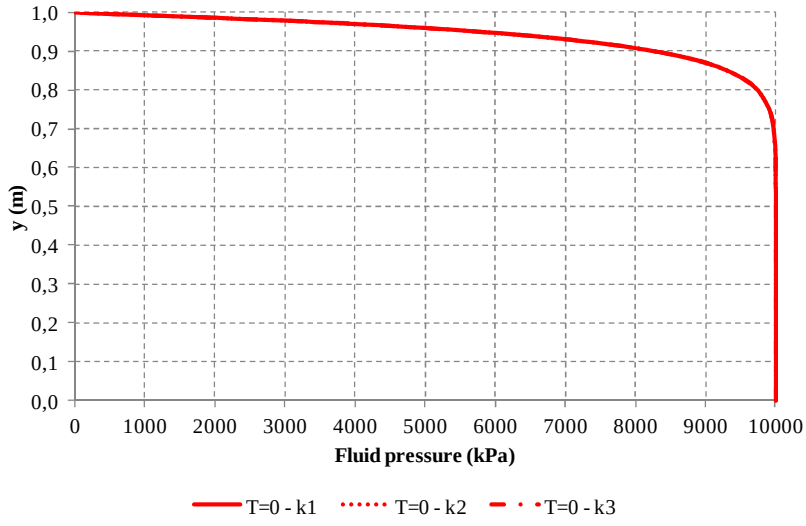

Figure 6.9 - Results of fluid pressure for linear elastic model - compressible fluid (T=0).

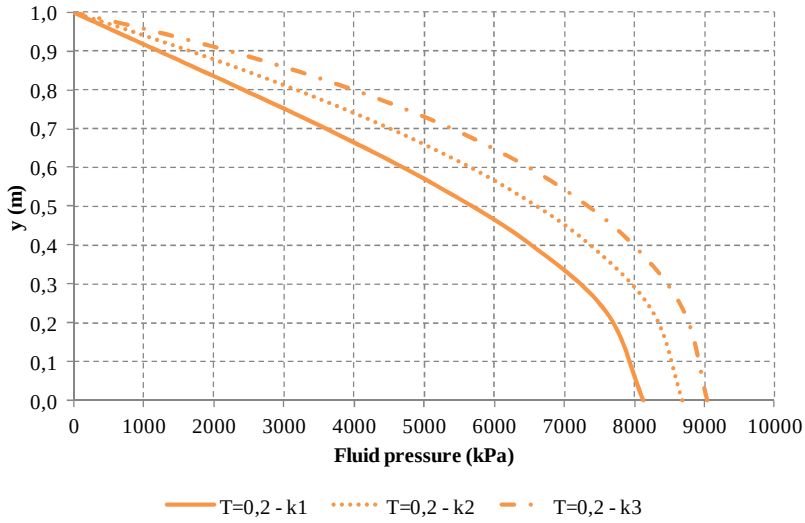

Figure 6.10 - Results of fluid pressure for linear elastic model - compressible fluid (T=0,2).

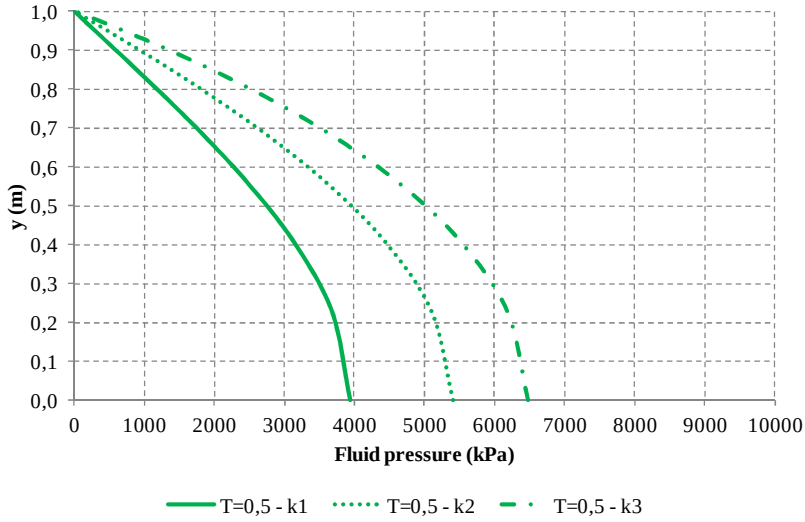

Figure 6.11 - Results of fluid pressure for linear elastic model - compressible fluid (T=0,5).

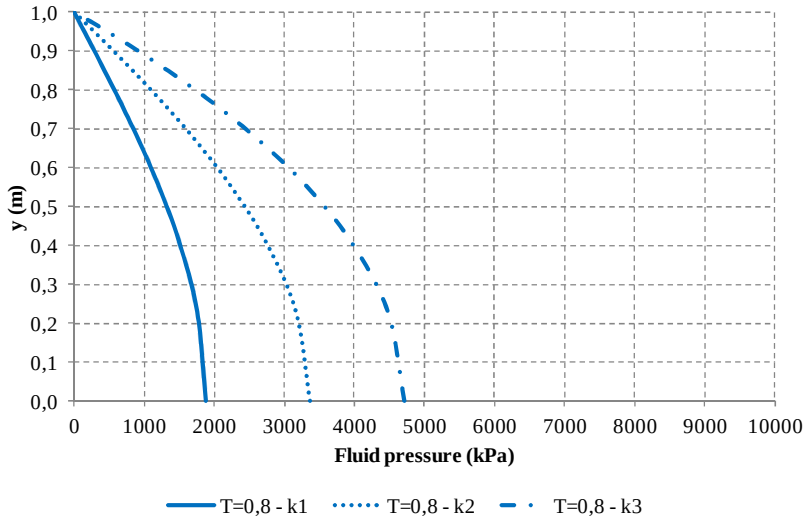

Figure 6.12 - Results of fluid pressure for linear elastic model - compressible fluid (T=0,8).

The results for simulations with the compressible fluid follow the same behavior tendency of the incompressible fluid analysis. In the first time stage, the fluid pressure is equal for all permeability functions. Then, in the following time stages, fluid pressure dissipates faster for constant permeability (k_1 function) and slower for the function which reaches a permeability value 100 times lower than the initial value (k_3 function).

In comparison to the results achieved with incompressible fluid permeability analyses simulations, it is fair to state that the difference between the values of pressure for both types of fluids is related to its compressibility, not being associated to the permeability functions.

The analysis of the fluid pressure curves over time format shows fluid flow tendency is the same (the shape of the curves is maintained), regardless fluid compressibility.

In order to complement this analysis, the void ratio and permeability profiles for functions k_2 and k_3 of this soil sample are shown in Figure 6.13, in Figure 6.14 and Figure 6.15, respectively.

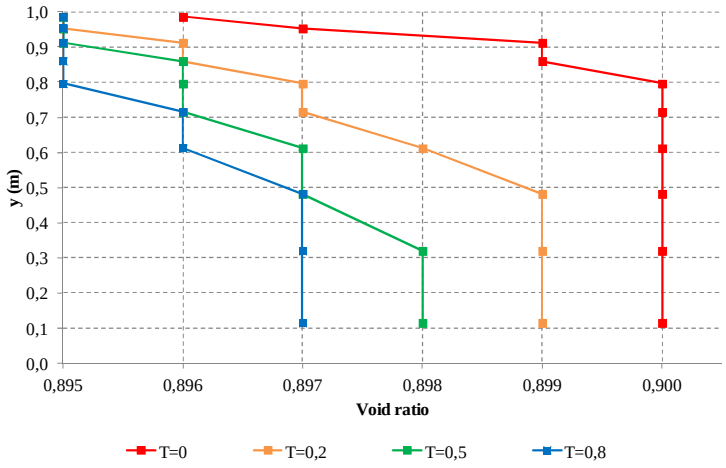

Figure 6.13 - Void ratio profile (compressible fluid - linear elastic model).

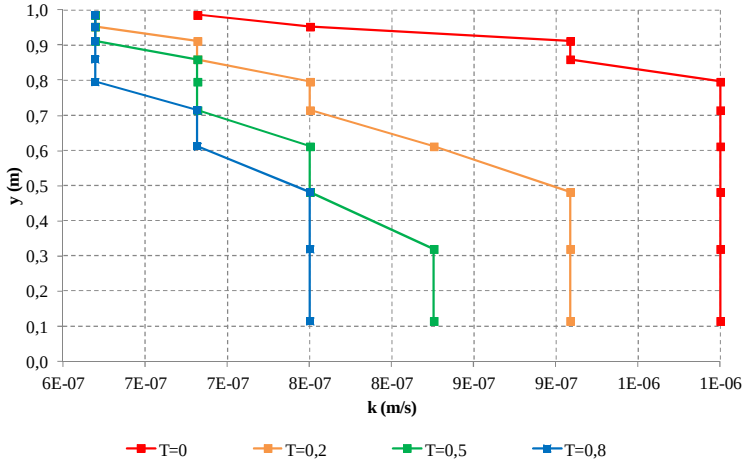

Figure 6.14 - Permeability profile for function k_2 (compressible fluid - linear elastic model).

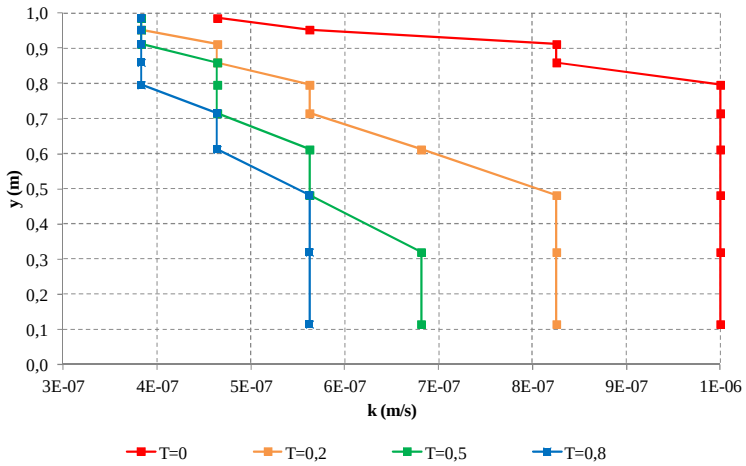

Figure 6.15 - Permeability profile for function k_3 (compressible fluid - linear elastic model).

6.4 MODIFIED CAM-CLAY MODEL RESPONSES

The analyses performed with this model use the parameters shown in Table 6.3. The values of permeability vary according to the permeability functions defined in section 6.2.

Table 6.3 - Parameters of modified Cam-clay model for one-dimensional consolidation problem (permeability analysis).

M	1
p_0	5000 kPa
Overconsolidation ratio (OCR)	0,20
λ	0,0030
κ	0,0003
Initial void ratio (e_0)	0,90
Poisson coefficient (ν)	0,31
Density of the solids (ρ_s)	2,65 kg/m³
Solids bulk modulus (k_s)	$1{,}0 \times 10^{15}$ kPa
Density of the fluid (ρ_f)	1,00 kg/m³

The values of final void ratio for the modified Cam-clay model analyses are presented in Table 6.4. There were no differences between final void ratio values for incompressible and compressible fluids. The volume change is small, but the effects of permeability variation can be noticed in fluid pressure results due to the chosen permeability functions. The evolution of the fluid pressure during the simulation of the consolidation process is monitored

for specific time factors (T=0; 0,2; 0,5 e 0,8). The results for incompressible and compressible fluid analysis are presented in sections 6.4.1 and 6.4.2, respectively.

Table 6.4 - Final void ratio values for modified Cam-clay model simulations.

Permeability	**Final void ratio**
k_1 function	0,876
k_2 function	0,877
k_3 function	0,877

6.4.1 INCOMPRESSIBLE FLUID

The simulations with incompressible fluid (k_f =1x10^{12} kPa) were performed for the three permeability functions, k_1, k_2 and k_3. The fluid pressure results for each time factor (T=0; 0,2; 0,5 e 0,8) are presented in Figure 6.16, Figure 6.17, Figure 6.18 and Figure 6.19.

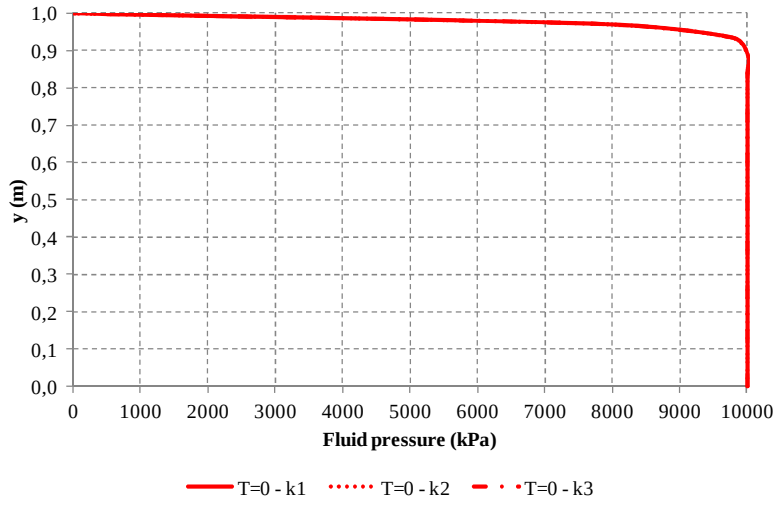

Figure 6.16 - Results of fluid pressure for modified Cam-clay model - incomp. fluid (T=0).

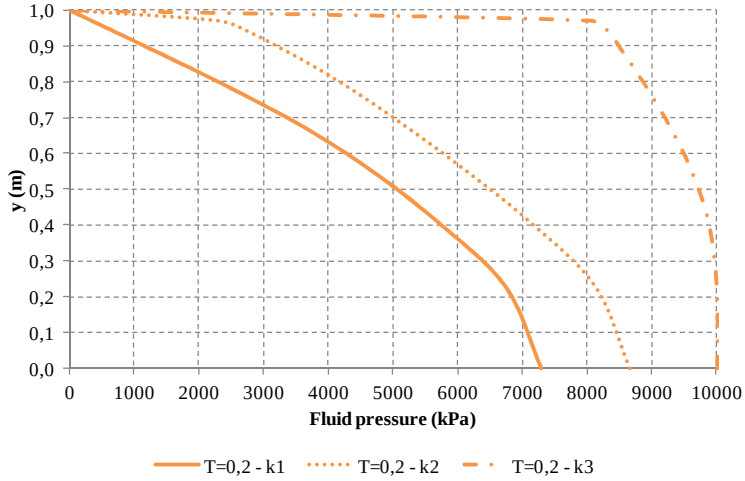

Figure 6.17 - Results of fluid pressure for modified Cam-clay model - incomp. fluid (T=0,2).

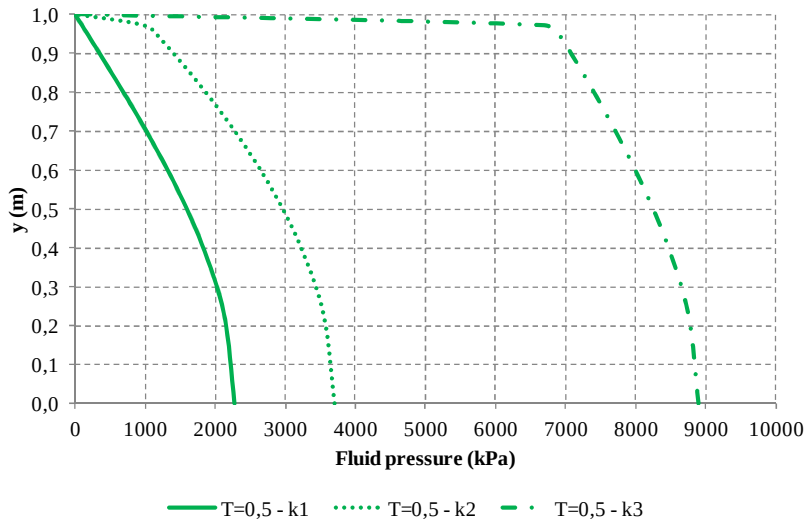

Figure 6.18 - Results of fluid pressure for modified Cam-clay model - incomp. fluid (T=0,5).

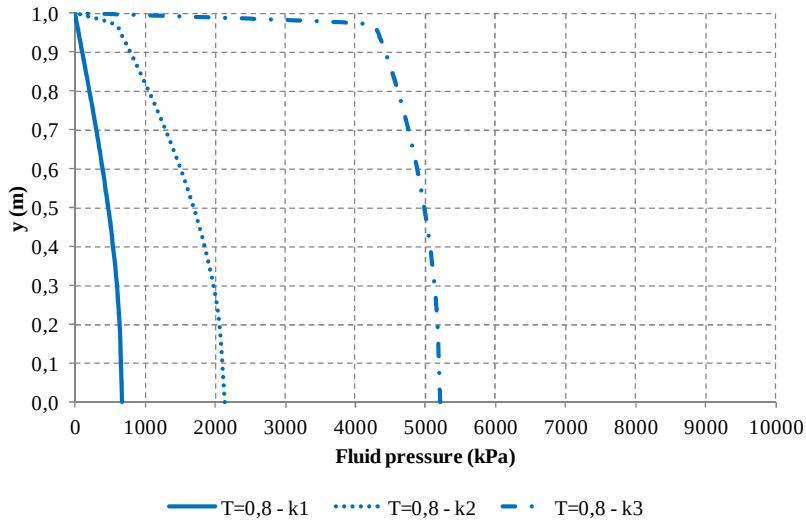

Figure 6.19 - Results of fluid pressure for modified Cam-clay model - incomp. fluid (T=0,8).

The behavior tendency of the porous medium is the same observed for the linear elastic model. In the first time stage (T=0), the values of fluid pressure are equal for all permeability functions simulations. Then, in the following time stages, fluid pressure dissipates over time, faster for the constant permeability function (k_1 function) and slower for the function which reaches a permeability value 100 times lower than the initial value (k_3 function).

It can be inferred from these results that the values of fluid pressure are influenced by permeability, even for low void ratio changes. This attests the effect observed with the linear elastic model, confirming that the straining the porous medium suffers is sufficient to make the permeability function influence noticeable.

Analyzing the shape of the curves, it can be noticed that for permeability function k_3, fluid pressure is high for the lower layers of the soil sample and it decreases abruptly for the superficial layers (surface at 1 m).

During the process, the superficial layers consolidate first, having their pores closed, forming a low-permeability zone. The observed pore closing influences more drastically permeability values for permeability function k_3 for these simulations. This causes fluid flow decrease, making the values of fluid pressure higher in other layers of the sample.

The effect of pores closing in superficial layers is explained by the use of modified Cam-clay model. This model represents the strains a porous medium suffers due to applied stress more adequately than the linear elastic model. Thus, the void ratio of the soil is appropriately calculated and updated during the simulations and the effect of pore closing during the consolidation process is better represented.

In order to complement this analysis, the void ratio and permeability profiles for functions k_2 and k_3 of this soil sample are shown in Figure 6.20, Figure 6.21 and Figure 6.22, respectively.

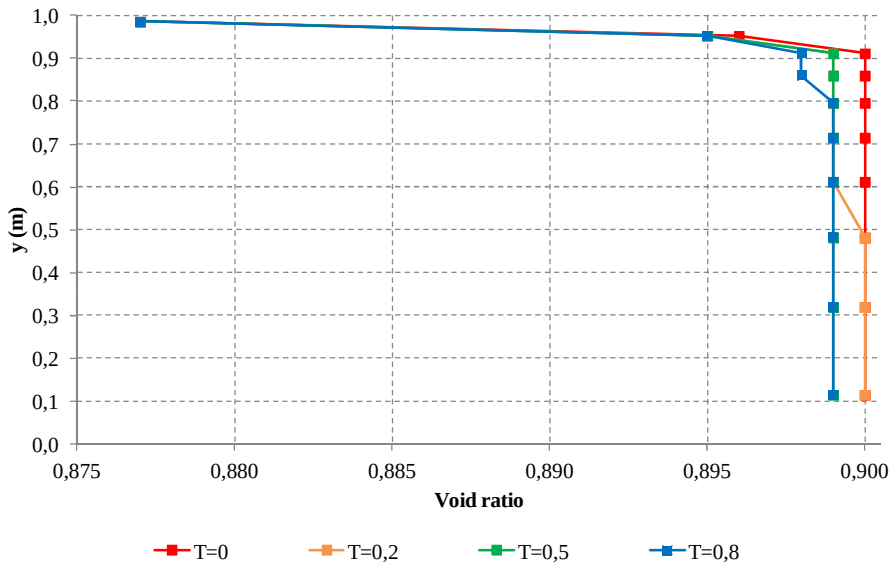

Figure 6.20 - Void ratio profile (incompressible fluid - modified Cam-clay model).

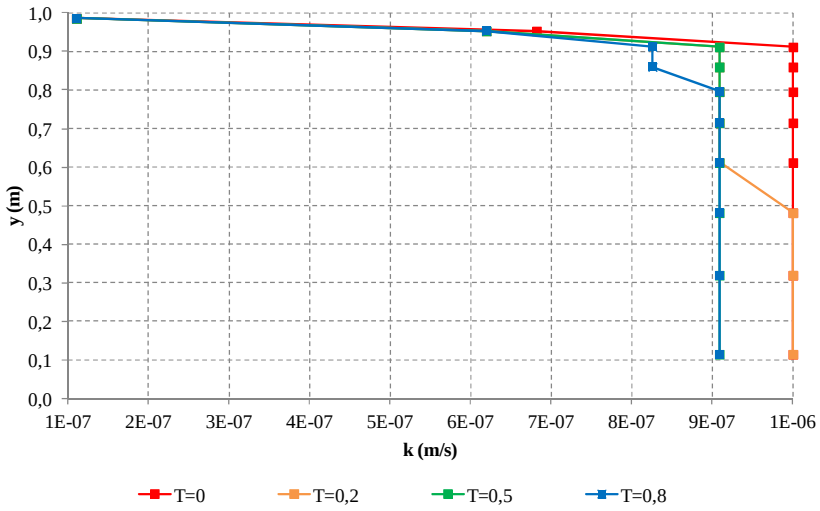

Figure 6.21 - Permeability profile for function k_2 (incomp. fluid - modified Cam-clay model).

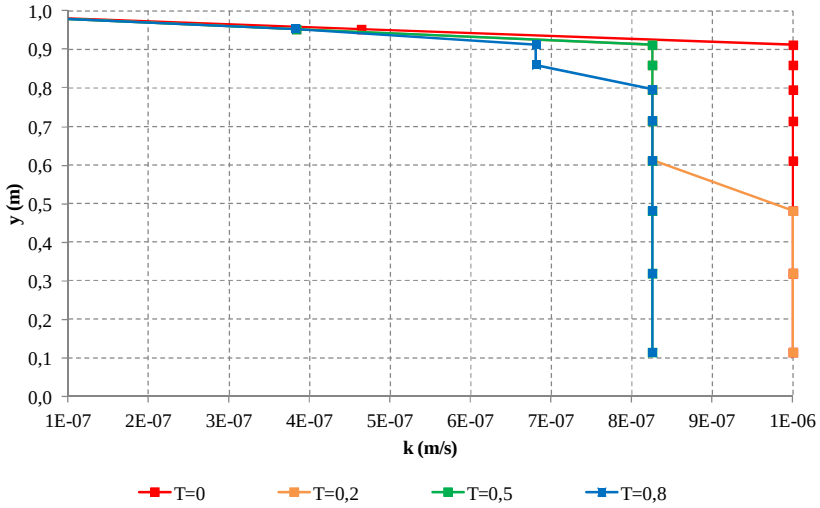

Figure 6.22 - Permeability profile for function k_3 (incomp. fluid - modified Cam-clay model).

In Figure 6.23, two curves are plotted, one for void ratio and other for permeability. These curves complement the understanding of the pore closing process during consolidation when performing simulations with modified Cam-clay model. It can be observed how void ratio gradually until it reaches initial stress (5000 kPa), when it starts to decrease abruptly. As expected, being the permeability a function of void ratio, it follows the same tendency.

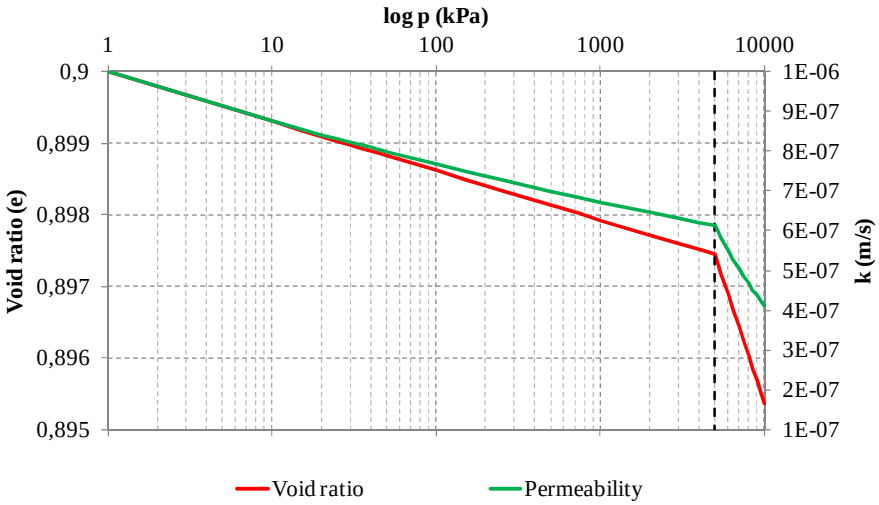

Figure 6.23 - Void ratio and permeability changes with stress increase.

With these conclusions, one can deduce the need for an appropriate permeability function, with adequate parameters to represent the pore volume changes over time. The porous medium permeability influences directly fluid pressure and flow, representing an important aspect of numerical modeling.

6.4.2 COMPRESSIBLE FLUID

The simulations with compressible fluid (k_f =1x10^5 kPa) were performed for the three permeability functions, k_1, k_2 and k_3. The fluid pressure results for each time factor (T=0; 0,2; 0,5 e 0,8) are presented in Figure 6.24, Figure 6.25, Figure 6.26 and Figure 6.27.

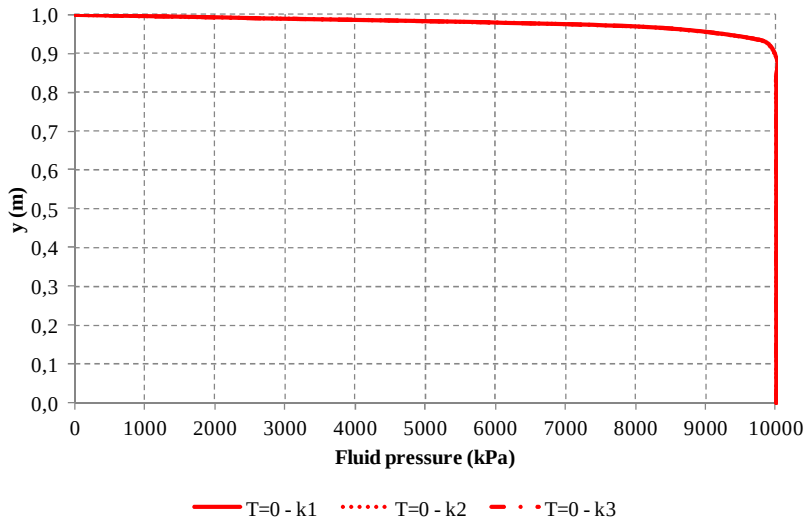

Figure 6.24 - Results of fluid pressure for modified Cam-clay model - comp. fluid (T=0).

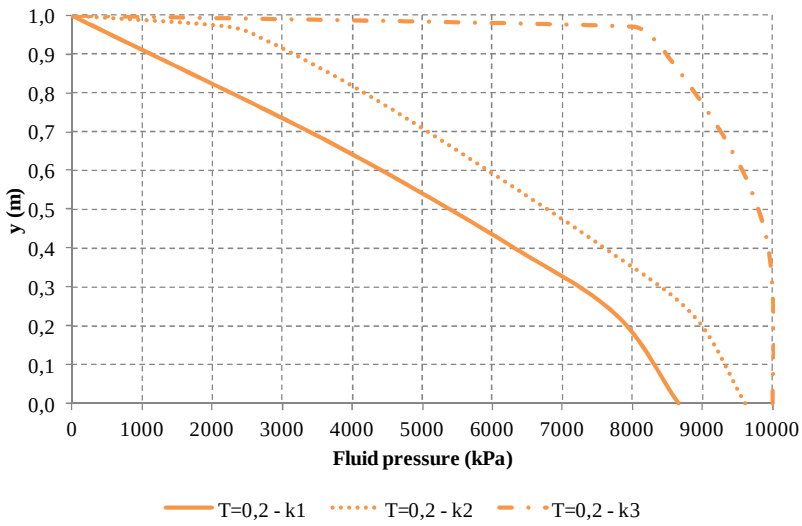

Figure 6.25 - Results of fluid pressure for modified Cam-clay model - comp. fluid (T=0,2).

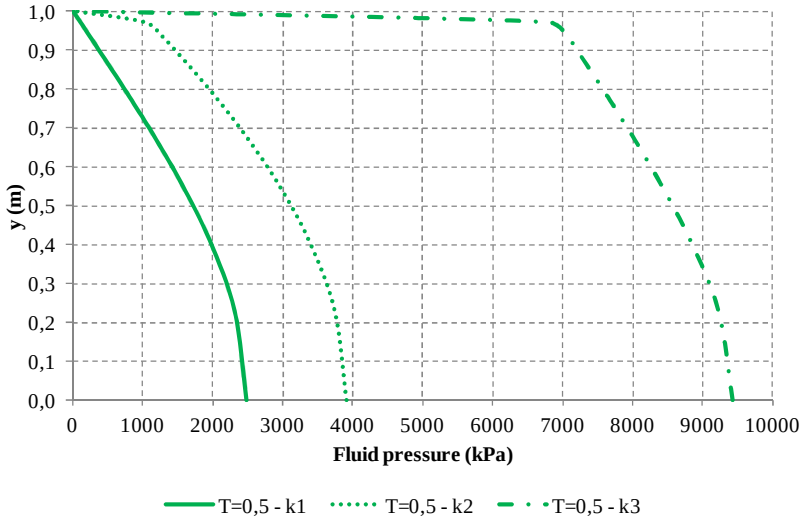

Figure 6.26 - Results of fluid pressure for modified Cam-clay model - comp. fluid (T=0,5).

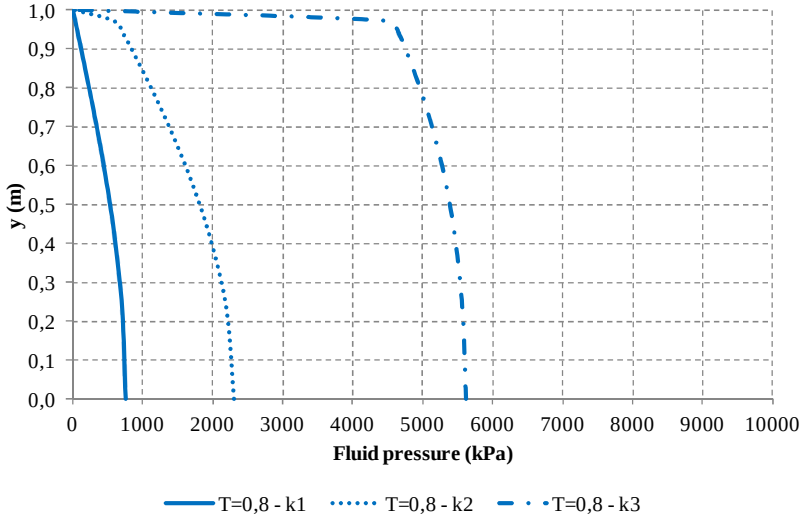

Figure 6.27 - Results of fluid pressure for modified Cam-clay model - comp. fluid (T=0,8).

As observed in the linear elastic analysis, the results of the simulations with the compressible fluid follow the same behavior tendency of the incompressible fluid. For the first time stage, the fluid pressure is equal for all permeability functions. Then, for the following time stages, fluid pressure dissipates faster for the constant permeability function (k_1 function) and slower for the function which reaches a permeability value 100 times lower than the initial value (k_3 function).

Again, it is fair to state that the only difference between the values of pressure for both types of fluids is related to its compressibility, not being associated to the permeability functions.

Thus, by analyzing the format of the fluid pressure curves over time, it can be inferred that the fluid flow tendency is the same (the shape of the curves is maintained), regardless the fluid compressibility.

The effect of fluid pressure increase and abrupt decrease for the permeability function k_3 is again observed. It can be explained by features of modified Cam-clay model. The superficial layers of the porous medium suffer consolidation first. Thus, this process creates a low-permeability zone at the surface of the sample, making difficult fluid flow through this region. Therefore, fluid pressure within the porous medium increases, as observed for the results of all time stages for permeability function k_3 curves.

In order to complement the analyses of influence of fluid compressibility in the permeability of the soil sample, the void ratio and permeability profiles are shown in Figure 6.28, in Figure 6.29 and Figure 6.30, respectively.

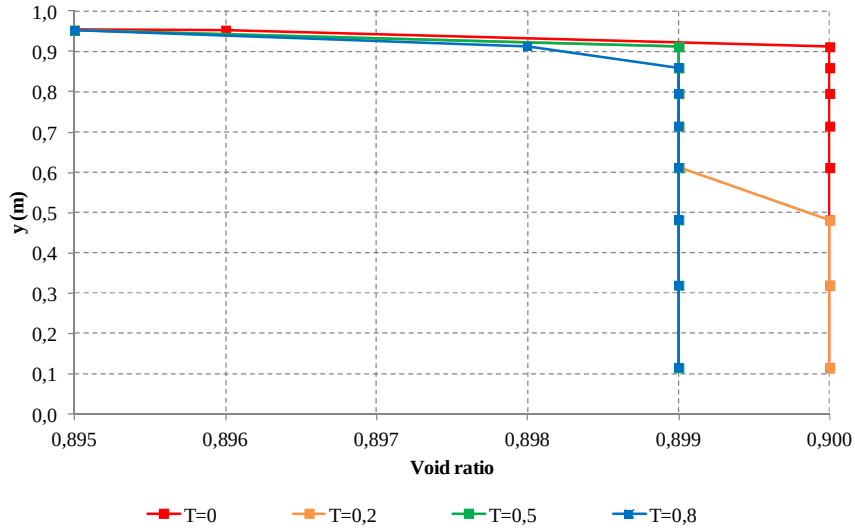

Figure 6.28 - Void ratio profile (compressible fluid - modified Cam-clay model).

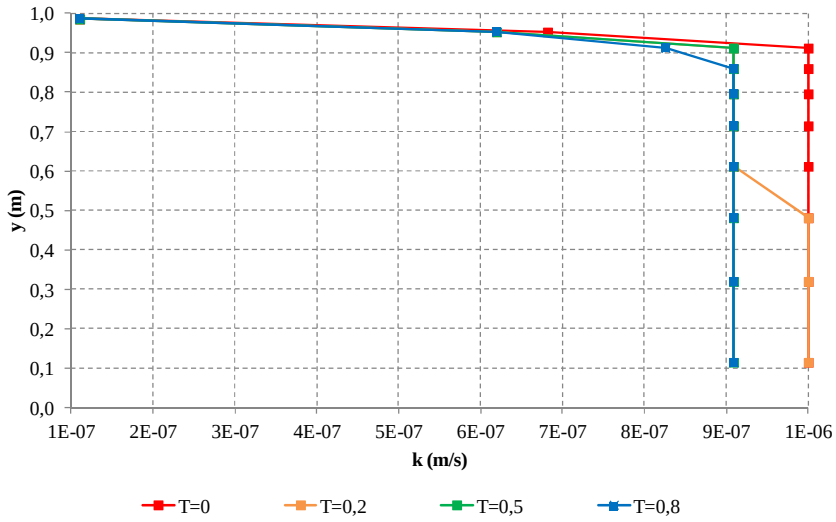

Figure 6.29 - Permeability profile for function k_2 (comp. fluid - modified Cam-clay model).

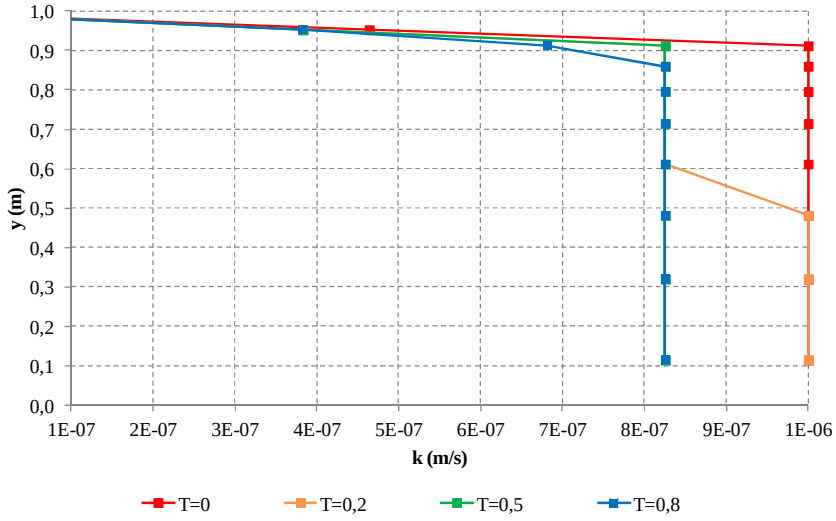

Figure 6.30 - Permeability profile for function k_3 (comp. fluid - modified Cam-clay model).

6.5 COMPARISON BETWEEN INCOMPRESSIBLE AND COMPRESSIBLE FLUID RESULTS

The combined effect of fluid compressibility and permeability changes has already been verified, being stated that fluid flow is only affected by permeability, regardless fluid properties.

Comparing the results for incompressible and compressible fluid simulations, it is possible to observe that only the effect of delay in fluid pressure dissipation is associated to fluid compressibility.

Considering this, in Figure 6.31, Figure 6.32 and Figure 6.33, the results of the simulations are plotted again, allowing the comparison between incompressible and compressible fluid results and results for different permeability functions (k_2 and k_3). The plotted values of fluid pressure correspond to the results of the simulations performed with the linear elastic model.

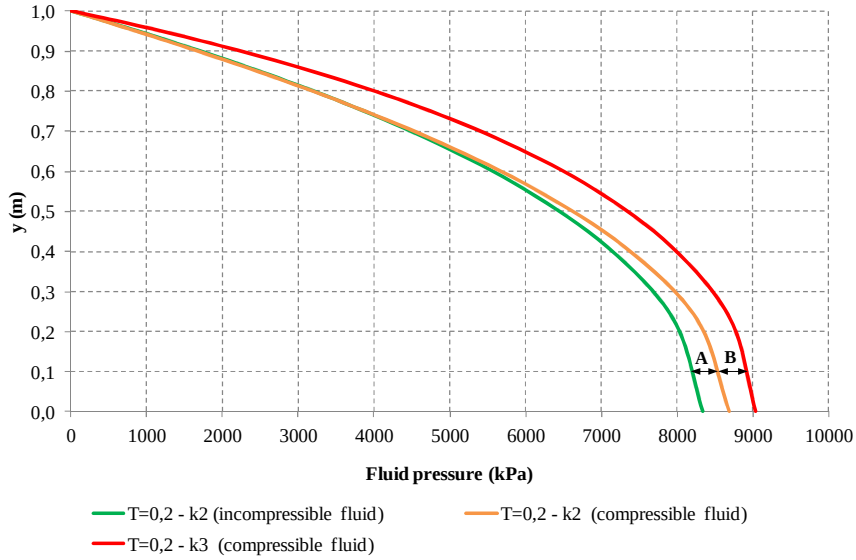

Figure 6.31 - Comparison between results of incompressible and compressible fluid simulation for different permeability functions (T=0,2).

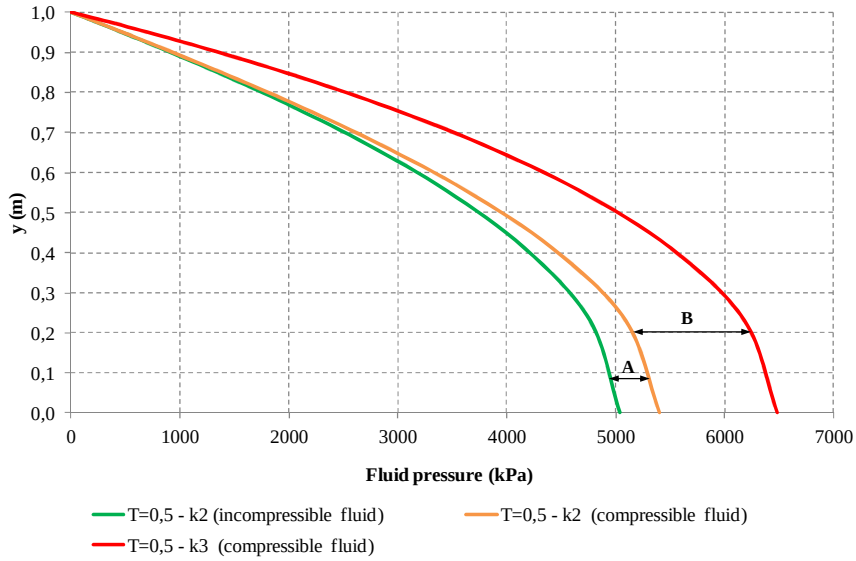

Figure 6.32 - Comparison between results of incompressible and compressible fluid simulation for different permeability functions (T=0,5).

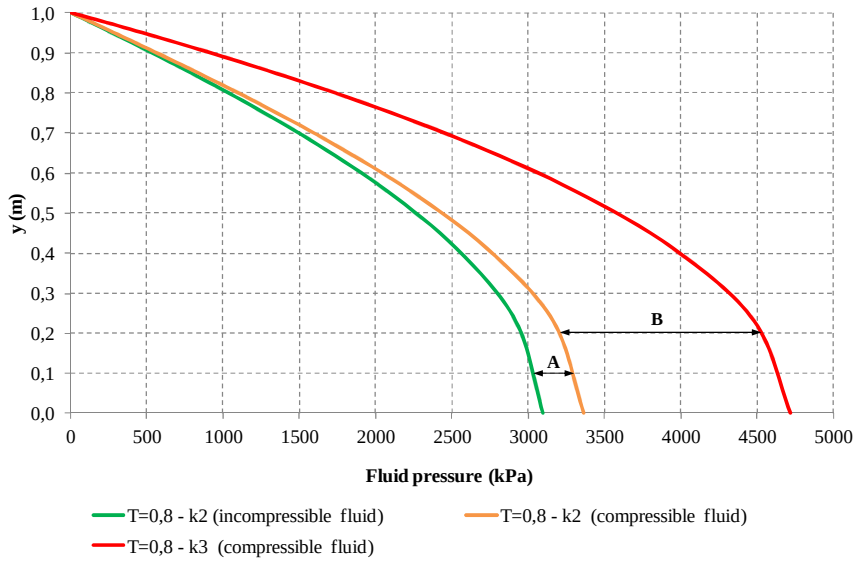

Figure 6.33 - Comparison between results of incompressible and compressible fluid simulation for different permeability functions (T=0,8).

Analyzing the results for all three time stages, it is possible to observe two distinct zones, A and B. The first zone, indicated by A in the graphs, refers to the difference in fluid pressure values associated to the fluid compressibility. The results of the curves that delimitate zone A in the graphs are governed by the same permeability function (k_2). Therewith, zone A corresponds only to the fluid compressibility effect.

The second zone, indicated by B in the graphs, refers to the difference of fluid pressure values due to permeability changes. The curves that delimitate zone B correspond to results of simulations made with the same fluid bulk modulus value. However, they are governed by different permeability functions, k_2 and k_3. Thus, zone B corresponds only to the permeability effect.

With this approach of results presentation, one can conclude the influence limit of each parameter effect, allowing a more accurate analysis of the causes for fluid pressure increase in porous media during consolidation.

6.6 SUMMARY

The objective of this chapter was to evaluate the effects of permeability variation in fluid pressure dissipation during a consolidation process. Furthermore, the combined effect of permeability changes and fluid compressibility was analyzed. This allowed a better understanding of the hydraulic behavior of porous media.

The analyses performed for permeability influence evaluation proved that there is need of developing appropriate permeability functions for porous media studies. The pore volume changes influence directly fluid percolation through the porous medium, evidencing that the different permeability functions may alter significantly the responses achieved with the proposed numerical model.

On the other hand, fluid compressibility does not alter percolation through the porous medium. The fluid flow takes place with the same tendency observed in incompressible fluid simulations. However, the effect of fluid pressure dissipation delay is still registered.

An interesting result was noticed in modified Cam-clay analyses. For the simulations made with permeability function k_3, it could be observed that fluid pressure values were high for lower layers of the soil sample. On the other hand, fluid pressure for superficial layers was extremely low, causing an abrupt change in fluid pressure curve format, as observed in the correspondent graphs. This is explained by the consolidation process in this porous medium. The modified Cam-clay model reproduced the pore closing effect more accurately than the linear elastic model. Thus, the applied load which starts the consolidation process of this soil sample reproduced significant changes in void ratio for the superficial layers of the sample first. Therefore, a low-permeability zone which prevented fluid pressure dissipation for lower layers (fluid flow out of the sample) was formed.

These analyses highlighted the importance of studying permeability functions for porous medium, in order to better represent its hydraulic behavior.

Finally, the results of incompressible and compressible fluid simulations were compared for two different permeability functions. This allowed the division of zones of causes for fluid pressure delay in dissipation, one correspondent only to fluid compressibility influence, other to permeability decrease influence.

7 CONCLUSIONS

The main objective of this research was to define a numerical model for coupled hydro-mechanical analyses for compaction and subsidence problems in petroleum reservoirs considering fluid compressibility valid.

Compaction during primary recovery simulation in an oil reservoir is a problem of dissipation of fluid pressure, with no external loading applied. This kind of problem is adequately reproduced with formulation which uses the iterative coupling strategy. In terms of physical behavior of the porous medium, the level of coupling of this kind of problem is not so strong and the application of the iterative coupling strategy would not imply on numerical model accuracy loss.

On the other hand, the application in traditional geotechnics of the same type of formulation requires a stronger coupling strategy. In cases such as consolidation in soil samples, where load is applied, the level of coupling may influence more the results of the simulation. The separate solution of the equations which describe the problem does not represent adequately the physics of the phenomenon. A fully coupled model is the most appropriate for representing the case, providing greater accuracy to the simulations.

Considering these analyses, the formulation proposed in this research is based on a fully coupled approach. Therewith, it can be applied not only in reservoir geomechanics simulations, but also in consolidation analyses in geotechnics. This formulation has been tested with parametric analyses related to mechanical and hydraulic behavior in porous media.

There have been performed sensitivity analyses for fluid compressibility. Results show that considering this affects fluid pressure responses significantly. It is important to highlight that defining if a certain value of fluid bulk modulus is equivalent to a compressible fluid property depends on the stress level to which this fluid subjected. High stress levels magnify the effects of fluid compressibility. This is extremely relevant for reservoir geomechanics considering the stress level reservoirs are usually subjected.

Important results have been achieved when performing simulations with the modified Cam-clay model. This constitutive model allowed the reproduction of the compaction drive mechanism. Values of fluid pressure reduced for high levels of stress due to this effect.

The consideration of fluid compressibility influences greatly the results of fluid pressure in numerical modeling for this type of problem. Therefore, one can deduce that this

assumption may improve reservoir simulations, providing more accurate results of geomechanical and hydraulic responses.

Besides this, solids compressibility has been tested. The sensitivity analyses for this parameter have revealed that the effect of considering it does not influence fluid pressure results significantly when the simulations are performed for low stress levels (100 kPa). Therefore, in these conditions, solids compressibility could be neglected in numerical models with no losses in model response adequacy.

However, for high stress levels (10000 kPa), Biot's coefficient is largely influenced. This reflects on analyses performed with the modified Cam-clay model. This effect could be associated to specific features of this constitutive model, not only to solids compressibility. Nevertheless, considering the solids compressibility effect may be significant for reservoir simulations. Values of Biot's coefficient suffer significant changes for typical solids bulk modulus (quartz crystals - $4x10^7$ kPa), indicating the importance of taking into account solids compressibility effects when high stress levels are imposed to the porous medium.

Finally, the influence of permeability changes and the combined effect of permeability variation and fluid compressibility have been analyzed. It is important to state that the effect of permeability changes is not influenced by fluid compressibility. The two effects, permeability changes and fluid compressibility, can be separately analyzed. Thus, it is possible to define to which point the fluid pressure increase is related only to permeability changes or to fluid compressibility. In the presented results, there were defined zones of permeability changes influence and fluid compressibility influence. This type of analysis is extremely significant in practical terms, facilitating the understanding of degree of influence for each parameter.

Another interesting result is related to the modified Cam-clay model. The consolidation process is characterized by pore closing and fluid flow in a porous medium. Depending on the load this medium is subjected, the superficial layers of the sample can consolidate first, forming a low-permeability zone. This zone stops fluid flow, making fluid pressure increase within the porous medium.

This analysis can be extremely relevant for reservoir geomechanics application of the model. Fluid flow may be disturbed or even interrupted by this low-permeability zone, decreasing oil production rate.

In an overall analysis, the proposed formulation is adequate to describe the parameters studied during this research. However, there are some limitations. This formulation is

exclusively for isothermal media and its application is limited to simulations of saturated porous media, only for liquid fluids (regardless its compressibility).

These assumptions were made in order to restrict the simulations to analyses with fluid compressibility influence consideration. Therefore, the simplifications proposed may prevent a full representation of the problem, but are sufficient to allow the evaluation of the specific mentioned effects.

7.1 RECOMMENDATIONS FOR FURTHER RESEARCH

Some aspects have not been studied during this research and these are suggested as themes for future work. This proposal includes some themes which are beyond the scope of this dissertation and difficulties encountered in performing some tasks during the development of this research. There are recommendations for further research in other areas which could contribute to improve the results with the model proposed in this dissertation.

These suggestions are:

- To enhance reservoir modeling considering other phases, such as gaseous phase and water phase;
- To consider the effects of temperature in reservoir simulation;
- To consider the effects of gas compressibility;
- To develop a formulation appropriate to represent chemical interaction among phases;
- To simulate a real case of petroleum reservoir, comparing simulation and field responses;
- To employ different constitutive model in reservoir simulation, such as subloading model;
- To develop appropriate constitutive models for permeability, emphasizing the relation between void ratio and transmissibility of fluids;
- To improve numerical simulation with ALLFINE by implementing subroutines for the non-linearity problems in flux for this proposed formulation.

REFERENCES

Ahmed, T. (2001). Reservoir Engineering Handbook. Butterworth-Heinemann, Woburn, Massachusetts, USA, 2 ed. 1191 p.

Ahmed, T., McKinney, P. D. (2005). Advanced Reservoir Engineering. Elsevier Inc. & GPP, USA. 407 p.

Alonso, E. E., Gens, A., Josa, A. (1990). A constitutive model for partially satured soils. *Géotechnique*. 40: 3, 405-430.

Biot, M. A. (1940). *General theory of three-dimensional consolidation*. J. Appl. Phys., 12:155-164.

Britto, A. M. and Gunn, M. J. (1987). *Critical state soil mechanics via finite element*. John Wiley & Sons Ltd., West Sussex, England. 488 p.

Callari, C., Auricchio, F., Sacco, E. (1998). A finite-strain Cam-clay model in the framework of multiplicative elasto-plasticity. *International Journal of Plasticity*. 14, 1155-1187.

Chen, Z., Huan, G., Ma, Y. (2006). *Computational methods for multiphase flow in porous media*. SIAM, Computational & Science Engineering. 549 p.

Cordão Neto, M. P. (2005). *Análise hidro-mecânica de barragens de terra construídas com materiais colapsíveis.* Tese de Doutorado, Publicação G.TD – 028/05, Departamento de Eng. Civil e Ambiental, Universidade de Brasília, Brasília, DF, 152 p.

Dake, L. P. (1978). *Fundamentals of reservoir engineering*. Elsevier Inc., The Hague, Netherlands, 1 ed. 437 p.

Dean, R. H., Gai, X., Stone, C. M., Minkoff, S. E. (2006). A comparison of techniques for coupling porous flow and geomechanics. *SPE Reservoir Simulation Symposium*, SPE 79709, Houston, Texas, EUA, 132-140.

Desai, C. S., Siriwardane, H. J. (1984). *Constitutive laws for engineering materials with emphasis on geologic materials*. Prentice-Hall, Inc, Englewood Cliffs, New Jersey. 468 p.

Dhawan, S., Rawat, S., Kumar, S., Kapoor, S. (2011). Solution of advection diffusion equation using Finite Element Method. *Institute of Electrical and Electronics Engineers*.

Dung, T. Q. (2007). *Coupled fluid flow-geomechanics simulation applied to compaction and subsidence estimation in stress sensitive & heterogeneous reservoirs*. Doctorate thesis. Australian School of Petroleum, South Australia. University of Adelaide. 174 p.

Falcão, F. de O. L. (2002). *Efeitos geomecânicos na simulação de reservatórios*. Dissertação de Mestrado, Departament of Civil Engineering, Pontifícia Universidade Católica do Rio de Janeiro, Rio de Janeiro, RJ. 152 p.

Farias, M. M. (1993). *Numerical analysis of clay core dams*. Ph.D. Thesis, University of Wales – University College of Swansea. 161 p.

Fredlund, D. G.; Radharjo, H. (1993). *Soil mechanics for unsaturated soils*. John Wiley & Sons, USA. 552 p.

Geertsma, J. (1973). Land Subsidence Above Compacting Oil and Gas Reservoirs. *Journal of Petroleum Technology*. 25, p. 734-744.

Gomes, I. F. (2009). *Implementação em elementos finitos das equações de pressão e saturação para simulação de fluxo bifásico em reservatórios de petróleo deformáveis*. Doctorate thesis, Department of Civil Engineering, Civil Engineering Post-graduate Program, Universidade Federal de Pernambuco, Recife, PE. 188 f.

Iglesias, R. (2009). *Conceitos de engenharia de reservatório*. CEPAC – Centro de Excelência em Pesquisas sobre Armazenamento de Carbono, PUC-RS.

Jesus, S. R. C. B. P. de, Cavalcante, A. L. B. (2011). Estudo de modelos numéricos para descrição do fenômeno de advecção. *VI Simpósio Brasileiro de Aplicações de Informática em Geotecnia.* Universidade de Brasília, Brasília, Brasil, 167-176.

Jha, B. (2005). *A mixed finite element framework for modeling coupled fluid flow and reservoir geomechanics*. Master report. Departament of Petroleum Engineering of Standford University. 154 p.

Lewis, R. W., Makurat, A., Pao, W. K. S. (2003). Fully coupled modeling of seabed subsidence and reservoir compaction of north sea oil fields. *Hydrogeology Journal*. 11, 142-161.

Li, X., Thomas, H. R., Fan, Y. (1999). Finite element method and constitutive modeling and computation for unsaturated soils. *Computer methods in applied mechanics and engineering*. 169, 135-159.

McCain Jr., W. D. (1933). *The properties of petroleum fluids*. PennWell Publishing Books, Tulsa, Oklahoma, 2 ed. 548 p.

Nonaka, N., Nakayama, T. (1998). A simple scheme for the finite element solution of a pure advection equation. *Computational Mechanics*. 22, 308-316.

Pastor, J. A. S. C. (2001). *Modelagem de reservatórios de petróleo utilizando formulação acoplada de elementos finitos*. Doctorate thesis, Department of Civil Engineering, Pontifícia Universidade Católica do Rio de Janeiro, Rio de Janeiro, RJ. 67 p.

Peaceman, D. W. (1977). *Fundamentals of numerical reservoir simulation*. Elsevier, Amsterdan, Netherlands. 192p.

Pereira, L. C. (2007). *Simulação de fluxo em reservatórios sob efeito da compactação*. Master dissertation, Department of Civil Engineering, Universidade Federal do Rio de Janeiro – COPPE/UFRJ, Rio de Janeiro, RJ. 136 p.

Richardson, M. D., Williams, K. L., Briggs, K. B., Thorsos, E. I. (2002). Dynamic measurement of sediment grain compressibility at atmospheric pressure: acoustic applications. *IEEE Journal of Oceanic Engineering*. Vol. 27, n. 3: 593-601.

Rosa, A. J., Carvalho, R. de S., Xavier, J. A. D. (2006). *Engenharia de reservatórios de petróleo*. Interciência, 1 ed. 808 p.

Samier, P., De Gennaro, S. (2007). Practical iterative coupling of geomechanics with reservoir simulation. *SPE Reservoir Simulation Symposium,* SPE 106188, Houston, Texas, USA, 1-10.

Samier, P., Onaisi, A., Fontaine, G. (2003). Coupled Analysis of Geomechanics and Fluid Flow in Reservoir Simulation. *SPE Reservoir Simulation Symposium*, SPE 79698, Houston, Texas, USA, 1-16.

Schrefler, B. A., Scotta, R. (2001). A fully coupled dynamic model for two-phase fluid flow in deformable porous media. *Computer methods in applied mechanics and engineering*. 3223, 3223-3246.

Settari, A. (2002). Reservoir compaction. *SPE Distinguished Author Series*, SPE 76805, Calgary, Alberta, Canada, 62-69.

Settari, A., Walters, D. A. (2001). Advances in Coupled Geomechanics and Reservoir Modeling with Applications to Reservoir Compaction. *SPE Reservoir Simulation Symposium*, SPE 51927, Houston, Texas, USA, 14-17.

Tran, D., Ngheim, L., Buchanan, L. (2005). An overview of iterative coupling between geomechanical deformation and reservoir flow. *SPE International Thermal Operations and Heavy Oil Symposium*, SPE 97879, Calgary, Alberta, Canada, 1-9.

Wan, J. (2002). *Stabilized finite element methods for coupled geomechanics and multiphase flow*. Doctorate dissertation. Departament of Petroleum Engineering of Standford University. 162 p.

Zienkiewicz, O. C. (1977). *The Finite Element Method*. McGraw-Hill, London, United Kingdom, 3 ed., 787 p.